Information from the Universe: Cosmological Branes and Perturbation of Strong Gravity

Elcio Abdalla

Instituto de Fisica, Universidade de São Paulo
C.P.66.318, CEP 05315-970, São Paulo, Brazil.

Abstract

We aim at gathering information from gravitational interaction in the Universe, especially in limiting situations, where gravity can be tested at its most extreme forms.

First we briefly consider perturbations of strong gravity solutions to Einstein Equations, and the type of signs derived thereof.

Subsequently, using the solutions to Einstein equations and boundary conditions we study the kind of constraints to the number of e-foldings in inflation.

Later we analyse a dynamical membrane world in a space-time with scalar bulk matter described by domain walls, as well as a dynamical membrane world in empty Anti de Sitter space-time.

We finally investigate the possibility of having shortcuts for gravitons leaving the membrane and returning subsequently. In comparison with photons following a geodesic inside the brane, we verify that shortcuts exist. For some Universes they are small, but sometimes are quite effective.

In the case of matter branes, we argue that at times just before nucleosynthesis the effect is sufficiently large to provide corrections to the inflationary scenario, especially as concerning the horizon problem and the Cosmological Radiation Background.

1 Introduction

Although standard model of particle physics has been established as the uncontested theory of all interactions down to distances of 10^{-17}m, there are good reasons to believe that there is a new physics arising soon at the experimental level [1]. On the other hand, string theory provides an excelent background to solve long standing problems of theoretical high energy physics. It is by now a widespread idea that M-theory [2] can be a reasonable description of our Universe. In the field theory limit, it is described by a solution of the (eventually 11-dimensional) Einstein equations with a cosmological constant by means of a four dimensional membrane. In this picture only gravity survives in the extra dimensions, while the remaining matter and gauge interactions are typically four dimensional.

This avenue presents us a possibility of tackling with two different problems at the same time, namely provide a means of testing the up to now far from experimental and observational data string theory, and providing a theoretical framework to cosmology, whose theoretical background needs a full understanding of quantum gravity in order to correctly deal with the puzzling question of the initial singularity.

General Relativity always evaded quantization. Einstein gravity is a non-renormalizable theory at a low loop level[110], and atempts to include supersymmetry in order to cancel divergencies only postponed the problem to a higher loop [4]. String Theory showed a way, from its very basis of how to succesfully quantize gravity. At the same time, and especially after the discovery of the anomaly cancellation mechanism[5], now even sometimes quoted as the first superstring revolution, strings are quasi unique in their descriptio. Moreover, the further discovery of the duality symmetry, such a uniqueness has been further enhanced [6], leading to the concept of a universal theory, the so called M-theory, largely unknown, describing an eleven dimensional misteiors, master theory, mother of all string descriptions on their side related by duality, and containing in their field theory limit a version of 11-dimensional supergravity [7].

The key question however lies on what can turn a higher dimensional theory into something realistic, describing our four dimensional world. Some hints are know since almost a century, and which have been used before in the context of supergravity. It is the Kaluza Klein approach [8], where extra dimensions are compactified, namely they are curled up into culrs of such a size that they cannot be observed in the daily life. Such an approach, although appealing has encountered several problems, being still an active field of inquire. Still there are proposals where some of these dimensions are lasge enough to be probed by microphysics [9].

Recently, Horava and Witten [10] considered M-theory in a rather intriguing situation. It has been argued that our universe can be seen as a solution of a higher dimensional theory. Strings can be open or closed. The closed string sector contains gravity and further components. The open string sector contains matter fields, isolated into their extremities. In this proposed picture the open string extremities containing the matter fields are restrained to live in the physical universe. In Horava and Witten proposal the physical universe is thus described by such a membrane.

Later on, Randall and Sundrum described the universe as a solution os the higher dimensional field equations with boundary conditions describing the membrane. As a result, they obtained a space with full fledged extra dimensions, but with a warp, such that the effective penetration of gravitons in the extra dimensions is small, and the effective gravitational interaction is, observationally, four dimensional. In this picture, there is a possibility that gravitational fields, while propagating out of the brane speed up, reaching farther distances in smaller time as compared to light propagating inside the brane, a scenario that for a resident of the brane (as ourselves) implies shortcuts [11]—[15].

It is our aim in this work to further develop these ideas in the case of a FRW brane Universe [16]. The subject was developed until now from the point of view of the brane [17], where all time dependence is embedded in the bulk metric written in gaussian coordinates. The price payed for the knownledge of the position of the brane in the bulk is the complicated form of the bulk metric and, consequently, the complicated behaviour of geodesics in the bulk. However, if we treat the problem from the point of view of the bulk, where the brane evolves in a non-trivial way in a static AdS background, we can construct explicitly the causal structure of null geodesics leaving and subsequently returning to the brane. As it turns out, shortcuts are common, although harmless at the present days (the delay is vanishingly small), but could be large in the era before nucleosynthesis if high redshits were available.

Moreover, one of the main goals of string theory nowadays is to prove itself able of coping with experimental evidences. Branes have been shown to be useful tools to understand the physics of strings and M-theory [58]. As it has also recently been pointed out [57], brane Universes such as the one described above could imply the existence of relics of the extra dimensions in the cosmic microwave background. Unfortunately, recent developments with inflation guided by a scalar field in the brane indicate that the consistency equation is preserved [59]. In this work however, we show that if inflation took part on the brane, the causal structure is definitely changed by those gravitational shortcuts, possibly leading to a non-usual period of causal evolution of scales. This could be responsible for distinct predictions in the cosmic microwave background structure for inflationary models.

This scenario has been proposed as an actually realizable possibility [18]—[55]. In [20] it has been shown that in some scenarios shortcuts are very difficult to be detected today because of the extremely short delay of the photon as compared to the graviton coming from the same source.

Recently it has been proved [57] that brane Universes can provide a means for finding relics of the higher dimensions in the cosmic microwave background as well. Thus it is worthwhile further pursuing brane models as useful tools to understand the physics of strings and M-theory [58], which proves them as very important instances to try a better insight of the Universe and its properties.

At last, we should stress that this is a toy model where the universe is replaced by a domain wall. The more realistic case deserves attention as well (see also [20]).

2 Further Motivations and Brane Cosmology

The Planck mass is the natural scale where string effects becomes important. However, it is not possible to achieve such an energy level in particle physics accelerators. Nonetheless, as we mentioned above, cosmology may provide an alternative laboratory for string theory. From the eighties several authors tried to analysed the kind of cosmology arising from string inspired models, which are essentially general relativity in higher dimensions together with scalar and tensor fields. In case we introduce also the brane concept, a consistent picture of the brane universe is achieved, and we can describe the evoltion of the universe by means of solutions of the Einstein field equations in higher dimensions, with a four dimensional membrane.

Extensive used of specific properties of strings, such as the T-duality may provide simple explanations of several properties of the universe, though of course an observational check is always missing. Nonetheless, a pre big-bang scenario turns out to be described, providing a very sophisticated physical picture of the universe. Several solutions indicating inflationary results have been obtained, in what is now usually called brane cosmology.

It is thus essential to provide means of comparing those results to some observational data, which is the largest difficulty in string theory. The best proposal is to use the extremely sophisticated data of the Cosmic Microwave Background, first obtained from the pioneering COBE satelite, and more recently by the detailed analysis of the WMAP. Such observations are opening the avenue for precision cosmology, and results with error bars less and a percent are now available. In such a case one can compare the predictions of inflationary models with observations, and even quantitatively distinguish between different inflationary scenarios, with a chance of favouring, or discarding, string inspired models of cosmology, or brane cosmology.

The definition of a scalar potential directly from string theory has been an important issue. In [21] an attempt was made in order to derive the scalar interaction from a brane-brane interaction. This kind of approach reviewed in [22] has been very recently taken over in [23]. A few different and new forms for the inflaton potential have been derived, showing that at least one can hope to derive inflationary models directly from the properties which caracterize string theory and its consequences, namely M-theory and branes.

3 Perturbations of Einstein Equations in a General Setup and consequences

Exact solutions of Einstein Equations are many, but reality can be much more difficult, and much more is needed, what goes beyond usually known exact solutions, and one has to go beyond them. Moreover, one has to physically separate properties of the whole universe, such as those described by the Friedmann-Robertson-Walker solution and generalizations and information details arising from small perturbations thereof, describing waves that can bring information both in the form of waves from distant objects, in a class of problems, as well as describing small inhomogeneities caracterized in the observation of anisotropies of the Cosmic Microwave Background.

3.1 Perturbations of Black Hole Solutions

The study of wave dynamics outside black holes has been an intriguing subject for the last few decades (for a review, see [24]). In virtue of previous works, we now have the schematic picture regarding the dynamics of waves outside a spherical collapsing object. A static observer outside the black hole can indicate three successive stages of the wave evolution. First the exact shape of the wave front depends on the initial pulse. This stage is followed by a quasi–normal ringing, which carries information about the structure of the background spacetime and is believed to be a unique fingerprint to directly identify the black hole existence. Detection of these quasinormal modes is expected to be realized through gravitational wave observation in the near future [24]. Finally, at late times, quasinormal oscillations are swamped by the relaxation process. This relaxation is the requirement of the black hole no–hair theorem [25]. Besides the dynamical mechanism of shedding the perturbation hair near black hole event horizon is of direct interest to the problem of stability of Cauchy horizons [26].

The mechanism responsible for the relaxation of neutral external perturbations was first exhibited by Price [27]. Studying the behavior of a massless scalar field propagating on a fixed Schwarzschild background, he showed that for a fixed position the field dies off with a power–law tail. The behavior of neutral perturbations along null infinity and future event horizon was further studied by Gundlach, Price and Pullin [28] and similar power–law tails have been obtained. These results were later confirmed using several different techniques, both analytic and numerical [29, 30, 31], and were generalized to *Reissner–Nordström* (RN) background [28, 32]. The application of linear approaches is encouraged by numerical analysis of the fully nonlinear dynamics of the fields [33, 34], which indicates the same late time pattern of decay.

Extending the basic scenario to study the asymptotic evolution of charged fields and self–interacting massive scalar field around a RN black hole, Hod and Piran [35, 36] found that although usual inverse power–law relations of these fields present at timelike infinity and null infinity, along the future black hole event horizon this power–law tail is accompanied by an oscillatory behavior. Recently, Brady et al. [37, 38] studied scalar wave dynamics in non–asymptotically flat exteriors of Schwarzschild–de Sitter and RN de Sitter black holes. Contrary to the asymptotically flat geometries, no power–law tails were detected in these cases. Instead the waves were found to decay exponentially at late times. For $l = 0$, they found that the field does not decay, but settles down to a nonzero constant. Moreover, for a field strongly coupled to curvature, they obtained that the wave function oscillates with an exponentially decaying amplitude. These observations support the earlier argument by Ching et al. [39] that usual inverse power–law tails as seen in asymptotically flat black hole spacetimes are not a general feature of wave propagation in curved spacetime. Besides some relation to the perturbative field, the relaxation process reflects a characteristic of the background geometry.

It is of interest to extend this study to *Anti–de Sitter* (AdS) spacetime. In addition to three major aspects that the evolution of test–field is associated with, including the no–hair theorem, the stability of Cauchy horizon and direct evidence of the existence of black hole provided by quasinormal ringing, the recent discovery of the *Anti–de Sitter/Conformal Field Theory* (AdS/CFT) correspondence makes the investigation in AdS black hole background more appealing. The quasinormal frequencies of AdS black hole have direct interpretation in terms of the dual *Conformal Field Theory* (CFT). In terms of the AdS/CFT correspondence [40, 41, 42], the black hole corresponds to an approximately thermal state in the field theory, and the decay of the test–field corresponds to the decay of the perturbation of the state. The first study of the scalar quasinormal modes in AdS space was performed by Horowitz and Hubeny [43] on the background of Schwarzschild AdS black holes in four, five and seven dimensions. They claimed that for large black holes both the real and imaginary parts of the quasinormal frequencies scale linearly with the black hole temperature. The time scale for approaching the thermal equilibrium is detected by the imaginary part of the lowest quasinormal frequency and is proportional to the inverse of the black hole temperature. Considering that the RN AdS solution provides a better framework than the Schwarzschild AdS geometry and may contribute significantly to our understanding of space and time, we generalized the study made in our previous work [89]. We found that the charge in RN AdS black hole showed a richer physics concerning quasinormal modes and further information on AdS/CFT correspondence. The bigger the black hole charge is, the quicker for their approach to thermal equilibrium in CFT. However these studies focused much on frequencies of the quasinormal modes, the object–picture of the evolution of test–field around the AdS background is lacking.

Now we are at the verge of opening a new window of information from the cosmos by means of the hopefully nearly coming discovery of gravitational waves [44]. The latter must be especially strong when emitted by black holes, thus the reason to further study field in such a background. Moreover, as it has been recently discovered, our universe is expanding with acceleration [45], possibly implying the existence of a small but non vanishing (and positive) cosmological constant [46]. The case of a negative cosmological constant (Anti de Sitter spacetime) has been discussed elsewhere [89, 48, 49].

According to the analysis of Leaver [50], after the initial burst of perturbation there are two main contributions to the resulting wave. First we find the so called quasinormal modes, and later the tails. The first can be understood as candidates to normal modes which however decay, the would be energy eigenstates becoming complex, in a mechanism first engenously described by G. Gamow in the content of nuclear physics [51] at the end, the wave describes properties more connected with the background space rather than the font itself. In the flat universes backgrounds the tails decay according to a power law, whereas in a space with a cosmological constant the decay is exponential. Solutions of the wave equation in a non trivial back ground has also been used to infer intrinsic properties of the spacetime [95].

On the other hand, the higher order WKB method proposed by Schutz and Will [96], and improved by Iyer and Will[97], provide an accurate and systematic means to study black hole quasinormal modes. In this work, we apply it to the study of various fields in a non-asymptotically flat geometry. We thus compute the quasinormal modes also according to this approximation, comparing the results whenever appropriate, what provides a quite complete picture of the question of quasinormal perturbations.

The results here cannot in general be obtained in analytic form, but describe reasonably the behaviour of waves scattered by the black hole solutions providing information about the caracteristics of the background. As examples, we provide the comparison between a numerical simulation and a semi analytic method in an Anti de Sitter black hole solution, and also between a numerical method and a WKB procedure for a de Sitter Black Hole solution.

Our intention here is to provide methods for dealing with perturbations of strong gravity solutions.

4 Scalar, Electromagnetic and Gravitational Perturbations

The metric describing a spherically black hole in the presence of a cosmological constant is well known in the literature. Written in spherical coordinates, the Schwarzschild-de Sitter metric is given by

$$ds^2 = -h(r)dt^2 + h(r)^{-1}dr^2 + r^2\left(d\theta^2 + \sin^2\theta d\phi^2\right) \ , \tag{1}$$

where the function $h(r)$ is

$$h(r) = 1 - \frac{2m}{r} - \frac{\Lambda r^2}{3} \ . \tag{2}$$

The integration constant m is the black hole mass, and if the cosmological constant is positive, the spacetime is asymptotically de Sitter. In this case, Λ is usually written in terms of a "cosmological radius" a as

$$\Lambda = \frac{3}{a^2} \ . \tag{3}$$

Assuming $m > 0$ and $\Lambda > 0$, the function $h(r)$ has three zeros r_+, r_c and r_n given by

$$r_+ = \frac{2}{\Lambda^{1/2}}\sin\left[\frac{1}{3}\sin^{-1}\left(3m\Lambda^{1/2}\right)\right] \ , \tag{4}$$

$$r_c = \frac{2}{\Lambda^{1/2}}\sin\left[\frac{1}{3}\sin^{-1}\left(3m\Lambda^{1/2}\right) + \frac{2\pi}{3}\right] \ , \tag{5}$$

$$r_n = -(r_+ + r_c) \ . \tag{6}$$

The constants m and a are related with the roots by

$$a^2 = r_+^2 + r_c^2 + r_+ r_c \ , \tag{7}$$

$$2ma^2 = r_+ r_c (r_+ + r_c) \ , \tag{8}$$

If $m^2\Lambda > 1$, there is no real positive zeros, and the metric (71) does not describe a black hole. If $m^2\Lambda = 1$, the zeros r_+ and r_c degenerate in a double root. This is the extreme SdS black hole. On the other hand, if $m^2\Lambda < 1$, then r_+ and r_c are real and positive. This is the Schwarzschild-de Sitter geometry, which we are interested.

More specifically, we will introduce scalar, electromagnetic and gravitational fields in the submanifold given by the block

$$T_+ = \{(t, r, \theta, \phi), r_+ < r < r_c\} \ . \tag{9}$$

In this region, we define the "tortoise" radial coordinate by

$$x(r) = \frac{1}{2\kappa_c}\ln(r_c - r) - \frac{1}{2\kappa_+}\ln(r - r_+) + \frac{1}{2\kappa_n}\ln(r - r_n) \ , \tag{10}$$

with

$$\kappa_i = \frac{1}{2}\left|\frac{dh(r)}{dr}\right|_{r=r_i} \ . \tag{11}$$

The constants κ_+ and κ_c are the surface gravity associated with the event and cosmological horizons.

For a scalar field Φ obeying the massless Klein-Gordon equation

$$\Box\Phi = 0 \ , \tag{12}$$

the usual separation of variables in terms of a radial field and a spherical harmonic $Y_{\ell,m}(\theta,\varphi)$, together with the tortoise coordinate leads to a Schrödinger-type equation. Indeed, expanding the field in spherical harmonics, in the form

$$\Phi = \sum_{\ell m} \frac{1}{r}\psi_\ell^{es}(t,r)Y_\ell(\theta,\phi) \ , \tag{13}$$

we get a decoupled wave equation for each value of ℓ. In terms of the coordinates t and x, this equation reads

$$-\frac{\partial^2\psi_\ell^{es}}{\partial t^2} + \frac{\partial^2\psi_\ell^{es}}{\partial x^2} = V^{es}(x)\psi_\ell \ , \tag{14}$$

with the effective potential V^{es} given by

$$V^{es}(r) = h(r)\left[\frac{\ell(\ell+1)}{r^2} + \frac{2m}{r^3} - \frac{2}{a^2}\right] \ . \tag{15}$$

In the non charged black hole geometry, it is possible to have pure electromagnetic and gravitational perturbations. In this case, the potential of the corresponding Schrödinger type equation is given [99] by the expression

$$V^{el}(r) = h(r)\frac{\ell(\ell+1)}{r^2} \ . \tag{16}$$

The perturbation theory for the exterior Schwarzschild-de Sitter geometry has been developed by [84, 87]. We consider

$$V^{ax}(r) = h(r)\left[\frac{\ell(\ell+1)}{r^2} - \frac{6m}{r^3}\right] \ , \tag{17}$$

$$V^{po}(r) = \frac{2h(r)}{r^3}\frac{9m^3 + 3c^2mr^2 + c^2(1+c)r^3 + 3m^2(3cr - \Lambda r^3)}{(3m+cr)^2} , \tag{18}$$

with $c = (\ell - 1)(\ell + 2)/2 = [\ell(\ell + 1) - 2]/2$.

For perturbations with $\ell > 0$, we can show explicitilly that the effective potentials $V(x) \equiv V(r(x))$ are positive definite. For scalar perturbations with $\ell = 0$, its effective potential has one zero point x_n, and it is negative for $x > x_n$.

5 Numerical and Semi-analytic Methods

5.1 Characteristc integration

In the pioneering work of Price [100] a very simple but at the same time very efficient way of dialing with two-dimensional d'Alembertians has been set up. The author introduced light-cone variables $u = t - x$ and $v = t + x$, in terms of which all the wave equations introduced have the same form. We call V the generic effective potential and ψ the generic field, and the equations can be written, in terms of the null coordinates, as

$$-4\frac{\partial^2}{\partial u \partial v}\psi(u,v) = V(r(u,v))\psi(u,v) . \tag{19}$$

In the characteristic initial value problem, initial data is specified on the two null surfaces $u = u_0$ and $v = v_0$. Since the basic aspects of the field decay are independent of the initial conditions, we begin with a Gaussian pulse on $u = u_0$ and set the field to zero on $v = v_0$,

$$\psi(u = u_0, v) = \exp\left[-\frac{(v - v_c)^2}{2\sigma^2}\right] , \tag{20}$$

$$\psi(u, v = v_0) = 0 . \tag{21}$$

Since in general we do not have analytic solutions to the time-dependent wave equation with the effective potentials introduced, one approach is to discretize the equation (19), and then implement a finite differencing scheme to solve it numerically. One possible discretization, used for example in [89, 105, 106], is

$$\begin{aligned}\psi(N) &= \psi(W) + \psi(E) - \psi(S) \\ &\quad - \Delta^2 V(S)\frac{\psi(W)+\psi(E)}{8} + \mathcal{O}(\cdot^{\triangle})\ ,\end{aligned} \tag{22}$$

where we have used the definitions for the points: $N = (u+\Delta, v+\Delta)$, $W = (u+\Delta, v)$, $E = (u, v+\Delta)$, $S = (u, v)$ and $S = (u+\Delta/2, v+\Delta/2)$. With the use of expression (22), the basic algorithm will cover the region of interest in the $u-v$ plane, using the value of the field at three points in order to calculate it at a forth one.

After the integration is completed, the values $\psi_l(u_{max}, v)$ and $\psi_l(u, v_{max})$ are extracted, where u_{max} (v_{max}) is the maximum value of u (v) on the numerical grid. Taking sufficiently large u_{max} and v_{max}, we have good approximations for the wave function at the event and cosmological horizons.

5.2 Non-characteristc integration

It is not difficult to set up a numeric algorithm to solve equation (14) with Cauchy data specified on $t = t_0$ surface. We used 4^{th} order in x and 2^{nd} in t scheme[**?**]. The second spatial derivative at a point (t, x) is given by

$$\psi''(t,x) = \frac{\psi(t,x+2dx) - 16\psi(t,x+dx) + 30\psi(t,x) - 16\psi(t,x-dx) + \psi(t,x-2dx)}{12dx^2}, \tag{23}$$

while the second time derivative is

$$\ddot{\psi}(t,x) = \frac{\psi(t+dt,x) - 2\psi(t,x) + \psi(t-dt,x)}{dt^2}. \tag{24}$$

Given $\psi(t = t_0, x)$ and $\psi = (t = t_0 - dt, x)$ (or $\dot{\psi}(t = t_0, x)$), we can use (23) and (24) discretization to solve (14) and calculate $\psi(t = t_0 + dt, x)$. This is the basic algorithm. At each interaction, one can control the error by using the invariant integral (the wave energy) associate to (14)

$$E = \frac{1}{2}\int \left(\left(\psi'(t,x)\right)^2 + \left(\dot{\psi}(t,x)\right)^2 + V\psi(t,x)^2 \right)\, dx. \tag{25}$$

We make exhaustive analysis of the asymptotic behavior of the solutions of (14) with quite general initial conditions of the form

$$\begin{aligned}
\psi(0,x) &= C_0 \exp\left[-\frac{(x-x_0)^2}{2\sigma_0^2}\right], \\
\dot{\psi}(0,x) &= C_1 \exp\left[-\frac{(x-x_1)^2}{2\sigma_1^2}\right].
\end{aligned} \tag{26}$$

The results, that indeed do not depend on the details of initial conditions, are compatible with the ones obtained by the usual characteristic integration. As we will see, $\dot{\psi}(0,x)$ determines the asymptotic value for the $\ell=0$ modes of scalar fields.

5.3 WKB analysis

Let us consider now the time-independent version of the problem, Laplace transforming the wave equations (12), or equivalently an expression of the type (14), such that the problem can be rewritten as a Cauchy initial value problem. The ordinary differential equations obtained have the form

$$\frac{d^2\psi(x)}{dx^2} - \left[s^2 + V(x)\right]\psi(x) = 0 \ . \tag{27}$$

One thus finds that there is a discrete set of possible values to s such that the function $\hat{\psi}_\ell$, the Laplace transformed field, satisfies both boundary conditions,

$$\lim_{x\to-\infty} \hat{\psi}_\ell\, e^{sx} = 1 \ , \tag{28}$$

$$\lim_{x\to+\infty} \hat{\psi}_\ell\, e^{-sx} = 1 \ . \tag{29}$$

By making the formal replacement $s = i\omega$, we have the usual quasinormal mode boundary conditions. The frequencies ω (or s) are called quasinormal frequencies.

We will use in this work a high order WKB approximation scheme introduced by Schutz and Will [96], and later improved by Iyer and Will [97]. It is a very efficient algorithm to calculate the quasinormal frequencies, which have been applied in a variety of situations [98]. With this method, the quasinormal modes are given by

$$\omega_n = (V_0 + P) - i\left(n + \frac{1}{2}\right)\left(-2V_0^{(2)}\right)^{1/2}(1+Q) \tag{30}$$

where the quantities P and Q are determined using

$$P = \frac{1}{8}\left[\frac{V_0^{(4)}}{V_0^{(2)}}\right]\left(\frac{1}{4}+\alpha^2\right) - \frac{1}{288}\left[\frac{V_0^{(3)}}{V_0^{(2)}}\right]^2\left(7+60\alpha^2\right) , \tag{31}$$

$$\begin{aligned} Q \;=\; & \frac{1}{-2V_0^{(2)}}\left\{\frac{5}{6912}\left[\frac{V_0^{(3)}}{V_0^{(2)}}\right]^4\left(77+188\alpha^2\right) - \frac{1}{384}\left[\frac{V_0^{(3)2}V_0^{(4)}}{V_0^{(2)}}\right]\left(51+100\alpha^2\right)\right. \\ & + \frac{1}{2304}\left[\frac{V_0^{(4)}}{V_0^{(2)}}\right]^2\left(67+68\alpha^2\right) + \frac{1}{288}\left[\frac{V_0^{(3)}V_0^{(5)}}{V_0^{(2)2}}\right]\left(19+28\alpha^2\right) \\ & \left. - \frac{1}{288}\left[\frac{V_0^{(6)}}{V_0^{(2)}}\right]\left(5+4\alpha^2\right)\right\} \end{aligned} \tag{32}$$

In the equations (30) to (32) $\alpha = n + 1/2$ and the superscript (n) denote differentiation with respect to x of the potential $V(x)$. The potential and its derivatives are then calculated in the point $x(r_0$, where $V(x)$ is an extremum. The integer n labels the modes

$$\begin{aligned} n \;=\; & 0, 1, 2, \ldots \mathrm{Re}(\omega) > 0 , \\ & -1, -2, -3, \ldots \mathrm{Re}(\omega) < 0 . \end{aligned}$$

6 Intermediary Region in Parameter Space

6.1 Scalar Fields with $\ell = 0$

In the zero angular momentum sector, we only have the possibility of scalar fields. Solutions of ( ) for $\ell = 0$ leads to a constant tail, as already shown in [105]. This is confirmed in figure (). The novelty here is the dependence of the asymptotic value on the $\dot{\psi}(0, x)$ initial condition. Figure n reveals the appearance of the constant value ϕ_0 for large t, and its dependence on $\dot{\psi}(0, x)$. Note that ϕ_0 falls below 10^{-7} for $\dot{\psi}(0, x) = 0$.

6.2 Fields with $\ell > 0$

We can have scalar and vector fields with angular momentum $\ell = 1$, and with $\ell > 1$, it is possible to introduce also gravitational fields. Their behavior is described in general by three phases. The first, related to the black hole itself, corresponds to the quasinormal modes generated from the presence of the black hole itself. A little later there is a region of posses law decay, which continues indefinitely in a flat space. In the presence of a cosmological constant an exponential decay takes over in the latest period. There is not constant (or growing) mode.

Some qualitative different effects show up when we turn away from the quasi extreme limit. For a small cosmological constant the asymptotic behavior is dominated by an exponential decaying mode rather than by a quasinormal mode. Such exponential decays will characterize the de Sitter space in general. We will later comment about the pure de Sitter limit, which is exactly solvable, though we do not have definite answers about the respective behavior. The exponential decay also characterizes the electromagnetic as well as the gravitational perturbations.

As the separation of the horizons increases, the quasinormal frequencies deviate from the predicted by expressions (**??**) and (**??**). In figure 1, this is illustrated for $\ell = 1, 2$.

It is interesting to compare the values obtained for the fundamental modes using the numerical and semi-analytic methods. We find that the agreement between then is good, for the hole range of Λ. The difference is better for the first values of ℓ. This is expected, since the numerical calculations are better in this region. In the table 1, we illustrate these observations with a few values of Λ. It is important to mention that quasinormal frequencies for the SdS black hole were already calculated in a recent paper [103], applying a variation of the WKB method used here [104].

Higher modes cannot be obtained from the numerical solution, but can be calculated by the semi-analytical method. As the cosmological constant decreases, the real and imaginary parts of the frequencies increase, up to the limit where the geometry is asymptotically flat. The behavior of the modes is illustrated in figure 2. The behavior of the electromagnetic field is similar.

Figure 3 shows that the massless scalar, electromagnetic and gravitational perturbations in SdS geometry behave as

$$\psi_\ell^{es} \sim e^{-k_{exp}^{es} t} \quad \text{com} \quad t \to \infty \tag{33}$$

$$\psi_\ell^{el} \sim e^{-k_{exp}^{el} t} \quad \text{com} \quad t \to \infty \tag{34}$$

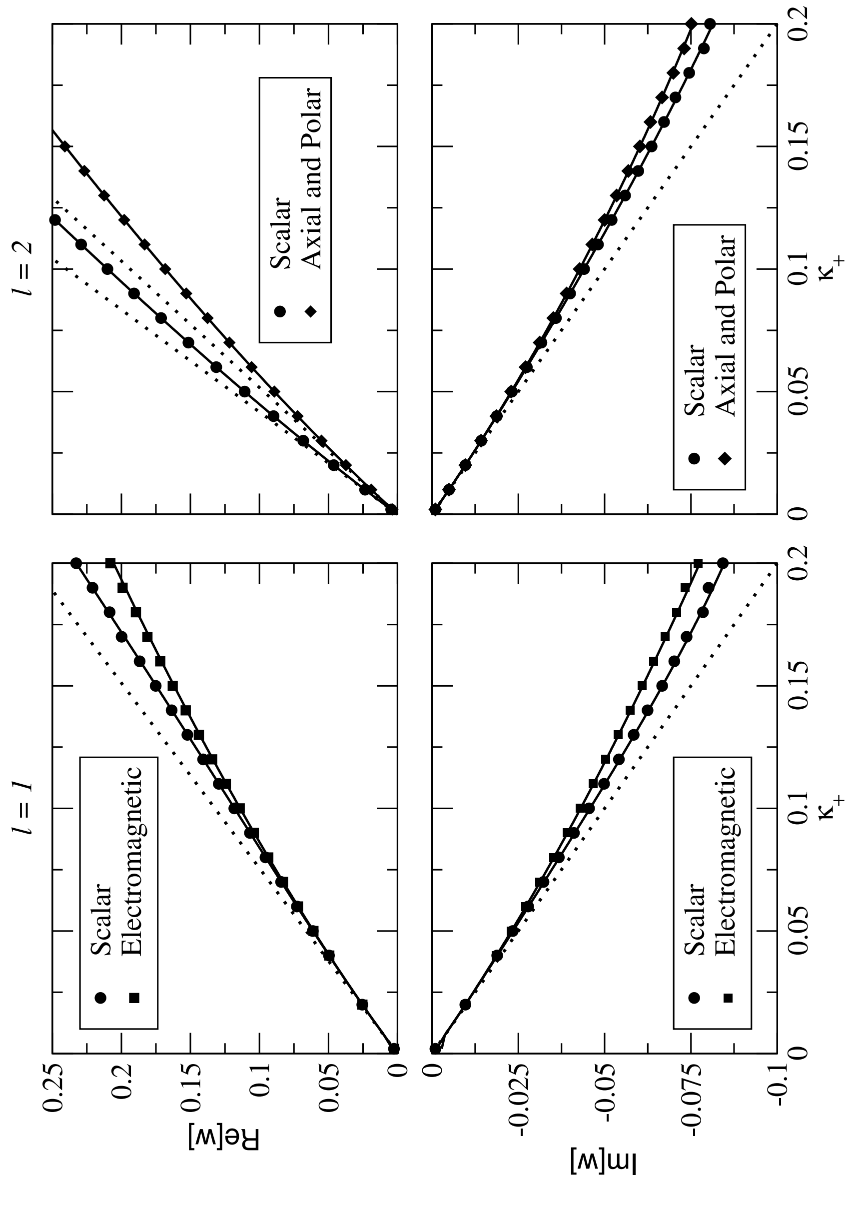

Figure 1: *Graph of the real and imaginary part of the fundamental frequencies* $(n = 0)$ *with* κ_+. *The dotted lines are the near extreme results, the symbols are the numerical results and the continuous curves are the semi-analytic results.*

		Numerical		Semi-analytical	
ℓ	Λ	Re(ω)	-Im(ω)	Re(ω)	-Im(ω)
1	1.000E-5	2.930E-01	9.753E-01	2.911E-01	9.780E-02
	1.000E-4	2.928E-01	9.764E-02	2.910E-01	9.797E-02
	1.000E-3	2.914E-01	9.726E-02	2.896E-01	9.771E-02
	1.000E-2	2.770E-01	9.455E-02	2.753E-01	9.490E-02
	1.000E-1	8.159E-02	3.123E-02	8.144E-02	3.137E-02
2	1.000E-5	4.840E-01	9.653E-02	4.832E-01	9.680E-02
	1.000E-4	4.833E-01	8.948E-02	4.830E-01	9.677E-02
	1.000E-3	4.816E-01	8.998E-02	4.809E-01	9.643E-02
	1.000E-2	4.598E-01	8.880E-02	4.592E-01	9.290E-02
	1.000E-1	1.466E-01	3.068E-02	1.466E-01	3.070E-02
3	1.000E-5	6.769E-01	8.662E-02	6.752E-01	9.651E-02
	1.000E-4	6.754E-01	8.654E-02	6.749E-01	9.647E-02
	1.000E-3	6.732E-01	8.660E-02	6.720E-01	9.611E-02
	1.000E-2	6.437E-02	9.200E-02	6.428E-02	9.235E-02
	1.000E-1	2.091E-02	3.054E-02	2.091E-02	3.056E-02

Table 1: *Fundamental frequency ($n = 0$) of the scalar field, obtained using the numerical and semi-analytical methods.*

		Numerical		Semi-analytical	
ℓ	Λ	Re(ω)	-Im(ω)	Re(ω)	-Im(ω)
1	1.000E-5	2.481E-01	9.226E-02	2.459E-01	9.310E-02
	1.000E-4	2.481E-01	9.223E-02	2.457E-01	9.307E-02
	1.000E-3	2.475E-01	9.176E-02	2.448E-01	9.270E-02
	1.000E-2	2.374E-01	8.839E-02	2.352E-01	8.896E-02
	1.000E-1	8.035E-02	3.027E-02	8.023E-02	3.033E-02
2	1.000E-5	4.577E-01	8.985E-02	4.571E-01	9.506E-02
	1.000E-4	4.575E-01	8.991E-02	4.569E-01	9.502E-02
	1.000E-3	4.559E-01	9.439E-02	4.551E-01	9.464E-02
	1.000E-2	4.371E-01	8.941E-02	4.364E-01	9.074E-02
	1.000E-1	1.458E-01	3.037E-02	1.458E-01	3.038E-02
3	1.000E-5	6.578E-01	8.365E-02	6.567E-01	9.563E-02
	1.000E-4	6.576E-01	8.349E-02	6.564E-01	9.559E-02
	1.000E-3	6.547E-01	8.399E-02	6.538E-01	9.520E-02
	1.000E-2	6.276E-02	8.852E-02	6.267E-01	9.125E-02
	1.000E-1	2.085E-02	3.039E-03	2.085E-01	3.040E-02

Table 2: *Fundamental frequency ($n = 0$) of the electromagnetic field, obtained using the numerical and semi-analytical methods.*

		Numerical		Semi-analytical	
ℓ	Λ	Re(ω)	-Im(ω)	Re(ω)	-Im(ω)
2	1.000E-5	3.738E-01	8.883E-02	3.731E-01	8.921E-02
	1.000E-4	3.737E-01	8.880E-02	3.730E-01	8.918E-02
	1.000E-3	3.721E-01	8.850E-02	3.715E-01	8.888E-02
	1.000E-2	3.566E-01	8.538E-02	3.560E-01	8.572E-02
	1.000E-1	1.179E-01	3.020E-02	1.179E-01	3.023E-02
3	1.000E-5	5.999E-01	8.677E-02	5.992E-01	9.272E-02
	1.000E-4	5.996E-01	8.676E-02	5.990E-01	9.269E-02
	1.000E-3	5.972E-01	8.971E-02	5.966E-01	9.234E-02
	1.000E-2	5.725E-01	8.695E-02	5.718E-01	8.874E-02
	1.000E-1	1.900E-01	3.030E-02	1.900E-02	3.032E-02
4	1.000E-5	8.106E-01	8.810E-02	8.091E-01	9.417E-02
	1.000E-4	8.102E-01	8.781E-02	8.087E-01	9.413E-02
	1.000E-3	8.070E-01	8.799E-02	8.055E-01	9.376E-02
	1.000E-2	7.733E-02	8.714E-02	7.720E-01	9.000E-02
	1.000E-1	2.564E-02	3.034E-03	2.563E-01	3.036E-02

Table 3: *Fundamental frequency ($n = 0$) of the axial and polar gravitational fields, obtained using the numerical and semi-analytical methods.*

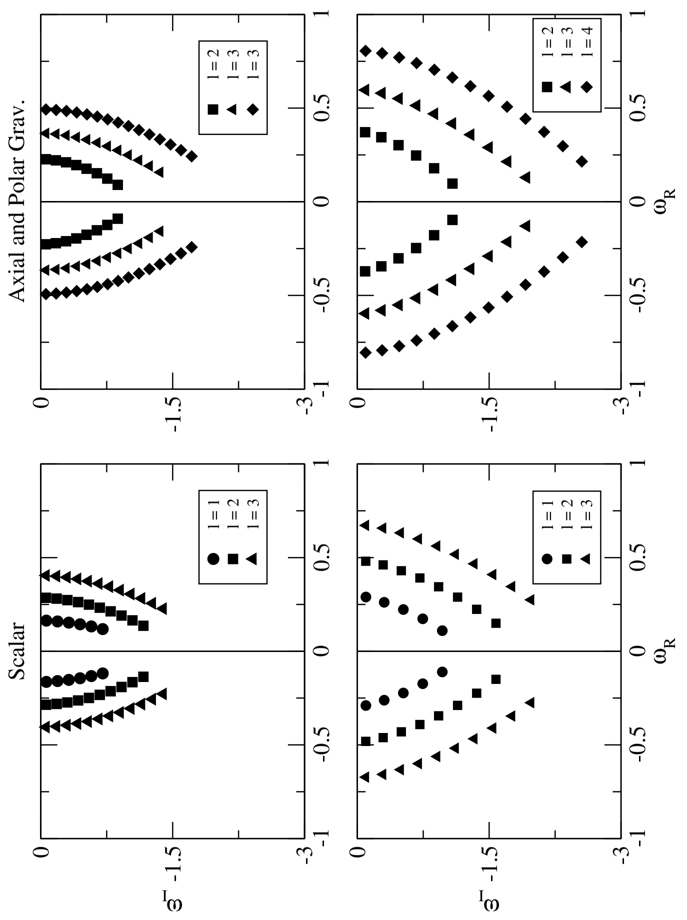

Figure 2: *Quasinormal modes of the scalar, axial and polar gravitational fields, for higher modes.*

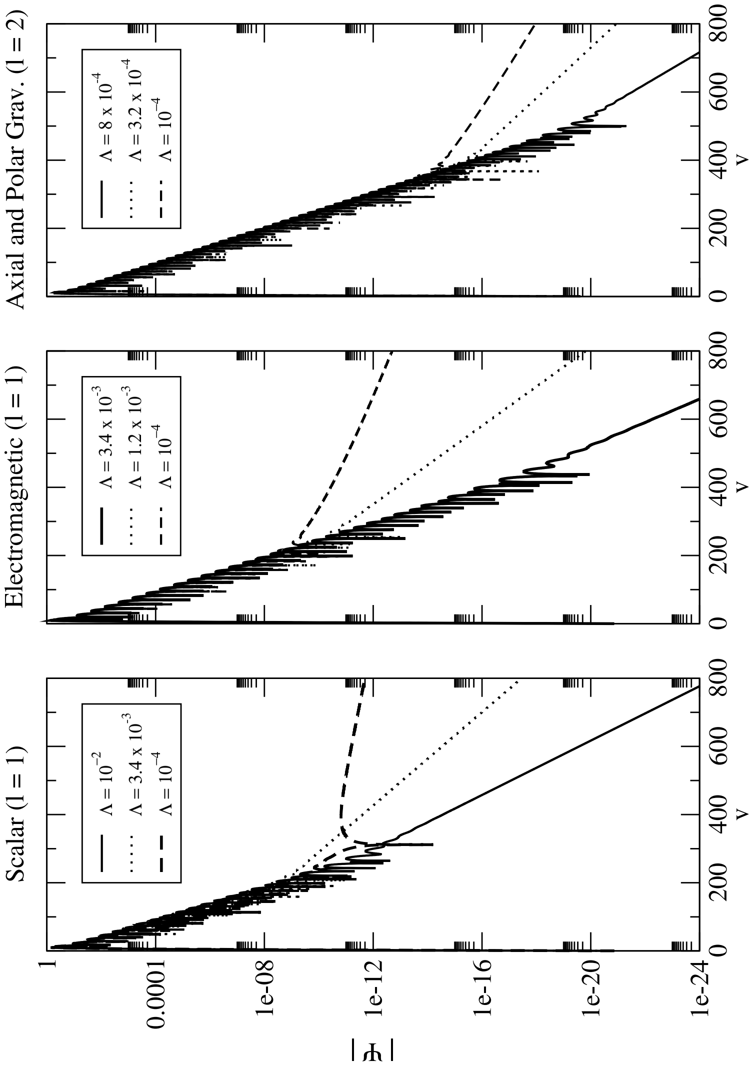

Figure 3: *Exponential tail for the scalar and electromagnetic fields with $\ell = 1$, and for the axial and polar gravitational field with $\ell = 2$.*

$$\psi_\ell^{ax} \sim e^{-k_{exp}^{ax} t} \quad \text{com} \quad t \to \infty \tag{35}$$

$$\psi_\ell^{po} \sim e^{-k_{exp}^{po} t} \quad \text{com} \quad t \to \infty \tag{36}$$

for t sufficiently large. At the event and the cosmological horizons t is substituted, respectively by v and u.

The numerical simulations developed in the present work reveal an interesting transition between oscillatory modes and exponentially decaying modes. As shown in figure (4), as the cosmological constant decreases, the absolute value of $-\mathrm{Im}(\omega)$ decreases as well.

Up to a certain critical value of Λ we do not observe the exponential tail, since the coefficient k_{exp} is larger than $-\mathrm{Im}(\omega)$ thus the decaying quasinormal mode dominates. But for Λ smaller than this critical value, $-\mathrm{Im}(\omega)$ turns out to be larger than k_{exp} and the exponential tail dominates. Certainly, for a small enough cosmological constant the exponential tail dominates in the various cases considered here.

Another aspect worth mentioning in the intermediate region is the dependence of the parameters k_{exp}^{es}, k_{exp}^{el}, k_{exp}^{ax} and k_{exp}^{po} with ℓ and κ_c. The results suggest that the k_{exp} are at least second differentiable functions of κ_c. Therefore, close to $\kappa_c = 0$, we approximate

$$k_{exp}^{es}(\kappa_c) \approx \ell \left(\kappa_c + c^{es}\kappa_c^2\right) \tag{37}$$

$$k_{exp}^{el}(\kappa_c) \approx k_{exp}^{ax}(\kappa_c) \approx k_{exp}^{po}(\kappa_c) \approx (\ell+1) \left(\kappa_c + c^{e-g}\kappa_c^2\right) \tag{38}$$

Previous results are illustrated in figure 5.

6.3 Perturbations of Early Universe and Relics of Inflation

Not very much is known from the early universe prior to nucleosynthesis. However, from the experimental fact that the Cosmic Microwave Background is homogeneous to one part in a hundred thousand, a fact that is not statistically expected, and further caracteristics of the universe as e.g. absence of magnetic monopoles and flatness, one generally believes that before nucleosynthesis the universe underwent an epoch of high inflation, that is, an era when the universe was filled with basically nothing but a scalar field,

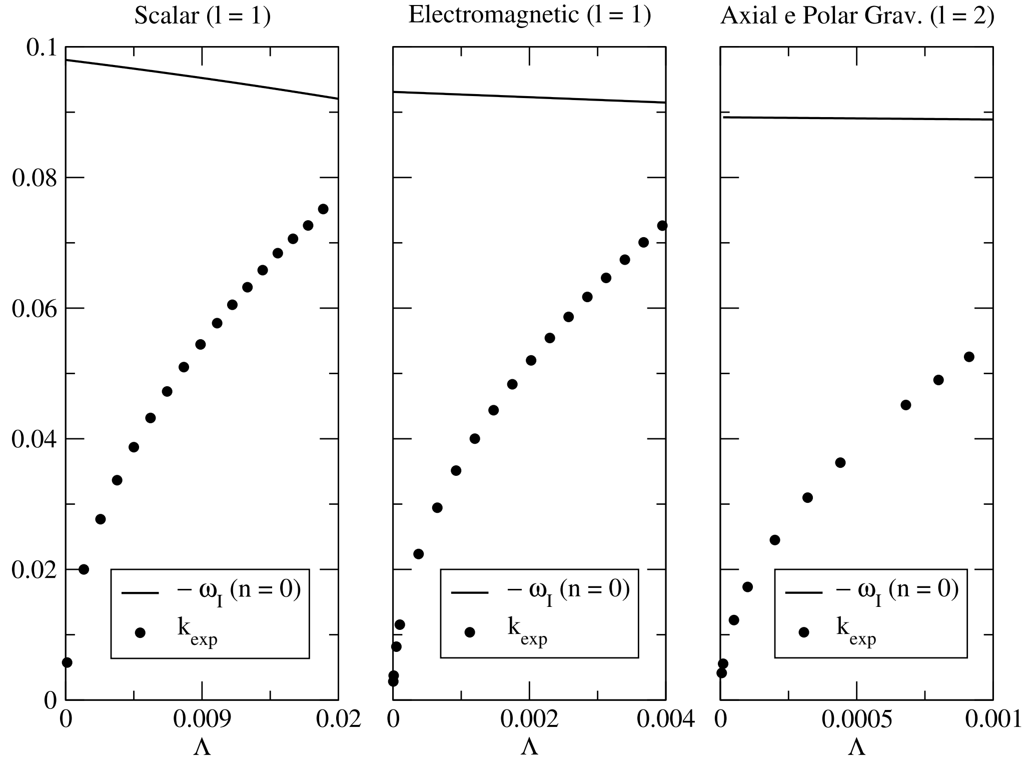

Figure 4: *Approaching of the constants $-Im(\omega)$ (fundamental mode) and k_{exp}, for the scalar, electromagnetic and gravitational fields.*

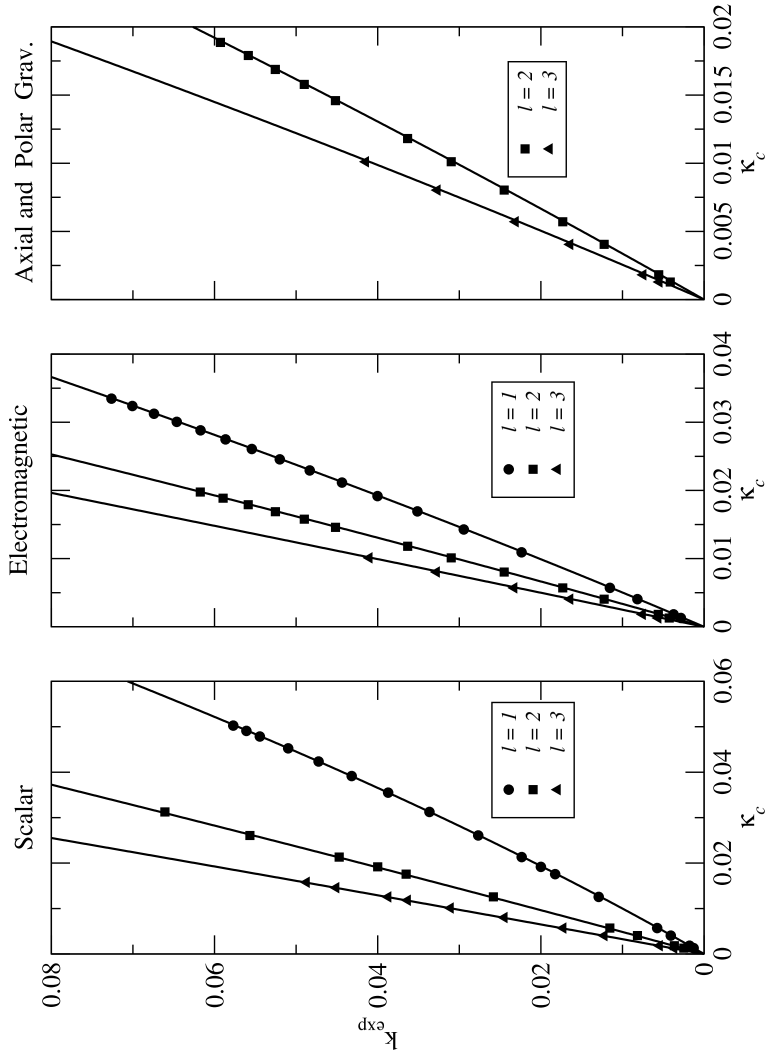

Figure 5: *Dependence of the coefficient k_{exp} with κ_c and ℓ. The symbols indicate the estimated numerical values. The solid lines are the appropriate quadratic fittings.*

dominating the energy density, and which drove a very strong expansion, increasing the overall sizes by at least fifty orders of magnitude.

The observational likeliness of the inflationary scenario has been deepened by the COBE/WMAP experiments. However, very little is known about a possible derivation of inflation from first principles. On the other hand, we have a very arid theory in search of experimental support, namely string theory. It is very desirable that both can find a meeting point, what would be a new era in the physics of fundamental objects.

The main calculations in inflationary models concern the density perturbations, or else its Fourier components $\delta_{\vec{k}}$. Its modulus squared, $|\delta_{\vec{k}}|^2$ defines the power spectrum, $\mathcal{P}(\vec{k})$, which is the main experimental data available from the CMB results.

Main Results from Standard Inflationary Models

Inflationary models are a cornesrtone for the understanding of the origin and evolution of large scale structure, of the large scale isotropy of the Microwave Background radiation and of the flatness of the universe. It is not our aim to give a full account of the developments, which by itself is of a very large extension, and has been covered by books and various extensive reviews [60] [56].

Some facts that are under study are the main points we need from the whole amount of information. First we describe the universe in terms of an unperturbed Friedmann equation, derived from a perfect fluid of the form

$$T^{\mu\nu} = pg^{\mu\nu} + (\rho + p)u^\mu u^\nu \tag{39}$$

where ρ is the energy density, p the pressure and u^μ the fluid four-velocity. With the choice $u^\mu = \delta_0^\mu$ the metric is given by

$$ds^2 = dt^2 - a^2(t)\delta_{ij}dxdx^j \quad . \tag{40}$$

There is a set of independent modes of perturbations of these fields. There are perturbations of the density, pressure and velocity fields, as well as pure perturbations of the metric, generating gravitational waves.

In particular, Friedmann equation, usually written as

$$H^2 = \frac{8\pi G}{3}\rho - \frac{K}{a^2} \tag{41}$$

where $H = \frac{\dot{a}}{a}$ is the Hubble constant, and K a constant describing the curvature, is perturbed, leading to functions $\delta\rho$, δK describing the observed inhomogeneities. The spectrum pf perturbations is obtained, from the observational side, from the COBE/WMAP satelites describing the Cosmic Microwave Background.

From the theoretical side, the large scale quasi-homogeneity of the universe is predicted by inflation. As described initially by Guth [61], inflation is driven by a scalar field coupled to gravity, the inflaton field, contributing to the energy density and pressure as

$$\begin{aligned} \rho &= \frac{1}{2}\dot{\varphi}^2 + V(\varphi) \\ p &= \frac{1}{2}\dot{\varphi}^2 - V(\varphi) \quad , \end{aligned}$$

where $V(\varphi)$ is a potential for the inflaton. The inflaton field equation is

$$\ddot{\varphi} + 3H\dot{\varphi} + V'(\varphi) = 0 \quad . \tag{42}$$

Inflation is a phenomenon where the scale factor increses very fast, as *e. g.* exponentially, in which case we can consider the the potential is almost constant, and the kinetic energy is very small, giving rise to an effective cosmological constant, and a de Sitter like expantion. In such a slow roll approximation we define the very usefull parameters

$$\begin{aligned} \epsilon &= \\ \eta &= \\ \zeta &= \end{aligned}$$

The slow roll approximation means that these parameters are very small, that is, we neglect the second derivative of φ in 42 obtaining

$$\dot{\varphi} \approx -\frac{1}{3H}V' \quad . \tag{43}$$

An observationally important parameter describes the deviation from scale invariance of the density perturbation, that is,

$$\delta^2 \approx k^{n-1} \quad \Rightarrow n - 1 = \frac{d\ln\delta^2}{d\ln k} \quad . \tag{44}$$

In terms of the slow roll parameters

$$n = 1 + 2\eta - 6\epsilon \quad . \tag{45}$$

Observations give n near unit, somewhat larger than one at large scales, and smaller at small scales.

7 The junction conditions

The formulation of proper junction conditions at surfaces of discontinuity is a fundamental problem in gravitational theory. Well-known examples are the Schwarzschild and Oppenheimer-Snyder problems, which require the junction of the interior field of a static or collapsing star to the exterior vacuum field.

In newtonian theory the problem is directly solved by imposing the standard continuity and jump conditions connecting the potential and its first derivatives across the surface. In general relativity, however, the gravitational potential is not only determined by the smoothness of physical conditions but also by the smoothness of the coordinates we are using to describe spacetime.

A pioneering work on these subjects was made in 1922 by C. Lanczos [64], on which W. Israel [65] based his landmark formalism forty years later. Independent of these works, G. Darmois [66] derived junction conditions for the special case of a boundary surface, i.e. a surface through which both the metric and the extrinsic curvature tensor are continuous. All these ideas are now known as the Darmois-Israel junction/thin-shell formalism, which has found wide application in general relativity and cosmology, including further studies of gravitational collapse, the evolution of bubbles and domain walls in a cosmological setting, wormholes and more recently in brane cosmology.

In this section we review the junction formalism as it was first derived by Israel. We also derive the Darmois-Israel conditions from the gravitational action in the context of D-dimensional theories and give an alternative approach using distribution theory.

7.1 The Formalism

Consider a spacetime M (riemannian manifold with signature $(-+++)$) with metric $g_{\alpha\beta}(x^\gamma)$ in the coordinate system (x^γ). The absolute derivative of a smooth vector function **A** defined on a curve on this spacetime parametrized by t is given by

$$\nabla_t A^\alpha \equiv \frac{\partial A^\alpha}{\partial t} + A^\lambda \Gamma^\alpha_{\lambda\mu} \frac{dx^\mu}{dt} \,. \tag{46}$$

Let Σ be a smooth hypersurface in M with metric $g_{ij}(\xi^c)$ in the coordinates ξ^c, which separates M into two four-dimensional manifolds M^- and M^+, each containing Σ as part of its boundary.

The unit 4-normal $\mathbf{n}$ to this hypersurface in M labels Σ as timelike (spacelike) for $\epsilon(\mathbf{n}) \equiv \mathbf{n}\,.\,\mathbf{n} = -1\,(1)$.

We define a natural frame of three linearly independent tangent vectors $e^\alpha_{(i)}$ associated with the intrinsic coordinates ξ^i as

$$e^\alpha_{(i)} = \frac{\partial x^\alpha}{\partial \xi^i} \,, \tag{47}$$

which gives the induced metric on Σ as

$$g_{ij} \equiv \mathbf{e}_{(i)}\,.\,\mathbf{e}_{(j)} = \frac{\partial x^\alpha}{\partial \xi^i}\frac{\partial x^\beta}{\partial \xi^j} g_{\alpha\beta} \,. \tag{48}$$

The intrinsic covariant derivative of **A** with respect to ξ^i is the projection of the vector $\partial \mathbf{A}/\partial \xi^j$ onto Σ,

$$A_{i;j} = \mathbf{e}_{(i)} \cdot \frac{\partial \mathbf{A}}{\partial \xi^j} = \frac{\partial A}{\partial \xi^j} - A_h \Gamma^h_{ij} \,. \tag{49}$$

We see that intrinsic covariant differentiation does not depend on the nature of the embedding. Properties of a non-intrinsic character enter when we consider the way in which Σ "bends" in M. This is measured by the variations $\partial \mathbf{n}/\partial \xi^i$ of the unit normal,

$$\partial \mathbf{n}/\partial \xi^i = K^j_i \mathbf{e}_{(j)} \,, \tag{50}$$

what defines the *extrinsic curvature 3-tensor* K_{ij} of Σ,

$$K_{ij} = e_{(j)} \cdot \frac{\partial \mathbf{n}}{\partial \xi^i} \equiv \frac{\partial x^\alpha}{\partial \xi^i}\frac{\partial x^\beta}{\partial \xi^j} \nabla_\alpha n_\beta = -n_\gamma \left(\frac{\partial^2 x^\gamma}{\partial \xi^i \partial \xi^j} + \Gamma^\gamma_{\alpha\beta} \frac{\partial x^\alpha}{\partial \xi^i}\frac{\partial x^\beta}{\partial \xi^j} \right) \,. \tag{51}$$

Let K^-_{ij}, K^+_{ij} be the extrinsic curvatures of Σ associated with its embeddings in M^-, M^+. If $K^-_{ij} \neq K^+_{ij}$, Σ is called a singular hypersurface of order one, *surface layer* or *thin shell*. If $K^-_{ij} = K^+_{ij}$, Σ is called a hypersurface of higher order or *boundary surface*.

The Darmois conditions for the joining of M^- and M^+ through Σ are [66]

$$[g_{ij}] = 0\,, \tag{52}$$
$$[K_{ij}] = 0\,, \tag{53}$$

where $[X] = X^+ - X^-$ is the jump of X through the hypersurface Σ.

A boundary surface satisfies both equations, while a thin shell only satisfies (52). Condition (53) as it stands is ambiguous since the orientation of the 4-vector field $\mathbf{n}$ has not been specified. The Israel formalism will require the normals in M to point from M^- to M^+. We should stress that the majority of the existing literature deals with spherical symmetry where the direction of the normal is clear, but in more complicated cases great care must be taken.

The Israel formulation [65] of thin shells follows from the Lanczos equation [64]

$$[K_{ij}] - g_{ij}[K^a_a] = -8\pi G S_{ij}\,, \tag{54}$$

or equivalently

$$[K_{ij}] = -8\pi G(S_{ij} - \frac{1}{2}g_{ij}S)\,, \tag{55}$$

where S_{ij} is the surface stress-energy tensor of Σ.

By regarding a thin shell as the limit of a layer of uniform finite thickness ϵ as $\epsilon \to 0$, we can give a heuristic justification for the name *surface stress-energy tensor*.

Let Σ^-, Σ^+ be the two boundary surfaces separating the finite layer from the regions M^-, M^+. In gaussian coordinates the equations of Σ^- and Σ^+ are $x^1 = 0$, $x^1 = \epsilon$.

In terms of the extrinsic curvature tensor and in the gaussian system of coordinates the Ricci tensor can be written as

$$^4R_{ij} = \frac{\partial K_{ij}}{\partial x^1} + Z_{ij}\,, \tag{56}$$

where

$$Z_{ij} = {}^3R_{ij} - KK_{ij} + 2K^p_i K_{pj}\,. \tag{57}$$

Integration of the Einstein field equations

$$R_{\alpha\beta} = -8\pi G(T_{\alpha\beta} - \frac{1}{2}g_{\alpha\beta}T)\,, \tag{58}$$

through the layer gives

$$-8\pi G\int_0^\epsilon (T_{ij} - \frac{1}{2}g_{ij}T)dx^1 = [K_{ij}] + \int_0^\epsilon Z_{ij}dx^1\,. \tag{59}$$

In the limit $\epsilon \to 0$ for fixed K^-_{ij}, K^+_{ij}, K_{ij} remains bounded inside the layer. Hence, the integral of Z_{ij} tends to zero. Comparing this result with (55) we see that

$$S_{ij} = \lim_{\epsilon\to 0}\int_0^\epsilon T_{ij}dx^1\,. \tag{60}$$

Thus, S_{ij} is the integral of Einstein's energy tensor through the thickness of the layer.

7.2 Matching Conditions from the Action

We will consider now the problem of junction conditions in the context of D-dimensional theories [71]. In order to do this we will introduce the concept of *domain wall*. In a D-dimensional spacetime a domain wall can be defined as an extended object with $D-2$ spatial dimensions, which divides the spacetime in different domains. Here we will use this term to make reference to any $D-2$ brane moving in D dimensions.

Let M be a D-dimensional manifold containing a domain wall Σ, which splits M into two parts M^- and M^+. The metric must be continuous everywhere, while its derivatives must be continuous everywhere except on Σ. We will denote $\Sigma^\pm$ as being the two sides of Σ.

Varying the Einstein-Hilbert action in $M^\pm$ gives [1]

$$\delta S_{EH} = -\frac{1}{2}\int_{\Sigma^\pm} d^{D-1}x\sqrt{-h}\, g^{MN}n^P(\nabla_M\delta g_{NP} - \nabla_P\delta g_{MN})\,, \tag{61}$$

where n_M is the unit normal pointing into $M^\pm$ and the induced metric on $\Sigma^\pm$ is given by the tangential components of the projection tensor $h_{MN} = g_{MN} - n_Mn_N$. If we contract the quantity in parenthesis with $n^Mn^Nn^P$, it vanishes, so we can replace g^{MN} by h^{MN}.

[1] For convenience we use units such that $8\pi G = 1$

The expression (61) contains a normal derivative of the metric variation, which is discontinuous across Σ according to our initial hypothesis, so the contributions from $M^{\pm}$ will not necessarily cancel out. In this way, it is necessary to add a Gibbons-Hawking boundary term [68] on each side of the domain wall to cancel out this term,

$$S_{GH} = -\int_{\Sigma^{\pm}} d^{D-1}x\sqrt{-h}\, K \,, \tag{62}$$

with K being the trace of the extrinsic curvature of Σ, *i.e.* $K = h^{MN}K_{MN}$ where $K_{MN} = h^P_M h^Q_N \nabla_P n_Q$.

The variation of this new term is

$$\delta S_{GH} = -\int_{\Sigma^{\pm}} d^{D-1}x\sqrt{-h}\,(\delta K + \frac{1}{2}K h^{MN}\delta g_{MN})\,, \tag{63}$$

where

$$\delta K = -K^{MN}\delta g_{MN} - h^{MN}n^P(\nabla_M \delta g_{NP} - \frac{1}{2}\nabla_P \delta g_{MN}) + \frac{1}{2}K n^P n^Q \delta g_{PQ}\,. \tag{64}$$

Thus, the total variation is

$$\begin{aligned} \delta S_{EH} + \delta S_{GH} &= \int_{\Sigma^{\pm}} d^{D-1}x\sqrt{-h}\,\left[\frac{1}{2}h^{MN}n^P\nabla_M\delta g_{NP} + K^{MN}\delta g_{MN} - \right. \\ &\left. -\frac{1}{2}K n^M n^N \delta g_{MN} - \frac{1}{2}K h^{MN}\delta g_{MN}\right]\,. \end{aligned} \tag{65}$$

Notice that the first term in the rhs of (65) can be written as

$$h^{MN}n^P\nabla_M\delta g_{NP} = \bar{\nabla}_M(h^{MN}n^P\delta g_{NP}) + K n^M n^N \delta g_{MN} - K^{MN}\delta g_{MN}\,, \tag{66}$$

where $\bar{\nabla}$ is the covariant derivative associated to h. Then, we substitute this last result into (65) to get

$$\delta S_{EH} + \delta_{GH} = \frac{1}{2}\int_{\Sigma^{\pm}} d^{D-1}x\sqrt{-h}\,(K^{MN} - K h^{MN})\delta g_{MN}\,. \tag{67}$$

If the domain wall has an action given by

$$S_{dw} = \int_{\Sigma} d^{D-1}x\sqrt{-h}\, L_{dw}\,, \tag{68}$$

whose variation is

$$\delta S_{dw} = \int_{\Sigma} d^{D-1}x\sqrt{-h}\, t^{MN}\delta g_{MN}\,, \tag{69}$$

where $t^{MN} \equiv \frac{2}{\sqrt{-h}}\frac{\delta S_{dw}}{\delta h_{MN}}$ is tangential to the domain wall such that we can replace δh_{MN} by δg_{MN}.

Finally, the variation of the total action $S = S_{EH} + S_{GH} + S_{dw}$ gives the Darmois-Israel conditions

$$[K_{MN} - K h_{MN}] = -t_{MN}\,, \tag{70}$$

where the brackets stand for the jump of K through the domain wall Σ.

7.3 Junction Conditions from Distribution Theory

The Darmois-Israel conditions describe the motion of the domain wall through the bulk. However, sometimes it will be required to have a static brane, in this case the Darmois-Israel conditions reduce to some relations between the energy density and pressure on the brane and the coefficients of the bulk metric. An alternative derivation of these relations can be done using distribution theory as follows.

Let us consider as an example a 5-dimensional bulk metric of the form [69, 70]

$$ds^2_{(5)} = -n^2(t,y)dt^2 + a^2(t,y)\gamma_{ij}dx^k dx^j + b^2(\tau,y)dy^2\,, \tag{71}$$

where γ_{ij} represents a maximally symmetric metric on the 3-brane located in $y = 0$ with $k = -1, 0, 1$ parametrizing the spatial curvature.

The stress-energy tensor appearing in the Einstein's equations $G_{AB} = \kappa^2_{(5)}\mathcal{T}_{AB}$ can be written as

$$\mathcal{T}_{AB} = \hat{T}_{AB} + T_{AB}\,, \tag{72}$$

where $\hat{T}_{AB}$ is the stress-energy tensor of the matter on the bulk (and possibly other branes) which we do not need to specify here, and T_{AB} corresponds to the matter content on the brane which can be expressed quite generally as

$$T^A_B = \frac{\delta(y)}{b} diag(-\rho, p, p, p, 0) \quad . \tag{73}$$

The energy ρ and the pressure p are independent of the position on the brane in order to recover homogeneous cosmology on the brane.

From the metric (71) the Einstein's tensor components are found to be

$$\tilde{G}_{00} = 3\left\{\frac{\dot{a}}{a}\left(\frac{\dot{a}}{a}+\frac{\dot{b}}{b}\right)-\frac{n^2}{b^2}\left(\frac{a''}{a}+\frac{a'}{a}\left(\frac{a'}{a}-\frac{b'}{b}\right)\right)+k\frac{n^2}{a^2}\right\}, \tag{74}$$

$$\begin{aligned}\tilde{G}_{ij} &= \frac{a^2}{b^2}\gamma_{ij}\left\{\frac{a'}{a}\left(\frac{a'}{a}+2\frac{n'}{n}\right)-\frac{b'}{b}\left(\frac{n'}{n}+2\frac{a'}{a}\right)+2\frac{a''}{a}+\frac{n''}{n}\right\}+\\ &\quad +\frac{a^2}{n^2}\gamma_{ij}\left\{\frac{\dot{a}}{a}\left(-\frac{\dot{a}}{a}+2\frac{\dot{n}}{n}\right)-2\frac{\ddot{a}}{a}+\frac{\dot{b}}{b}\left(-2\frac{\dot{a}}{a}+\frac{\dot{n}}{n}\right)-\frac{\ddot{b}}{b}\right\}-k\gamma_{ij}\,,\end{aligned} \tag{75}$$

$$\tilde{G}_{05} = 3\left(\frac{n'}{n}\frac{\dot{a}}{a}+\frac{a'}{a}\frac{\dot{b}}{b}-\frac{\dot{a}'}{a}\right), \tag{76}$$

$$\tilde{G}_{55} = 3\left\{\frac{a'}{a}\left(\frac{a'}{a}+\frac{n'}{n}\right)-\frac{b^2}{n^2}\left(\frac{\dot{a}}{a}\left(\frac{\dot{a}}{a}-\frac{\dot{n}}{n}\right)+\frac{\ddot{a}}{a}\right)-k\frac{b^2}{a^2}\right\}, \tag{77}$$

where a prime stands for derivative with respect to y and the dot means derivative with respect to t.

In order to have a well defined geometry the metric must be continuous across the brane. However, its derivatives with respect to y can be discontinuous in $y=0$. Thus, there is a Dirac delta function in the second derivatives of the metric with respect to y. In general we will have

$$a'' = \hat{a}'' + [a']\delta(y)\,, \tag{78}$$

where $\hat{a}''$ stands for the non-distributional part of the second derivative of a (the ordinary second derivative), and $[a']$ is the jump of the first derivative across $y=0$ defined by

$$[a'] = a'(0^+) - a'(0^-)\,. \tag{79}$$

Hence, the resulting terms with a delta function appearing in the Einstein tensor must be matched to the distributional part of the stress-energy tensor in order to satisfy the Einstein's equations. Matching the Dirac delta functions in the components (74) and (75) of the Einstein's tensor we obtain the following relations

$$\frac{[a']}{a_0 b_0} = -\frac{\kappa_{(5)}^2}{3}\rho\,,$$

$$\frac{[n']}{n_0 b_0} = \frac{\kappa^2_{(5)}}{3}(3p + 2\rho)\,, \tag{80}$$

where the subscript 0 means that the metric coefficients take their values on the brane. This result is known as the *junction conditions* for a static brane embedded in a generic bulk.

7.4 Application of quantum cosmology: an upper bound for the number of e-foldings

Motivated by the well-known example of black hole entropy, an influential holographic principle has put forward, suggesting that microscopic degrees of freedom that build up the gravitational dynamics actually reside on the boundary of space-time [110]. This principle developed to the Maldacena's conjecture on AdS/CFT correspondence [111] and further very important consequences, such as Witten's [112] identification of the entropy, energy and temperature of CFT at high temperatures with the entropy, mass and Hawking temperature of the AdS black hole [113].

On the other hand, although standard model of particle physics has been established as the uncontested theory of all interactions down to distances of 10^{-17}m, there are good reasons to believe that there is a new physics arising soon at the experimental level, and this fact is going to appear in a clear fashion in the setup of cosmology, where a large number of quite exciting developments is giving rise to a precision cosmology. Thus cosmology may provide an alternative laboratory for string theory. From the eighties several authors tried to analyse the kind of cosmology arising from string inspired models, which are essentially general relativity in higher dimensions together with scalar and tensor fields. In case we introduce also the brane concept, a consistent picture of the brane universe is achieved, and we can describe the evoltion of the universe by means of solutions of the Einstein field equations in higher dimensions, with a four dimensional membrane. We thus seek at a description of the powerful holographic principle in cosmological settings, where its testing is subtle, and the question of hologrphy therein has been considered by several authors [114] have shown that for flat and open Friedmann-Lemaitre-Robertson-Walker(FLRW) universes the area of the particle horizon should bound the entropy on the backward-looking light cone. In addition to the study of holography in homogeneous cosmologies, attempts to generalize the holographic principle to a generic realistic inhomogeneous cosmological setting were carried out in [115]. Later, the very interesting study of the holographic principle in FLRW universe filled with CFT with a dual AdS description has been done by Verlinde [116], revealing that when a universe-sized black hole can be formed, an interesting and surprising correspondence appears between entropy of CFT and Friedmann equation governing the radiation dominated closed FLRW universes. Generalizing Verlinde's discussion to a broader class of universes including a cosmological constant [117], we found that matching of Friedmann equation to Cardy formula holds for de Sitter closed and AdS flat universes. However for the remaining de Sitter and AdS universes, the argument fails due to breaking down of the general philosophy of the holographic principle. In high dimensions, various other aspects of Verlinde's proposal have also been investigated in a number of works [118].

In a very recent paper [119], further light on the correspondence between Friedmann equation and Cardy formula has been shed from a Randall-Sundrum type brane-world perspective [120]. Considering the CFT dominated universe as a co-dimension one brane with fine-tuned tension in a background of an AdS black hole, Savonije and Verlinde found the correspondence between Friedmann equation and Cardy formula for the entropy of CFT when the brane crosses the black hole horizon. This result has been further confirmed by studying a brane-universe filled with radiation and stiff-matter, quantum-induced brane worlds and radially infalling brane [121]. The discovered relation between Friedmann equation and Cardy formula for the entropy shed significant light on the meaning of the holographic principle in a cosmological setting. However the general proof for this correspondence for all CFTs is still difficult at the moment. Other settings have also been considered as in *e. g.* [122]. It is worthwhile to further check the validity of the correspondence in broader classes of situations than [116, 119].

Our motivation here is the use of the correspondence between the CFT gas and the Friedmann equation establishing an upper bound for the number of e-foldings during inflation. Recently, Banks and Fischler [123] have considered the problem of the number of e-foldings in a universe displaying an asymptotic de Sitter phase, as our own. As a result the number of e-foldings is not larger than 65/85 depending on the type of matter considered.

Here we reconsider the problem from the point of view of the entropy content of the Universe, and considering the correspondence between the Friedmann equation and Cardy formula in Brane Universes, as discussed by us [124].

The existence of an upper bound for the number of e-foldings before the end of inflation was also studied recently in [125] and [126]. However in their investigation the number of e-foldings is related both to a possible reduction in energy scale during the late stages of inflation and to the complete cosmological evolution, being model dependent. The bound has been obtained in some very simple cosmological settings, while it is still difficult to be obtained in nonstandard models. Using the holographic principle, the consideration of physical details connected to the universe evolution can be avoided. We have obtained the upper bound for the number of e-foldings for a standard FRW universe as well as non-standard cosmology based on the brane inspired idea of Randall and Sundrum models.

The starting point is that the scalar factor, in case of the brane cosmology, is defined by the Darmois-Israel condition [127][124][128]. We consider a bulk metric defined by

$$ds_5^2 = -f dt^2 + f^{-1} dr^2 + r^2 d\Sigma_K^2, \tag{81}$$

where $f = k + \frac{r^2}{L^2} - \frac{m}{r^2}$ and L is the curvature radius of AdS spacetime. k takes the values $0, -1, +1$ corresponding to flat, open and closed geometrics, and $d\Sigma_k^2$ is the corresponding metric on the unit three dimensional plane, hyperboloid or sphere. The black hole horizon is located at

$$r_H^2 = \frac{L^2}{2}(-k + \sqrt{k^2 + 4m/L^2}). \tag{82}$$

The relation between the parameter m and the Arnowitt-Deser-Misner (ADM) mass of the five dimensional black hole M is [129]

$$M = \frac{3\omega_3}{16\pi G_5} m \tag{83}$$

where ω_3 is the volume of the unit 3 sphere.

Here, the location and the metric on the boundary are time dependent. We can choose the brane time such that $\dot{r}^2 = f^2 \dot{t}^2 - f$, in which case the metric on the brane is given by

$$ds_4^2 = -d\tau^2 + r^2(\tau) d\Sigma_3^2 \quad . \tag{84}$$

The Conformal Field Theory lives on the brane, which is the boundary of the AdS hole. The energy for a CFT on a sphere with volume $V = r^3\omega_3$ is given by $E = \frac{L}{r}M$. The density of the CFT energy can be expressed as

$$\rho_{CFT} = E/V = \frac{3mL}{16\pi G_5 a^4} = \frac{3m}{8\pi G_4 a^4} \quad . \tag{85}$$

The entropy of the CFT on the brane is equal to the Bekenstein-Hawking entropy of the AdS black hole [112][130],

$$S_{CFT}(4D) = S_{BH}(5D) = \frac{V_H}{4G_5}, \quad V_H = a_H^3\omega_3 \quad . \tag{86}$$

The entropy density of the CFT on the brane is

$$\sigma = \frac{S}{V} = \frac{a_H^3\omega_3}{4G_5}\frac{1}{a^3\omega_3} \overset{G_5=\frac{G_4L}{2}}{=} \frac{a_H^3}{2G_4La^3} \quad . \tag{87}$$

From the matching conditions we find now the cosmological equations in the brane,

$$H^2 = -\frac{k}{r^2} + \frac{m}{r^4} - \frac{1-(\sigma/\sigma_c)^2}{L^2} \quad , \tag{88}$$

where $\sigma_c = \frac{3}{8\pi G_5 L}$ is the critical brane tension. Taking $\sigma = \sigma_c$, (88) reduces to the Friedmann equation of CFT radiation dominated brane universe without cosmological constant discussed in [119]. If $\sigma > \sigma_c$ or $\sigma < \sigma_c$, the brane-world is a de Sitter universe or AdS universe, respectively. Using (85) the Friedmann equation can be written in the form

$$H^2 = -\frac{k}{a^2} + \frac{8\pi G_4}{3}\rho_{CFT} + \frac{\lambda}{3} \quad , \tag{89}$$

where λ is the effective positive cosmological constant in four dimensions.

The relation between the energy density and the entropy, $\rho = \frac{9mL}{16\pi^2 a_H^3 a^4}S$ can be used to rewrite the Friedmann equation as

$$(\dot{a})^2 + k - \frac{3G_4mLS}{2\pi a_H^3 a^2} - \frac{\lambda}{3}a^2 = 0 \quad , \tag{90}$$

which corresponds to the movement of a mechanical nonrelativistic particle in a given potential. For a closed universe there is a critical value for which the solution extends to infinity (no big crunch) which is

$$S < \frac{2\pi a_H^3\lambda a^4}{9G_4mL} \overset{a\approx\lambda^{-1/2}}{\rightarrow} \frac{2\pi a_H^3\lambda^{-1}}{9G_4mL} \quad . \tag{91}$$

The entropy in such a universe can be rewriten as

$$S = \sigma V = \frac{4}{3}\pi a^3 \frac{4\pi a_H^3 a}{3mL}\rho \tag{92}$$

at the end of inflation. We take ρ to be the energy density during inflation, that is, $\rho \sim \Lambda_I$, which for the scale factor at the exit of inflation leads to the value $a \approx \Lambda_I^{-1/2} e^{Ne}$, where $\Lambda_I^{-1/2}$ corresponds to the apparent horizon during inflation, and we obtain

$$N_e = \ln a + \frac{1}{2}\ln \Lambda_I \quad . \tag{93}$$

Using now (92) in (91) we get

$$a < (8\pi G_4 \Lambda_I \lambda)^{-1/4} \quad , \tag{94}$$

from which we arrive at

$$N_e < \frac{1}{4}\ln\frac{\Lambda_I}{\lambda} - \frac{1}{4}\ln(8\pi G_4) \approx 64 \quad , \tag{95}$$

where we used the usual values $\Lambda_I^{1/4} \approx 10^{16}$GeV and $\lambda^{1/4} \approx 10^{-3}$eV.

For this standard FRW universe, the bound obtained is in agreement with [125] and [126] as well as with [123] fir==or a universe filled with radiation.

Let us consider now very high energy brane corrections to the Friedmann equation. From the Darmois-Israel conditions we find

$$H^2 = -\frac{k}{a^2} + \frac{8\pi}{3M_4^2}\rho + \frac{4\pi}{3M_4^2}\frac{\rho^2}{l} + \frac{\lambda_4}{3} \approx -\frac{k}{a^2} + \frac{4\pi}{3M_4^2}\frac{\rho^2}{l} + \frac{\lambda_4}{3} \quad , \tag{96}$$

where l is the brane tension and in the very high energy limit the ρ^2 term dominates. Within the high-energy regime, the expansion laws corresponding to matter and radiation domination are slower than in the standard cosmology [126]. Slower expansion rates lead to a larger value of the number of e-foldings. However, the full calculation has not been obtained due to the lack of knowledge of this high-energy regime. Here we study this problem from the point of view of holography.

The energy density of the CFT and the entropy density are related as follows,

$$
\begin{aligned}
\rho_{CFT} &= \frac{3m}{8\pi G_4 a^4} \quad , \quad \sigma = \frac{a_H^3}{2G_4 L a^3} \quad , \\
\rho = \frac{9mLS}{16\pi^2 a_H^3 a^4} \quad , &
\end{aligned} \tag{97}
$$

which can be substituted in the Friedmann equation as before, leading to a bound for the entropy, as well as a bound for the scale factor, as given by

$$
\begin{aligned}
S^2 = \frac{256\pi^4 a_H^6 a^8 \rho^2}{81 m^2 L^2} &< \frac{64\pi^3 l a_H^6}{243 G_4 m^2 L^2 \lambda^3} \\
a^8 &< \frac{3l}{4\pi G_4 \rho^2 \lambda_4^3} \quad ,
\end{aligned} \tag{98}
$$

We consider the era when the quadratic energy density is important. The brane tension is required to be bounded by [132] $l < (1\mathrm{MeV})^4$. Combining the values of Λ_I and λ we chose before, a bound for N_e is given by

$$
N_e < 75 \quad . \tag{99}
$$

The number of e-foldings obtained is bigger than the value in standard FRW cosmology, which is consistent with the argument of [126].

In summary, we have derived the upper limit for the number of e-foldings based upon the arguments relating Friedmann equation and Cardy formula. For the standard FRW universe our result is in good agreement with [125] and [126] and in the radiation dominated case with [123]. For the brane inspired cosmology in four dimensions we obtained a larger bound. Considering such a high energy context, the expansion laws are slower than in the standard cosmology, and our result can again be considered to be consistent with the argument in [126]. The interesting point here is that using the holographic point of view, we can avoid a complicated physics during the universe evolution and give a reasonable value for the upper bound of the number of e-foldings.

8 The Scenarios

We shall consider two kinds of scenarios. In the first, a brane wall model based on the exact solution of Einstein Equations and boundary conditions, where the brane is a socalled domain wall embedded in a space-time containing a singularity (a type of black hole) and a cosmological constant. Subsequently we consider a Friedmann-Robertson-Walker type of membrane.

In the first case we have a scenario described by the gravitational action in a D-dimensional bulk with a scalar field, a bulk dilaton, a domain wall potential and a Gibbons-Hawking term [63],

$$S = \int_{bulk} d^D x\sqrt{-g}\left(\frac{1}{2}R - \frac{1}{2}(\partial\phi)^2 - V(\phi)\right) - \int_{dw} d^{D-1}x\sqrt{-h}([K] + \hat{V}(\phi))\,, \tag{100}$$

where ϕ is the bulk dilaton, K is the extrinsic curvature, $V(\phi)$ and $\hat{V}(\phi)$ are bulk and domain wall potentials respectively, and g and h denote the bulk and domain wall metrics. The potentials are here considered to be of the Liouville type:

$$\begin{aligned} V(\phi) &= V_0 e^{\beta\phi}\,, && (101)\\ \hat{V}(\phi) &= \hat{V}_0 e^{\alpha\phi}\,. && (102) \end{aligned}$$

We consider the bulk metric as being static and invariant under rotation, being given by

$$ds^2 = -U(r)dt^2 + U(r)^{-1}dr^2 + R(r)^2 d\Omega_k^2\,, \tag{103}$$

where $d\Omega_k^2$ is the line element on a $D-2$ dimensional space of constant curvature depending on a parameter k. We might also consider the brane to have a static metric, in which case the solution of the bulk would be more complicated. We come back to this point later. The above metric is supposed to have a mirror symmetry Z_2 with respect to the domain wall. Such a symmetry will be used in order to impose the Darmois-Israel conditions [65]. In fact, the variation of the total action (100) including the Gibbons-Hawking term leads directly to the Darmois-Israel conditions which in view of the Z_2 symmetry become

$$K_{MN} = -\frac{1}{2(D-2)}\hat{V}(\phi)h_{MN} \quad . \tag{104}$$

The extrinsic curvature can be computed as

$$K_{MN} = h_M^P h_N^Q \nabla_P n_Q \quad , \tag{105}$$

where the unit normal, which points into $r < r(t)$, is

$$n_M = \frac{1}{\sqrt{U - \frac{\dot{r}^2}{U}}}(\dot{r}\,,\,-1\,,\,0\ldots,\,0)\,. \tag{106}$$

Here a dot means derivative with respect to the bulk time t.

The ij component of (104) can be written as

$$\frac{R'}{R} = \frac{\hat{V}(\phi)}{2(D-2)U}\sqrt{U - \frac{\dot{r}^2}{U}}\,, \tag{107}$$

while the 00 component is

$$\left(\frac{R'}{R}\right)^{-1}\left(\frac{R'}{R}\right)' = \frac{\hat{V}'(\phi)}{\hat{V}(\phi)} - \frac{R'}{R}\,. \tag{108}$$

Here a prime denotes derivative with respect to the radial extra coordinate r.

The equation of motion for the dilaton obtained from the action (100), together with (108), can be simultaneously solved with the Ansatz (103), leading to [71]

$$\begin{aligned}\phi(r) &= \phi_\star - \frac{\alpha(D-2)}{\alpha^2(D-2)+1}\log r\,, & (109)\\ R(r) &= (\alpha^2(D-2)+1)C\hat{V}_0 e^{\alpha\phi_\star} r^{\frac{1}{\alpha^2(D-2)+1}}\,, & (110)\end{aligned}$$

where $\phi_\star$ and C are arbitrary integration constants.

The motion of the domain wall is governed by the ij component of the Darmois-Israel conditions (107). That equation can be written in terms of the brane proper time τ as

$$\frac{1}{2}\left(\frac{dR}{d\tau}\right)^2 + F(R) = 0\,. \tag{111}$$

The induced metric on the domain wall is Friedmann-Robertson-Walker and (111) describes the evolution of the scale factor $R(\tau)$. This equation is the same as that one for a particle of unit mass and zero energy rolling in a potential $F(R)$ given by

$$F(R) = \frac{1}{2}UR'^2 - \frac{1}{8(D-2)^2}\hat{V}^2R^2\,. \tag{112}$$

Notice that the solution only exists when $F(R) \leq 0$.

From the induced domain wall metric we find the relations between the time parameter on the brane (τ) and in the bulk (t) as given by

$$dt = \frac{\sqrt{U + \left(\frac{dr}{d\tau}\right)^2}}{U} d\tau \ ,$$

so that

$$\dot{r} \equiv \frac{dr}{dt} = \frac{dr}{d\tau}\frac{d\tau}{dt} = \frac{dr}{d\tau}\frac{U}{\sqrt{U + \left(\frac{dr}{d\tau}\right)^2}} \ , \tag{113}$$

where $\frac{dr}{d\tau} = \frac{dR}{d\tau}\left(\frac{dR}{dr}\right)^{-1}$ can be obtained from (111). Equation (113) describes the motion of a domain wall in the static background as seen by an observer in the bulk.

Consider two points on the brane. In general, there are more than one null geodesic connecting them in the D-dimensional spacetime. The trajectories of photons must be on the brane and those of gravitons may be outside. We consider the shortest path for both photons and gravitons. For the latter, the geodesic equation is the same as the one considered in [11], since the bulk metric is static:

$$\ddot{r}_g + \left(\frac{1}{r_g} - \frac{3}{2}\frac{U'}{U}\right)\dot{r}_g^2 + \frac{1}{2}U\,U' - \frac{U^2}{r_g} = 0 \ . \tag{114}$$

Again a dot means derivative with respect to the bulk time t.

The solutions of (113) and (114) in terms of the bulk proper time t were obtained by means of a **MAPLE** program. Now we discuss the possibility of shortcuts in the cases of the various solutions describing different Universes defined by the domain wall solution.

Subsequently, we have a scenario where the bulk is a purely Anti-de-Sitter space-time of the form [73],

$$ds^2 = h(a)dt^2 - \frac{da^2}{h(a)} - a^2 d\Sigma^2,$$

with $h(a) = k + \frac{a^2}{l^2}$, $l \sim 0.1mm$ is the Randall-Sundrum lenght scale [74] and $d\Sigma^2$ represents the metric of the three dimensional spatial sections with $k = 0\ ,\ \pm 1$,

$$d\Sigma^2 = \frac{dr^2}{1 - kr^2} + r^2[d\theta^2 + \sin^2(\theta)d\phi^2].$$

The brane is localized at $a_b(\tau)$, where τ is the proper time on the brane. The unit vector normal to the brane is defined as (overdot and prime superscript denote differentiation with respect to τ and a respectively)

$$n = \dot{a}_b(\tau)dt - \dot{t}(\tau)da \quad . \tag{115}$$

The normalization of n implies the relation between the bulk time t and the brane time τ,

$$h(a_b)\dot{t}^2 - \dot{a_b}^2 h^{-1}(a_b) = 1 \tag{116}$$

and also the usual FRW expression for the distance in the brane ,

$$ds^2 = d\tau^2 - a_b^2 d\Sigma^2 \quad .$$

Aiming at the Darmois-Israel conditions in the brane [65] we compute the second fundamental form

$$K_{ij} = e_i^\alpha e_j^\nu \nabla_\alpha n_\nu \quad ,$$

$$\begin{aligned} K_{rr} &= -\frac{a_b h}{(1-kr^2)}\dot{t} \quad , & (117)\\ K_{\theta\theta} &= -a_b r^2 h\dot{t} \quad , & (118)\\ K_{\phi\phi} &= -a_b r^2 \sin^2(\theta) h\dot{t} & (119)\\ & & (120) \end{aligned}$$

and

$$K_{\tau\tau} = \frac{1}{h\dot{t}}\Big(\ddot{a}_b + \frac{h'}{2}\Big) \quad . \tag{121}$$

With these results, using the Darmois-Israel conditions for a Z_2 symmetric configuration [65],

$$K_{ij} = \frac{1}{2}\kappa_{(5)}^2\Big(S_{ij} - \frac{1}{3}h_{ij}S\Big) \quad , \tag{122}$$

we relate the discontinuity in the second fundamental form through the brane and the energy momentum tensor in the brane, S_{ij}. For an isotropic distribution of matter, as given by

$$S_{ij} = \epsilon_T u_i u_j - p_T(h_{ij} - u_i u_j) \quad , \tag{123}$$

the following relations hold [75],[76], [77]

$$\frac{d\epsilon_T}{d\tau} = -3\frac{\dot{a}_b}{a_b}(\epsilon_T + p_T)$$

and

$$\frac{\dot{a}_b^2}{a_b^2} + \frac{h}{a_b^2} = \frac{\kappa_{(5)}^4 \epsilon_T^2}{36} \quad . \tag{124}$$

Following [78] and [79], we introduce an intrinsic non-dynamical energy density ϵ_0 defined by means of $\epsilon_T = \epsilon_0 + \epsilon$, $p_T = -\epsilon_0 + p$ where ϵ and p corresponds to the brane matter. Thus the junction equations imply the usual energy conservation in the brane,

$$\frac{d\epsilon}{d\tau} = -3\frac{\dot{a}_b}{a_b}(\epsilon + p) \tag{125}$$

and the modified Friedmann equation [80],

$$H^2 = \Big(\frac{\dot{a}_b}{a_b}\Big)^2 = \frac{\Lambda_4}{3} + \frac{1}{M_{Pl}^2}\Big(\frac{\epsilon}{3} + \frac{\epsilon^2}{6\epsilon_0}\Big) - \frac{k}{a_b^2} \quad , \tag{126}$$

with the hierarchy

$$M_{PL}^{-2} = \frac{\kappa_5^4 \epsilon_0}{6} \tag{127}$$

and the cosmological constant in the brane

$$\frac{\Lambda_4}{3} = \Big(\frac{\kappa_5^4 \epsilon_0^2}{36} - \frac{1}{l^2}\Big). \tag{128}$$

The present density of the Universe is

$$\epsilon(0) = \Omega_0 \epsilon_c = \Omega_0 3 M_{PL}^2 H_0^2 \quad ,$$

where Ω_0 is the ratio of the density and the critical density of the Universe. Aiming at the energy conservation, the Friedmann equation can be written as

$$H^2 = \frac{\Lambda_4}{3} + \Omega_0 H_0^2 \frac{a_{b0}^q}{a_b^q}\Big(1 + \frac{\Omega_0}{4(1+\Lambda_4 l^2/3)}\frac{L_c^q}{a_b^q}\Big) - \frac{k}{a_b^2} \quad , \tag{129}$$

where $L_c^q = a_{b0}^q l^2 H_0^2$.

We thus verify that there exist three phases in the evolution of the Universe. When $a_b >> L_c$ the linear term in the energy density prevails in the Friedmann equation, leading to the standard cosmology. Because $H_0 l \sim 10^{-29}$ this happens in a redshift of $a_{b0}/a_b \sim 10^{15}$, much earlier than the nucleosynthesis. For $a_b << L_c$ the Universe expands at a slower pace as compared to the standard model, $a_b \propto \tau^{1/q}$, and the quadratic term is the prevailing one. In an intermediate era where $a_b \sim L_c$, both phases coexist.

We see that all the cosmological information is already known: the position of the brane in the extra dimension, $a_b(\tau)$, is just the scale factor of the FRW metric and the junction conditions imply that the cosmological evolution of the brane is obtained by the usual energy conservation (125) and the modified Friedmann equations (126). However, in this work, we are particularly interested in the evolution of the brane with respect to the bulk. This relation can be obtained using (116) and transforming from the time of the brane to the time of the bulk. Thus the position of the brane can also be treated as a function of the bulk proper time satisfying the equation

$$\frac{da_b}{dt} = \frac{da_b}{d\tau}\frac{d\tau}{dt} = \dot{a}_b(\tau)\frac{h(a_b)}{\sqrt{h(a_b) + \dot{a}_b(\tau)^2}} \quad . \tag{130}$$

9 Solutions of the Geodesic Equation for a Domain Wall

9.1 Type I Solutions

We define the type I brane solutions as those for which $\alpha = \beta = 0$. Consequently, the potentials become cosmological constants. The solution also has a constant dilaton $\phi = \phi_0$. A simple rescaling in the metric leads us to

$$ds^2 = -U(R)dt^2 + U(R)^{-1}dR^2 + R^2 d\Omega_k^2 \ , \tag{131}$$

with

$$U(R) = k - 2MR^{-(D-3)} - \frac{2V_0}{(D-1)(D-2)}R^2 \ , \tag{132}$$

which corresponds to a topological black hole solution in D dimensions with a cosmological constant.

As discussed in Ref. [71], if the domain wall has positive energy density ($\hat{V}_0 > 0$), the relevant part of the bulk spacetime is $R < R(\tau)$, which is the region containing the singularity. If it has negative energy density ($\hat{V}_0 < 0$), the relevant part is $R > R(\tau)$, which is non-singular unless the wall reaches $R = 0$.

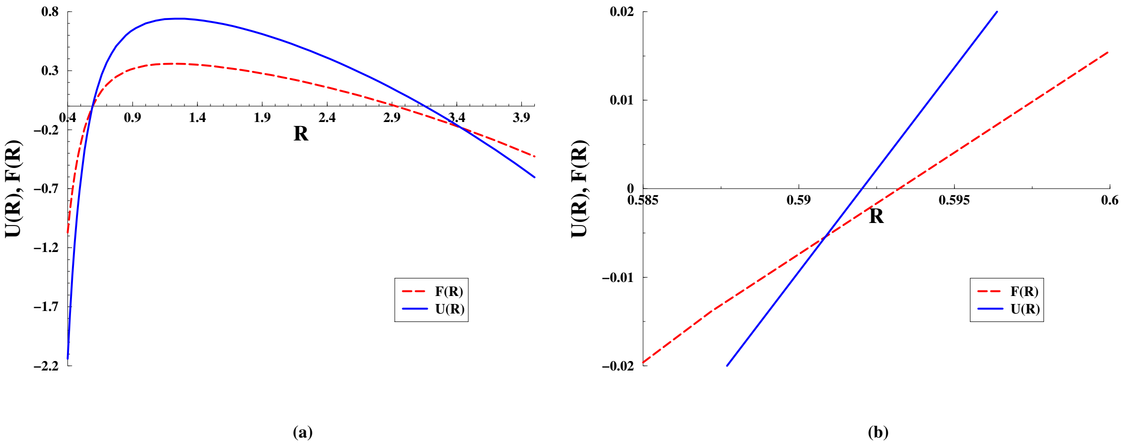

Figure 6: (a) $U(R)$ and $F(R)$ for type I solutions with $M = 1/10$, $V_0 = 1$ and $\hat{V}_0 = \pm 1$, (b) Zoom of the event horizon region.

The potential $F(R)$ ruling the evolution of the scale factor is

$$F(R) = \frac{k}{2} - MR^{-(D-3)} - \hat{\Lambda} R^2 \,, \tag{133}$$

where the effective cosmological constant on the domain wall is given by

$$\hat{\Lambda} = \frac{1}{D-2} \left[\frac{V_0}{D-1} + \frac{\hat{V}_0^2}{8(D-2)} \right] . \tag{134}$$

We shall analyze each of the four cases presented in [71]. As we have previously stated, the equation of motion (111) has a solution only when $F(R) \leq 0$. This is automatic only if $U(R) < 0$, i.e. if r is a time coordinate;

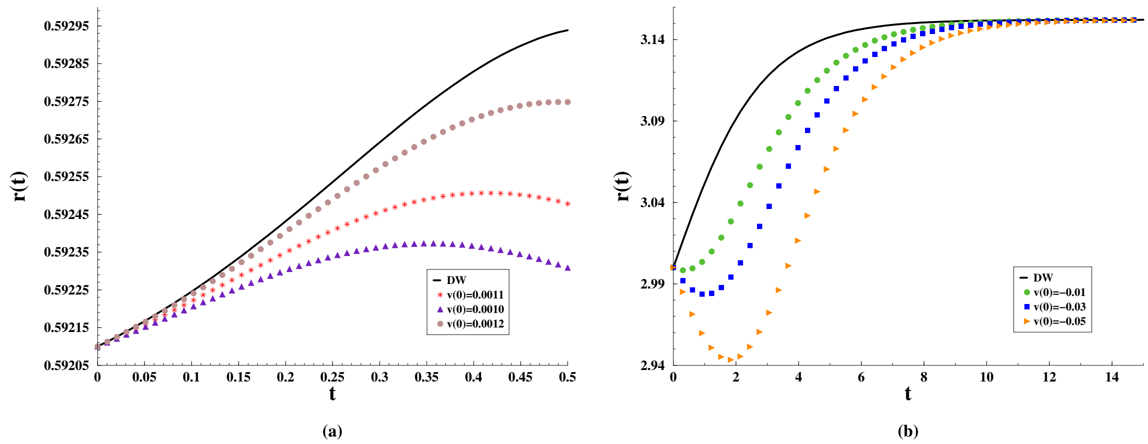

Figure 7: Domain wall motion and geodesics for type I solutions with $M = 1/10$, $V_0 = 1$ and $\hat{V}_0 = 1$ in (a) region I and, (b) region II.

therefore, we look for solutions with $U(R) > 0$. In fact, both conditions,

$$F(R) \leq 0 \qquad \text{and} \qquad U(R) > 0\,, \tag{135}$$

can coexist in some cases as we will see in what follows. In order to ilustrate the following examples we have chosen $D = 6$ dimensions.

9.1.1 $\hat{\Lambda} > 0$, $M > 0$

From the graph of $U(R)$ (see Fig.6) we can choose the initial condition for the domain wall assuming that (132) describes a dS-Schwarzschild bulk with event and cosmological horizons when $M > 0$ and $V_0 > 0$.

We thus choose the initial condition for the domain wall inside this region and where r is a space coordinate. From Fig.6 let us notice that there are two small regions, $r_H \leq r < 0.593$ and $2.93 \leq r < r_C$, where (135) holds. The results are shown in Fig.7. We see that for region I the geodesics follow the domain wall for a while and then decouple falling into the event horizon. For region II all the geodesics and the domain wall converge to the cosmological horizon r_C independently of the value of $\hat{V}_0$.

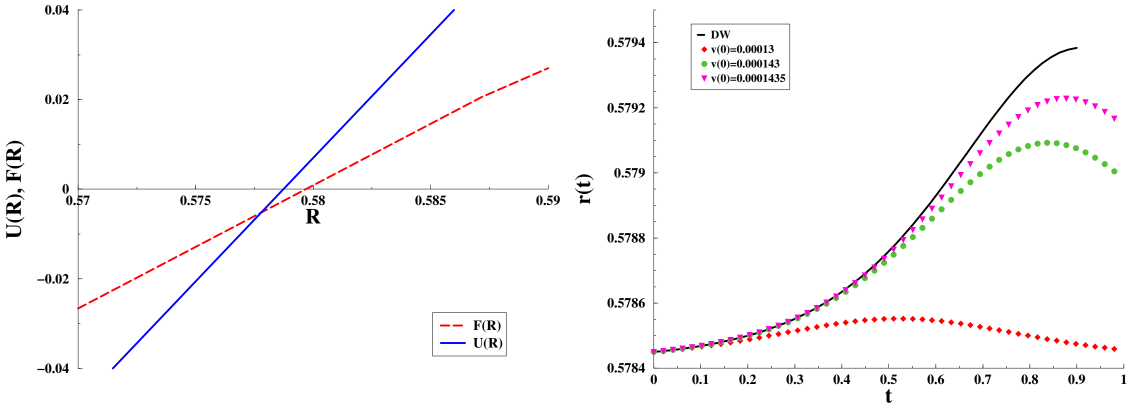

(a) (b)

Figure 8: (a) Zoom of the region where (135) holds from the graph of $U(R)$ and $F(R)$ with $\hat{\Lambda} < 0$ and $M > 0$ for type I solutions, (b) Domain wall motion and geodesics for type I solutions with $M = 1/10$, $V_0 = -1$ and $\hat{V}_0 = 1$.

9.1.2 $\hat{\Lambda} < 0$, $M > 0$

This case describes an AdS-Schwarzschild bulk. The condition (135) is fullfilled inside a very small range as we can see in Fig.8(a). However, all the geodesics fall into the event horizon after following some path on the brane (see Fig.8(b)).

9.1.3 $\hat{\Lambda} > 0$, $M < 0$

From Fig.9(a) we choose the initial condition for the domain wall equation of motion inside the region where (135) holds. As we can see from Fig.9(b), the domain wall and the geodesic converge to the cosmological horizon r_C. However, after some threshold initial velocity the geodesics diverge to the timelike naked singularity.

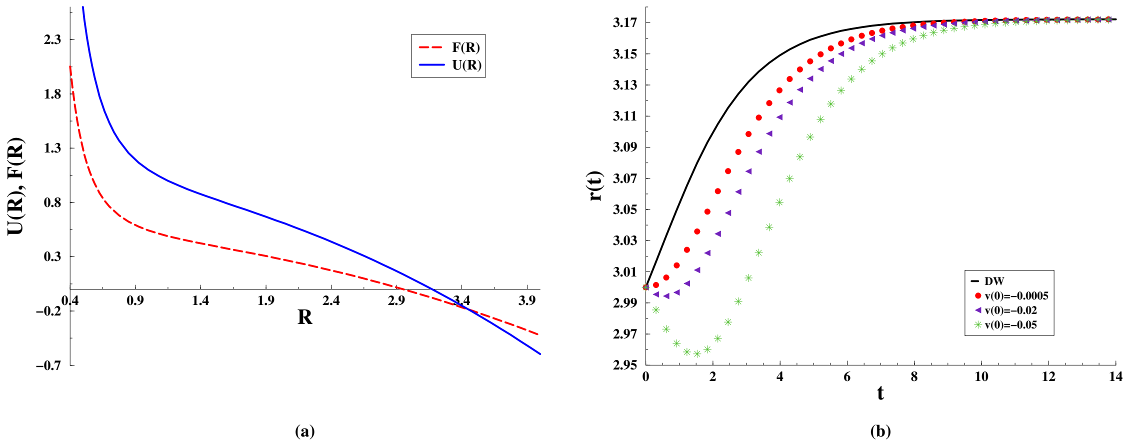

Figure 9: (a) $U(R)$ and $F(R)$ with $\hat{\Lambda} > 0$ and $M < 0$ for type I solutions, (b) Domain wall motion and geodesics for $M = -1/10$, $V_0 = 1$ and $\hat{V}_0 = 1$.

9.1.4 $\hat{\Lambda} < 0$, $M < 0$

In this case (111) can only have solution when $k = -1$. This is a topological black hole in an asymtotically AdS space. From Fig.10 we see that there is no solution fulfilling (135) between event and cosmological horizons.

9.2 Type II Solutions

The type II solutions have $\alpha = \beta/2$ and $k = 0$. The metric is given by

$$U(r) = (1+b^2)^2 r^{\frac{2}{1+b^2}} \left(-2Mr^{-\frac{D-1-b^2}{1+b^2}} - \frac{2\Lambda}{(D-1-b^2)} \right) , \tag{136}$$

and the scale factor is

$$R(r) = r^{\frac{1}{1+b^2}} , \tag{137}$$

where

$$\Lambda = \frac{V_0 e^{2b\phi_0}}{D-2} , \tag{138}$$

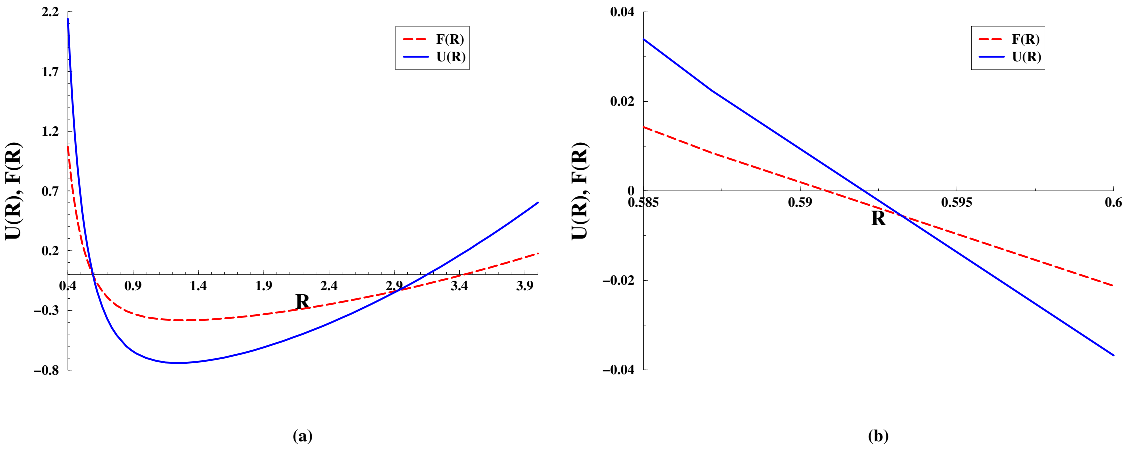

Figure 10: (a) $U(R)$ and $F(R)$ with $\hat{\Lambda} < 0$ and $M = -1/10$ for type I solutions, (b) Zoom of the event horizon region.

$$b \;=\; \frac{1}{2}\beta\sqrt{D-2}\,. \tag{139}$$

The potential is given by the expression

$$F(R) = -R^{2(1-b^2)}\left(MR^{-(D-1-b^2)} + \hat{\Lambda}\right)\;, \tag{140}$$

where

$$\hat{\Lambda} = \frac{e^{2b\phi_0}}{D-2}\left(\frac{V_0}{D-1-b^2} + \frac{\hat{V}_0^2}{8(D-2)}\right)\;. \tag{141}$$

There are twelve cases from which we choose those ones where r is a spatial coordinate. When $b^2 < D-1$, r is a spatial coordinate if $V_0 < 0$. When $b^2 > D-1$, r is spatial if $M < 0$.

We should also rewrite (135) as

$$F(r) \leq 0 \quad \text{and} \quad U(r) > 0\,. \tag{142}$$

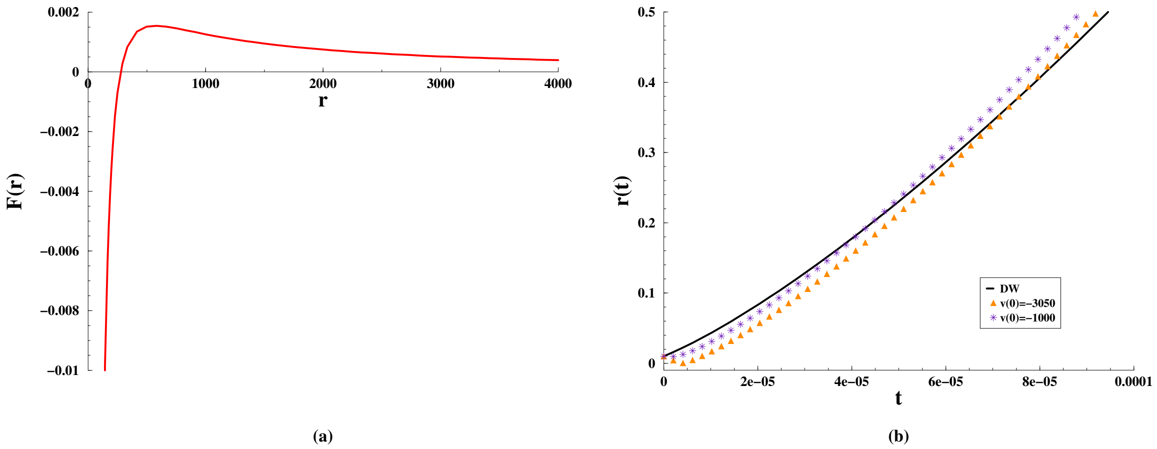

Figure 11: (a) $F(r)$ with $\hat{\Lambda} > 0$ and $M < 0$ for type II solutions, (b) Domain wall motion and geodesics for $V_0 = 1$, $\hat{V}_0 = 6$, $M = -10$ and $\beta = \sqrt{10}$.

9.2.1 $\hat{\Lambda} > 0$, $M < 0$, $b^2 > D - 1$

In this case $U(r)$ is always positive, whereas $F(r)$ is negative for small r. From Fig.11 we see that some microscopic shortcuts appear in the very beginning of the solution and after crossing the domain wall they escape to infinity.

9.2.2 $\hat{\Lambda} < 0$, $M > 0$, $b^2 < 1$

This case describes a black $(D-2)$ brane solution in AdS space. Here there is a very small region where (142) holds after the event horizon as we can see from Fig.12. We show the entire domain wall solution and we see that geodesics follow it and then decouple to fall into the event horizon at later times.

9.2.3 $\hat{\Lambda} < 0$, $M > 0$, $1 < b^2 < D - 1$

This case is also a black brane in AdS space. The region where (142) is respected is shown in Fig.13. As in the previous case all the geodesics follow

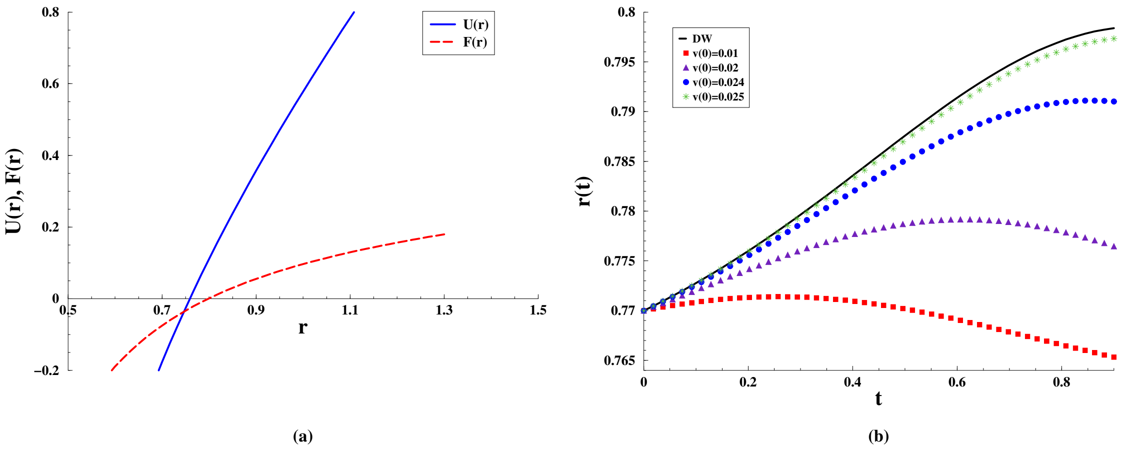

Figure 12: (a) $U(r)$ and $F(r)$ with $\hat{\Lambda} < 0$ and $M > 0$ for type II solutions, (b) Domain wall motion and geodesics for $V_0 = -1$, $\hat{V}_0 = 1$, $M = 1/10$ and $\beta = 1/\sqrt{2}$.

the domain wall and at later times fall into the event horizon.

9.2.4 $\hat{\Lambda} < 0$, $M < 0$

As $F(r)$ is always positive for all b^2, no solutions to (113) exist.

9.3 Type III Solutions

The type III solutions have $\alpha = \frac{2}{\beta(D-2)}$. In this case, the metric is given by

$$U(r) = (1+b^2)^2 r^{\frac{2}{1+b^2}} \left(-2Mr^{\frac{-1+b^2(D-3)}{1+b^2}} - \frac{2\Lambda}{(1+b^2(D-3))} \right) , \qquad (143)$$

and the scale factor is

$$R(r) = \gamma r^{\frac{b^2}{1+b^2}} , \qquad (144)$$

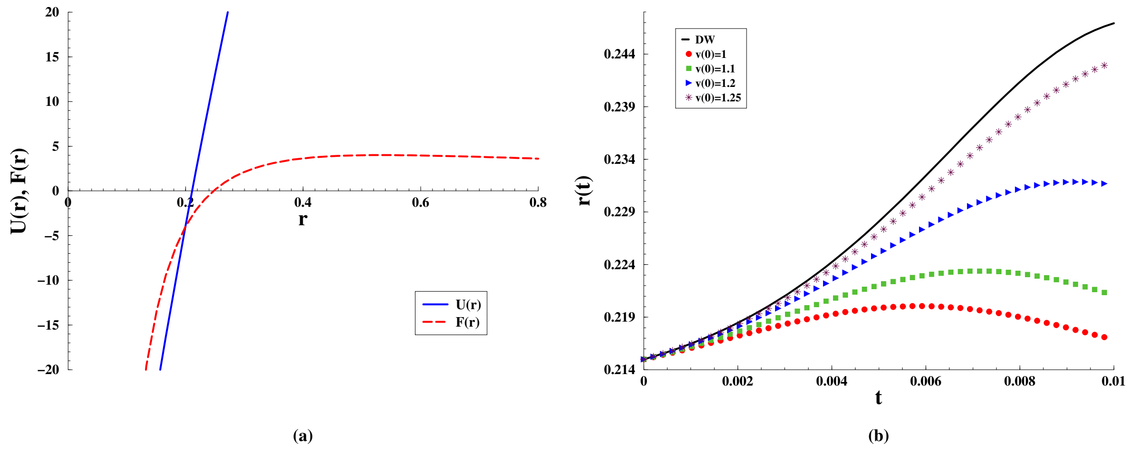

Figure 13: (a) $U(r)$ and $F(r)$ with $\hat{\Lambda} < 0$ and $M > 0$ for type II solutions, (b) Domain wall motion and geodesics for $V_0 = -1$, $\hat{V}_0 = 1$, $M = 10$ and $\beta = 2$.

where

$$\gamma = \left(\frac{(D-3)}{2k\Lambda(1-b^2)}\right)^{\frac{1}{2}} . \tag{145}$$

The values of Λ and b are the same as those given in (138) and (139).

The potential $F(R)$ is

$$\begin{aligned} F(R) &= -\frac{(D-3)b^4}{2k(1-b^2)(1+b^2(D-3))} - M\gamma^2 b^4 \left(\frac{R}{\gamma}\right)^{-\left(D-3+\frac{1}{b^2}\right)} - \\ &\quad -\frac{\hat{V}_0^2 e^{\frac{2\phi_0}{b}}\gamma^2}{8(D-2)^2}\left(\frac{R}{\gamma}\right)^{-2\left(\frac{1}{b^2}-1\right)} . \end{aligned} \tag{146}$$

If $V_0 > 0$, r turns out to be a time coordinate, while for $V_0 < 0$, it is a spatial coordinate. From the twelve cases shown in [71] we choose those where it is a spatial coordinate. For all these solutions the condition (142) applies.

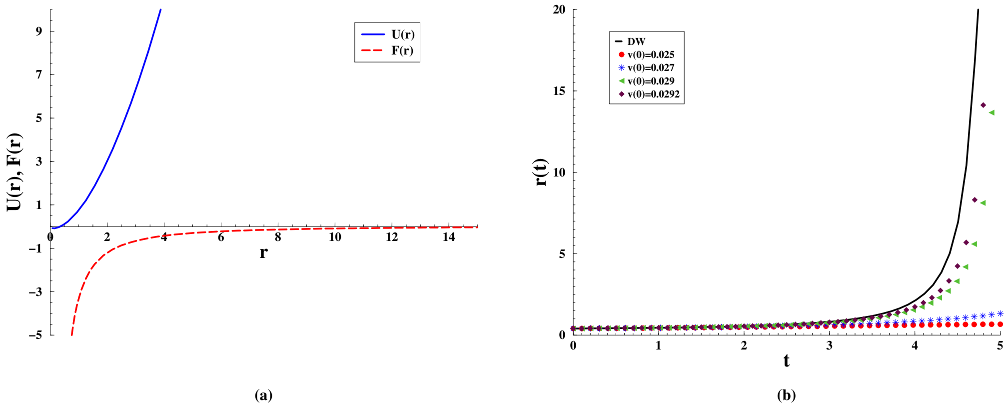

Figure 14: (a) $U(r)$ and $F(r)$ for Type III solutions with $k = -1$, $M = 1/10$ and $\beta^2 < \frac{1}{(D-2)}$, (b) Domain Wall motion and geodesics for $V_0 = -1$, $\hat{V}_0 = 1$, $\phi_0 = 1$ and $\beta = 1/\sqrt{6}$.

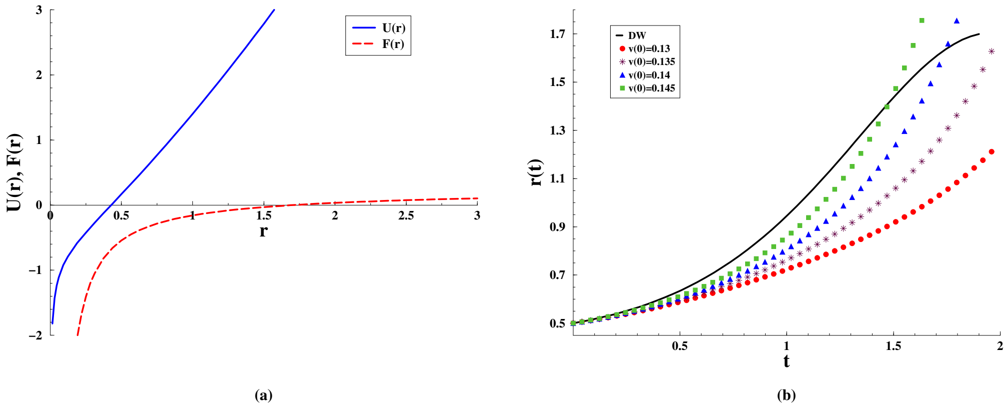

Figure 15: (a) $U(r)$ and $F(r)$ for $k = -1$, $M = 1/10$ and $V_0 < 0$ in Type III solutions, (b) Domain wall motion and geodesics with $V_0 = -1$, $\hat{V}_0 = 1$, $\phi_0 = 1$ and $\beta = 1/\sqrt{2}$.

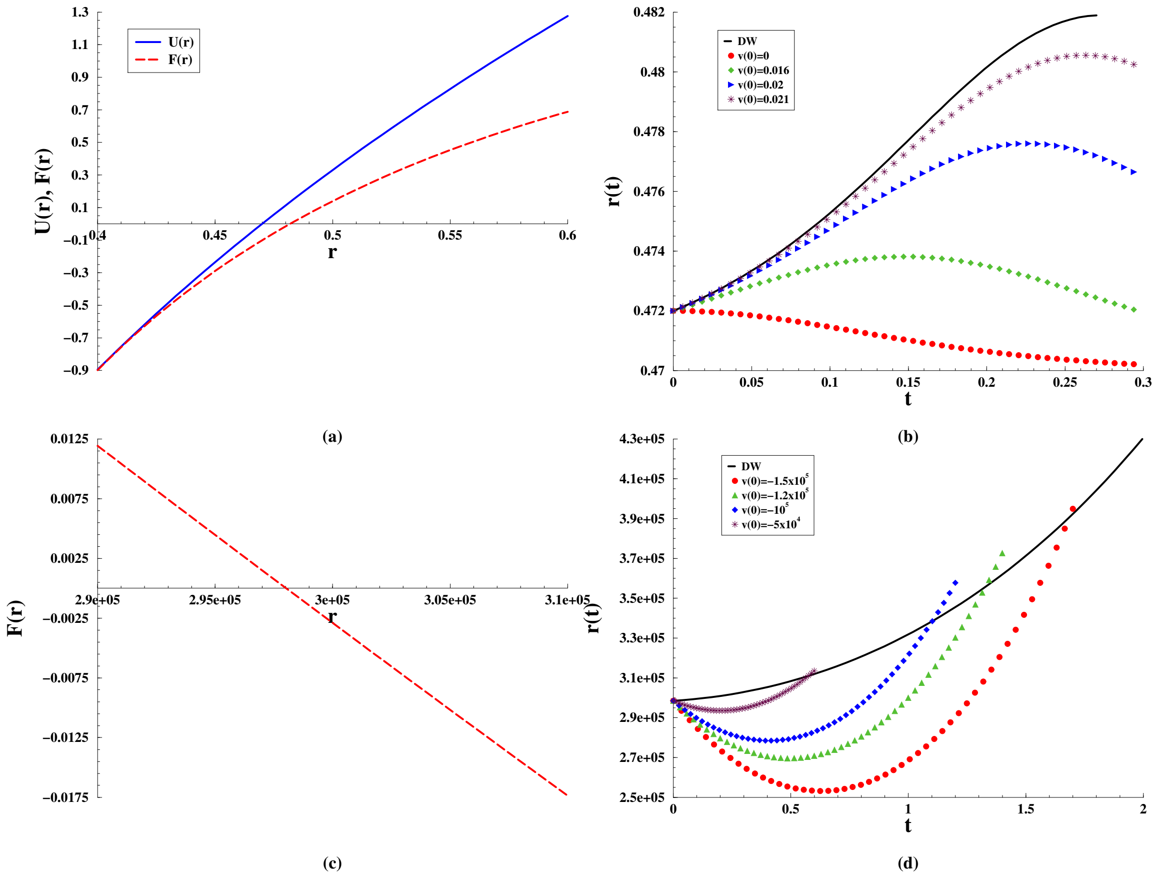

Figure 16: (a) $U(r)$ and $F(r)$ for $M = 1/10$ and $V_0 < 0$ in Type III solutions, (b) Domain wall motion and geodesics with $V_0 = -1$, $\hat{V}_0 = 1$, $\phi_0 = 1$ and $\beta = \sqrt{5}/2$, (c) $F(r)$ in the region of interest, (d) Domain wall motion and geodesics under the same conditions as (b).

9.3.1 $V_0 < 0$, $M > 0$, $b^2 < \frac{1}{(D-1)}$

This case describes a topological black hole in AdS space. From Fig.14 we can see the region where (142) holds. There are no shortcuts in this interval, and all the geodesics follow the brane and then either diverge to infinity or

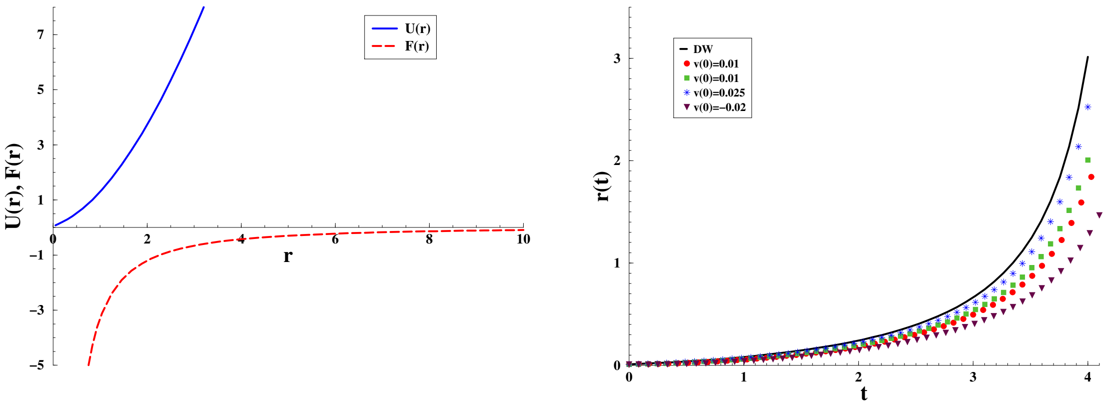

(a) (b)

Figure 17: (a) $U(r)$ and $F(r)$ for type III solutions when $k=-1$, $M=-1/10$ and $b^2<\frac{1}{(D-2)}$, (b) Domain wall motion and geodesics for $V_0=-1$, $\hat{V}_0=1$, $\phi_0=1$ and $\beta=1/\sqrt{6}$.

fall into the event horizon.

9.3.2 $V_0<0$, $M>0$, $\frac{1}{(D-1)}<b^2<1$

We again have a topological black hole in AdS space. There is a small interval where (113) has solution as we can see from Fig.15(a). Our results are shown in Fig.15(b). Notice that the domain wall equation of motion has a solution only inside the interval shown there. This means that only a group of geodesics with initial velocity $\dot{r}(0)>v_c$ can meet the domain wall after a roundabout in the bulk. It is also shown that negative initial velocities force geodesics to fall into the event horizon.

9.3.3 $V_0<0$, $M>0$, $b^2>1$

The black hole in AdS space appearing here has round spatial section. In this case $U(r)$ is always positive (then r is always a spatial coordinate); however,

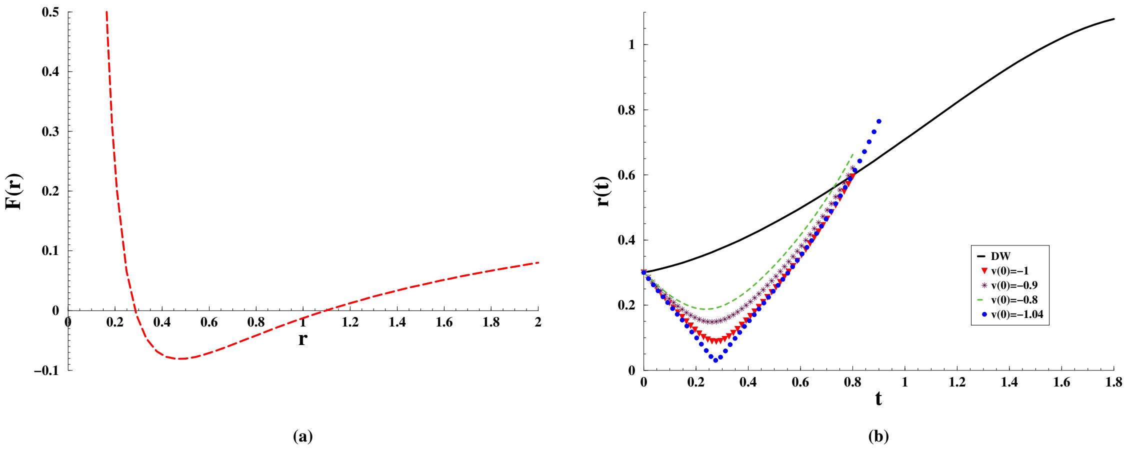

Figure 18: (a) $F(r)$ for type III solutions when $k = -1$, $M = -1/10$ and $\frac{1}{(D-2)} < b^2 < 1$, (b) Domain wall motion and geodesics for $V_0 = -1$, $\hat{V}_0 = 1$, $\phi_0 = 1$ and $\beta = 1/\sqrt{2}$.

as we must fulfill (142), we should notice that $F(r) \leq 0$ for $r \geq 3 * 10^5$. We found that shortcuts are possible for several initial velocities if $M = 0$.

The case $M > 0$ is shown in Fig.16. We have two regions of interest after the event horizon depending only on the sign of $F(r)$ since $U(r)$ is positive in this range. In the first region all the geodesics initially follow the brane and fall into the event horizon at later times. In the second region we have shortcuts again for several initial velocities.

9.3.4 $V_0 < 0$, $M < 0$, $b^2 < \frac{1}{(D-1)}$

Here $U(r)$ is always positive while $F(r)$ is negative in the range shown in Fig.17. The domain wall and the geodesics diverge after some time near the end of the range where (113) has a solution.

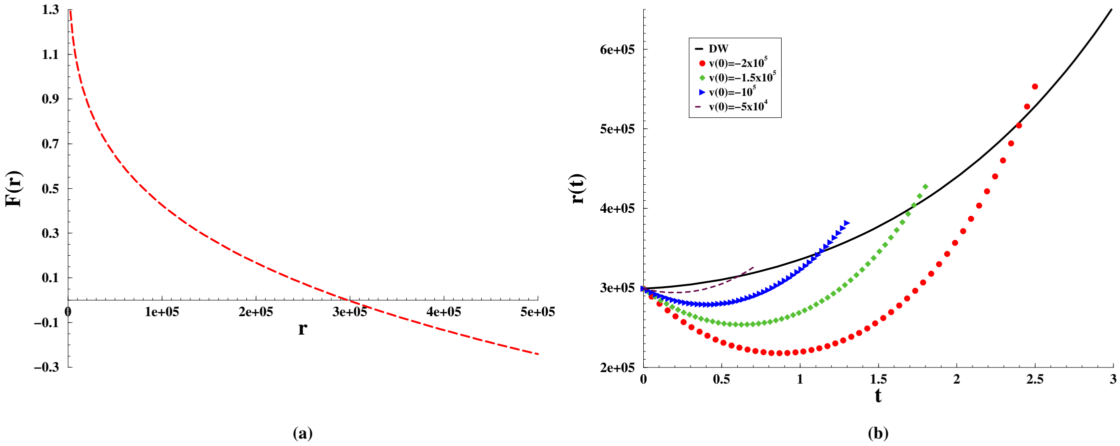

Figure 19: (a) $F(r)$ for type III solutions when $M = -1/10$ and $b^2 > 1$, (b) Domain wall motion and geodesics for $V_0 = -1$, $\hat{V}_0 = 1$, $\phi_0 = 1$ and $\beta = \sqrt{5}/2$.

9.3.5 $V_0 < 0$, $M < 0$, $\frac{1}{(D-1)} < b^2 < 1$

In this case $U(r)$ is always positive while $F(r)$ is negative for a small range as seen in Fig.18. There are several shortcuts in the region where the domain wall equation of motion has solution; nevertheless, there is a threshold velocity after which the geodesics can not return. As we can notice from Fig.18(b), the last curve displayed here ($v(0) = -1.04$) can not be consider a real shortcut since it is not a continuous solution of the geodesic equation, but represents a transition between shortcuts and geodesics falling into the naked singularity.

9.3.6 $V_0 < 0$, $M < 0$, $b^2 > 1$

Now $U(r)$ is always positive and $F(r)$ will determine the initial condition for the domain wall equation of motion. As we can see from Fig.19, several shortcuts appear.

10 Domain Wall Time and Time Delays

The time delay between the photon traveling on the domain wall and the gravitons traveling in the bulk [20] can be calculated as follows. Since the signals cover the same distance,

$$\int \frac{d\tau_\gamma}{r(\tau_\gamma)} = \int \frac{dt_g}{r_g(t_g)} \sqrt{U(r_g) - \frac{\dot{r}_g(t)^2}{U(r_g)}}\,, \tag{147}$$

the difference between photon and graviton time of flight can approximately be written as

$$\frac{\Delta\tau}{r} \simeq \int_0^{\tau_f+\Delta\tau} \frac{d\tau_\gamma}{r(\tau_\gamma)} - \int_0^{\tau_f} \frac{d\tau_g}{r(\tau_g)}\,, \tag{148}$$

or in terms of the bulk time

$$\Delta\tau \simeq r(t_f) \int_0^{t_f} dt \left(\frac{1}{r_g(t)} \sqrt{U(r_g) - \frac{\dot{r}_g(t)^2}{U(r_g)}} - \frac{1}{r(t)} \frac{d\tau}{dt} \right)\,. \tag{149}$$

The elapsed bulk time t, the corresponding domain wall time τ and the delays (149) are shown in Table 4 for all the shortcut examples considered in the present paper. Notice that $\Delta\tau < 0$ for the last geodesic solution in Fig.18 what, in fact, shows that this curve can not be considered a shortcut (it is probably falling into the naked singularity).

11 A Six-Dimensional Model

We consider a six-dimensional model, such as the one constructed by Kanti et. al. [72]. We also search for a solution of six-dimensional Einstein equation in AdS space of the form

$$ds^2 = -n^2(t,y,z)dt^2 + a^2(t,y,z)d\Sigma_k^2 + b^2(t,y,z)\left\{dy^2 + c^2(t,y,z)dz^2\right\} \tag{150}$$

where $d\Sigma_k^2$ represents the metric of the three dimensional spatial sections with $k = -1,\, 0,\, 1$ corresponding to a hyperbolic, a flat and an elliptic space, respectively.

Type II Shortcuts			
Conditions	t	τ	$\Delta\tau$
Fig.11, $v(0) = -3050$	7.5×10^{-5}	0.0025	0.0466
Fig.11, $v(0) = -1000$	4.4×10^{-5}	0.0014	0.0027
Type III Shortcuts			
Fig.15, $v(0) = 0.145$	1.49	0.970	0.210
Fig.15, $v(0) = 0.140$	1.75	1.394	0.523
Fig.16, $v(0) = -5 \times 10^4$	0.58	353	3.51
Fig.16, $v(0) = -10^5$	1.11	683	26.6
Fig.16, $v(0) = -1.2 \times 10^5$	1.33	823	48.1
Fig.16, $v(0) = -1.5 \times 10^5$	1.69	1058	104
Fig.18, $v(0) = -0.8$	0.73	0.753	0.123
Fig.18, $v(0) = -0.9$	0.78	0.808	0.148
Fig.18, $v(0) = -1$	0.81	0.842	0.111
Fig.18, $v(0) = -1.04$	0.80	0.831	-0.129
Fig.19, $v(0) = -5 \times 10^4$	0.61	372	4.11
Fig.19, $v(0) = -10^5$	1.14	703	29.2
Fig.19, $v(0) = -1.5 \times 10^5$	1.72	1081	112
Fig.19, $v(0) = -2 \times 10^5$	2.42	1568	354

Table 4: Domain wall time τ and time delays $\Delta\tau$ for shorcuts appearing in Type II and Type III Solutions

The total energy-momentum tensor can be decomposed in two parts corresponding to the bulk and the brane as

$$\tilde{T}^M_N = \breve{T}^{M(B)}_N + T^{M(b)}_N \,, \tag{151}$$

where the brane contribution can be written as

$$T^{M(b)}_N = \frac{\delta(z-z_0)}{bc}\, diag\,(-\rho, p, p, p, \hat{p}, 0)\,. \tag{152}$$

In order to have a well-defined geometry, the metric must be continuous across the brane; however, its derivatives with respect to z can be discontinuous at the position of the brane, generating a Dirac δ-function in the second derivatives of the metric with respect to z [81]. These δ function terms must be matched with the components of the brane energy-momentum tensor (152) in order to satisfy Einstein equations. Thus, we obtain the following Darmois-Israel conditions,

$$\begin{aligned}
\frac{[\partial_z a]}{a_0 b_0 c_0} &= -\frac{\kappa_{(6)}^2}{4}(p - \hat{p} + \rho)\,, \\
\frac{[\partial_z b]}{b_0^2 c_0} &= -\frac{\kappa_{(6)}^2}{4}\left\{\rho - 3(p - \hat{p})\right\}\,, \\
\frac{[\partial_z n]}{b_0 c_0 n_0} &= \frac{\kappa_{(6)}^2}{4}\left\{\hat{p} + 3(p + \rho)\right\}\,.
\end{aligned} \tag{153}$$

A metric of the form (150) satisfying six dimensional Einstein equations is given by

$$ds^2 = -h(z)dt^2 + \frac{z^2}{l^2}d\Sigma_k^2 + h^{-1}(z)dz^2\,, \tag{154}$$

where

$$d\Sigma_k^2 = \frac{dr^2}{1 - kr^2} + r^2 d\Omega_{(2)}^2 + (1 - kr^2)dy^2\,, \tag{155}$$

and

$$h(z) = k + \tfrac{z^2}{l^2} - \tfrac{M}{z^3} \quad , \quad \text{for AdS-Schwarzschild bulk}\,, \tag{156}$$

$$h(z) = k + \tfrac{z^2}{l^2} - \tfrac{M}{z^3} + \tfrac{Q^2}{z^6} \quad , \quad \text{for AdS-Reissner-Nordström bulk}\,, \tag{157}$$

with $l^{-2} \propto -\Lambda$ (Λ being the cosmological constant), which describes a black hole in the bulk, located at $z = 0$.

Following [12], we find a further solution by means of a Z_2 symmetry inverting the space with respect to the brane position. That is, considering a metric of the form

$$ds^2 = -A^2(z)dt^2 + B^2(z)d\Sigma_{(4)}^2 + C^2(z)dz^2 \tag{158}$$

and the brane to be defined at $z = z_0$, there is a solution given by

$$\begin{aligned}
&A(z),\ B(z),\ C(z) &&, \quad \text{for} \quad z \le z_0\,, \\
&A(z_0^2/z),\ B(z_0^2/z),\ C(z_0^2/z)\tfrac{z_0^2}{z^2} &&, \quad \text{for} \quad z \ge z_0\,.
\end{aligned} \tag{159}$$

The Z_2-symmetry corresponds to $z \to z_0^2/z$.

The static brane still has to obey the Darmois-Israel conditions (153), which for the metric (154) are written as

$$\begin{aligned}\frac{[\partial_z a]}{a_0^2 c_0} &= -\frac{\kappa_{(6)}^2}{4}\rho\,,\\ \frac{[\partial_z n]}{a_0 c_0 n_0} &= \frac{\kappa_{(6)}^2}{4}(4p+3\rho)\,,\end{aligned} \tag{160}$$

where here

$$\begin{aligned}[\partial_z a] &= -\frac{2}{l}\,,\\ [\partial_z n] &= -\frac{h'(z_0)}{\sqrt{h(z_0)}}\,.\end{aligned} \tag{161}$$

12 The Shortest Cut Equation

We consider the metric (150) with $k = 0$

$$ds^2 = -n^2(z)dt^2 + a^2(z)f^2(r)dr^2 + b^2(z)dy^2 + d^2(z)dz^2\,, \tag{162}$$

where the graviton path is defined equating (162) to zero. Therefore,

$$\int_{r_0}^{r} f(r')dr' = \int_{t_0}^{t} \frac{\sqrt{n^2(z) - b^2(z)\dot{y}^2 - d^2(z)\dot{z}^2}}{a(z)}dt \equiv \int_{t_0}^{t} \mathcal{L}\left[y(t), \dot{y}(t), z(t), \dot{z}(t); t\right] dt \tag{163}$$

which naturally defines a lagrangian density. The Euler-Lagrange equations of $\mathcal{L}$ define the graviton path. We first choose to work at a constant y to check on the very possibility of (162) allowing shortcuts. In this case the resulting equation is simple but far from trivial,

$$\ddot{z} + \left(\frac{a'}{a} - 2\frac{n'}{n} + \frac{d'}{d}\right)\dot{z}^2 + \left(\frac{nn'}{d^2} - \frac{a'}{a}\frac{n^2}{d^2}\right) = 0\,. \tag{164}$$

For $z \leq z_0$, $a = z/l$, $n = \sqrt{h(z)}$, and $d = 1/\sqrt{h(z)}$. For $z \geq z_0$ we have to use the Z_2 symmetry showed up in (159).

Notice that this case is equivalent to consider the problem in five dimensions with the metric shown in [12].

The most general case includes a y dependence on the graviton path; however, as we will show in what follows, this dependence turns to be superflous and does not affect z-equation since (164) is independently satisfied. This conclusion is not surprising if we notice that the metric (162) is y-independent.

The two Euler-Lagrange equations considering a y dependence are then given by

$$\begin{aligned}(n^2-d^2\dot{z}^2)\ddot{y}+\dot{z}\left\{\left(-\frac{a'}{a}+2\frac{b'}{b}\right)(n^2-d^2\dot{z}^2)-nn'+\right.\\ \left.+dd'\dot{z}^2+d^2\ddot{z}\right\}\dot{y}+b^2\left(\frac{a'}{a}-\frac{b'}{b}\right)\dot{z}\dot{y}^3=0\end{aligned} \tag{165}$$

and

$$\begin{aligned}(n^2-b^2\dot{y}^2)\ddot{z}+\left\{\left(\frac{a'}{a}+\frac{d'}{d}\right)(n^2-b^2\dot{y}^2)-2nn'+\right.\\ \left.+2bb'\dot{y}^2\right\}\dot{z}^2+(b^2\dot{y}\ddot{y})\dot{z}+\\ +\left\{-\frac{a'}{ad^2}(n^2-b^2\dot{y}^2)+\frac{nn'-bb'\dot{y}^2}{d^2}\right\}(n^2-b^2\dot{y}^2)=0\,.\end{aligned} \tag{166}$$

It is clear that the case $\dot{y}=0$ is a solution of this set of equations when at the same time z obeys (164).

This set of equations can be handled leading to

$$\begin{aligned}\frac{z\dot{z}\dot{y}}{h(z)}F_z+\left(h(z)-\frac{\dot{z}^2}{h(z)}\right)F_y &= 0\,,\\ \left(1-\frac{z^2\dot{y}^2}{h(z)}\right)F_z+\frac{z\dot{z}\dot{y}}{h(z)}F_y &= 0\,,\end{aligned} \tag{167}$$

where

$$\begin{aligned}F_y &= \ddot{y}+\dot{z}\left(\frac{2}{z}-\frac{h'(z)}{h(z)}\right)\dot{y}\,,\\ F_z &= \frac{\ddot{z}}{z}+\frac{\dot{z}^2}{z^2}\left(1-\frac{3}{2}z\frac{h'(z)}{h(z)}\right)+\frac{h(z)}{z}\left(\frac{h'(z)}{2}-\frac{h(z)}{z}\right)\,.\end{aligned} \tag{168}$$

Since the determinant of the set (167) is non-zero, the solutions of (165) and (166) must satisfy $F_y=0$ and $F_z=0$ independently. Furthermore, let us notice that $F_y = 0$ and $F_z = 0$ are the null geodesic equations for y and z respectively obtained from

$$\ddot{x}^\alpha + \Gamma^\alpha_{\mu\nu}\dot{x}^\mu\dot{x}^\nu = \lambda\dot{x}^\alpha \,. \tag{169}$$

Thus, a null curve is extreme if and only if it is a null geodesic.

Then, as (168) is the same as (164), our problem is reduced to the previous case with constant y described by (164).

For $k \neq 0$ cases we can also consider (164) as the shortcut equation if we assume the existence of a y-symmetry in our problem. In this way, our model represents a generalization of [12].

13 AdS-Schwarzschild Bulk

From the Darmois-Israel conditions (160) together with (161) we have

$$\frac{h}{z_0^2} = \frac{\kappa_{(6)}^4\rho^2}{64}\,, \tag{170}$$

$$\frac{h'}{2z_0} = -\frac{\kappa_{(6)}^4\rho^2}{64}(4\omega+3)\,, \tag{171}$$

and we can obtain the black hole mass M as a function of the brane energy density ρ, while ρ is fixed by a *fine-tunning*,

$$\frac{M}{z_0^5} = \frac{2}{5}\frac{k}{z_0^2} - (\omega+1)\frac{\kappa_{(6)}^4\rho^2}{40}\,, \tag{172}$$

$$\frac{\kappa_{(6)}^4\rho^2}{64} = -\frac{3k}{z_0^2(8\omega+3)} - \frac{5}{(8\omega+3)l^2}\,, \tag{173}$$

where $\omega = p/\rho$.

As we saw in the previous section, the shortcuts in six dimensions are determined from (164). We should also remember that the brane is static at $z = z_0$.

If a shortcut exists, there must be a time $t = v$ in the graviton path when $\dot{z}(v) = 0$ and $\ddot{z}(v) \geq 0$. Thus, (164) evaluated at this point will give

$$\ddot{z}(v) + h(z_v)\left(\frac{h'(z_v)}{2} - \frac{h(z_v)}{z_v}\right) = 0\,. \tag{174}$$

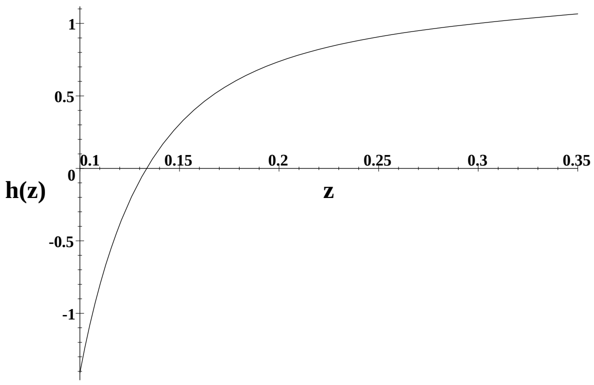

Figure 20: $h(z)$ in six-dimensional AdS-Schwarzschild bulk with the brane located at $z = 1/3$. Notice that the singularity is shielded by a horizon.

It is obvious that this minimum must be between the brane and the event horizon z_h, if a horizon exists. Otherwise, there is no turning point in the path since the graviton can not return after it goes through the event horizon. Hence, $h(z_v) > 0$. Thus, from (174) we require

$$F(z_v) = \frac{h'(z_v)}{2} - \frac{h(z_v)}{z_v} \leq 0 \quad \text{for} \quad z_h < z_v < z_0 \,. \tag{175}$$

Using (156) this implies

$$F(z_v) = \frac{5}{2}\frac{M}{z_v^4} - \frac{k}{z_v} \leq 0 \,. \tag{176}$$

This equation has a zero in $z = z_f \neq 0$ for $k \neq 0$

$$z_f^3 = \frac{5}{2k} M \,.$$

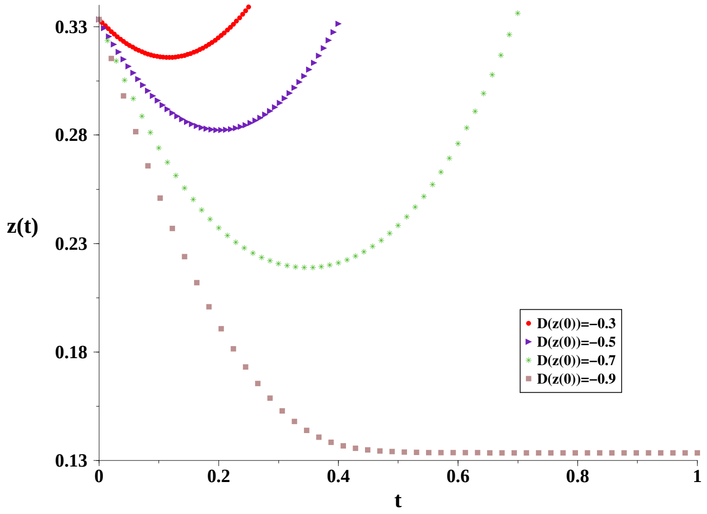

Figure 21: Shortcuts for several initial velocities in six-dimensional AdS-Schwarzschild bulk. Notice that there is a threshold initial velocity for which the graviton can not return to the brane and falls into the event horizon.

Thus, for the $k = 0$ or $k = -1$ cases there is no positive root. Since the mass, M, is positive, $F(z) > 0$ everywhere preventing the coexistence of shortcuts and horizons.

On the other hand, for $k = 1$ there is one real and positive root, which must satisfy $z_f < z_0$ in order to have shortcuts. This is

$$\frac{5M}{2z_0^3} - 1 < 0\,.$$

Taking into account (172) and the fact that ε^2 must be positive in (173) [2]

$$-4(\omega+1)\varepsilon^2 z_0^2 < 0\,, \tag{177}$$

[2]From now on, we will denote $\varepsilon^2 = \kappa_{(6)}^4 \rho^2/64$ in six dimensions.

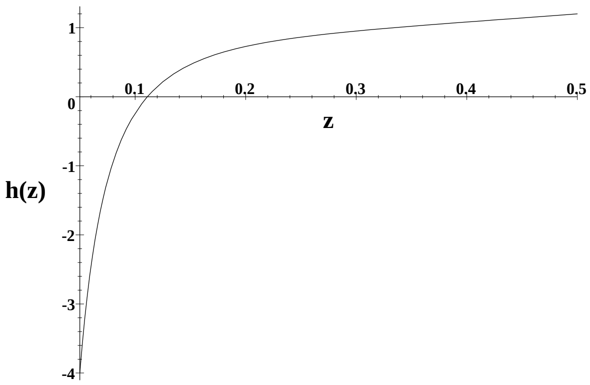

Figure 22: $h(z)$ in five-dimensional AdS-Schwarzschild bulk with the brane located at $z = 1/2$. Notice that the singularity is shielded by a horizon.

then

$$\omega + 1 > 0 \,. \tag{178}$$

Now, let us study the conditions under which the event horizon must appear. In general, the horizons occur at the zeros of $h(z)$, or equivalently at the zeros of

$$z^5 + z^3 l^2 - l^2 M \,.$$

In the meantime, the non-vanishing zeros of $h'(z)$ occur when

$$2z^5 + 3l^2 M = 0 \,.$$

Since the derivative has no positive zeros with $M > 0$, there is just one event horizon. Then as $h(z)$ goes to $-\infty$ at the origin, the conditions

$$M > 0 \tag{179}$$

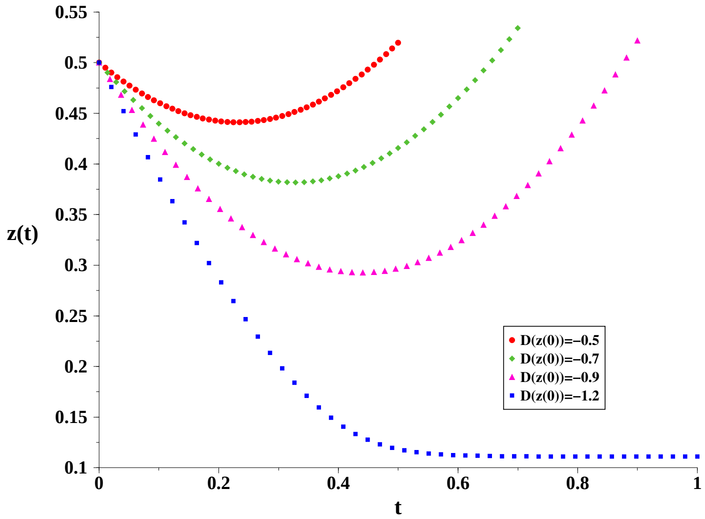

Figure 23: Shortcuts for several initial velocities in five-dimensional AdS-Schwarzschild bulk. As in the six dimensional case, there is a threshold initial velocity for which the graviton can not return to the brane and falls into the event horizon.

and

$$h(z_0) > 0 \tag{180}$$

are necessary and, in fact, enough to have a horizon and assure that the brane lies after it.

The condition (180) is automatically satisfied due to equation (170).

To fulfill (179) let us substitute (173) into (172) to have

$$(\omega + \frac{3}{4}) + (\omega + 1)\frac{z_0^2}{l^2} < 0\,.$$

If $\omega + 1 \leq 0$, this condition is always satisfied, but this configuration does not produce shortcuts as we would like. However, the condition is also satisfied with $\omega + 1 > 0$ if we require

$$-1 < \omega < -\frac{3}{4}\,, \tag{181}$$

and

$$\frac{z_0^2}{l^2} < -\frac{\omega + 3/4}{\omega + 1}\,. \tag{182}$$

If we follow both (181) and (182) together with the fine-tunning for the energy (173), we will have several shortcuts in AdS-Schwarzschild bulks with shielded singularity. In figures 20 and 21 we illustrate an example with $\omega = -4/5$, $z_0 = 1/3$, and $l = 1$. Notice in figure 20 that the horizon appears before the brane.

Since this case is equivalent to consider the problem in five dimensions with $h(z)$, M and ρ given in [12], analogous results are obtained. In this case, the fine-tunning in the energy is given by [3]

$$\varepsilon_{(5)}^2 = -\frac{1}{3\omega + 1}\left(\frac{1}{z_0^2} + \frac{2}{l^2}\right)\,, \tag{183}$$

and ω is confined to

$$-1 < \omega < -\frac{2}{3}\,, \tag{184}$$

while the brane position is given by

$$\frac{z_0^2}{l^2} < -\frac{\omega + 2/3}{\omega + 1}\,. \tag{185}$$

An example is shown in figures 22 and 23 for $\omega = -3/4$, $z_0 = 1/2$, and $l = 1$.

14 AdS-Reissner-Nordström Bulk

From the Darmois-Israel conditions (160) we will have for the black hole mass and charge,

$$\begin{aligned} \frac{M}{z_0^5} &= \frac{2k}{z_0^2} + \frac{8}{3l^2} + \frac{\kappa_{(6)}^4}{24}\rho^2\omega\,, \\ \frac{Q^2}{z_0^8} &= \frac{k}{z_0^2} + \frac{5}{3l^2} + \frac{8\omega + 3}{3}\,\frac{\kappa_{(6)}^4\rho^2}{64}\,. \end{aligned} \tag{186}$$

[3] In this case $\varepsilon_{(5)}^2 = \kappa_{(5)}^4\rho^2/36$.

At this stage it is convenient to carefully study the possibility of existence of shortcuts for every value of k.

14.1 $k = 0$ and $k = -1$ Cases

As it was found in the AdS-Schwarzschild case, (175) determines the existence of shortcuts. Using (157) we see that (175) has a zero in $z = z_f \neq 0$ when

$$\frac{5}{2} M z_f^3 - 4Q^2 - k z_f^6 = 0\,. \tag{187}$$

If $k = 0$, we have a real root in

$$z_f^3 = \frac{8Q}{5M}\,. \tag{188}$$

If $k = 1$, we have two roots in

$$z_f^3 = \frac{5}{4} M \pm \frac{1}{4}\sqrt{25M^2 - 64Q^2}\,. \tag{189}$$

Finally, if $k = -1$, we have

$$z_f^3 = -\frac{5}{4} M \pm \frac{1}{4}\sqrt{25M^2 + 64Q^2}\,. \tag{190}$$

Notice that $F(z)$ has at most one real and positive zero if $k = 0, -1$ and at most two positive zeros if $k = 1$.

Analyzing $h(z)$ and its derivative we see that $h(z)$ tends to $+\infty$ both at the singularity and at infinity, while $h'(z)$ tends to $-\infty$ at the singularity and to $+\infty$ at infinity.

The horizons occur at the zeros of $h(z)$, or equivalently, at the zeros of

$$z^8 + l^2 k z^6 - l^2 M z^3 + l^2 Q^2 = 0\,. \tag{191}$$

On the other hand, the non-vanishing zeros of $h'(z)$ occur when

$$2z^8 + 3l^2 M z^3 - 6l^2 Q^2 = 0\,. \tag{192}$$

This polynom grows at infinity being negative at the origin. Its derivative has non-vanishing roots when

$$16z^5 + 9l^2 M = 0\,. \tag{193}$$

For $M > 0$ this equation is never satisfied. Thus, as the derivative of (192) does not vanish and is positive outside the origin, the polynom (192) grows monotonically and has just one root. The zeros of this polynom are all non-vanishing zeros of $h'(z)$. Therefore, we conclude that for positive mass there is just one zero for $h'(z)$, and hence, at most two horizons for $h(z)$.

When there is one horizon, $h'(z)$ is negative before it and positive after, crossing $h(z)$ at the very horizon. If there are two horizons, $h'(z)$ vanishes at a point between Cauchy and event horizons, being negative before this point and positive after, while $h(z)$ is positive at all points except between both horizons. Taking into account both the sign and zeros of these functions, $h'(z)$ crosses $h(z)$ between the Cauchy horizon and the point at which $h'(z)$ vanishes.

Since $h'(z)/2$ has the same sign as $h'(z)$ and vanishes at the same point, and in the same way $h(z)/z$ has the same sign of $h(z)$ and vanishes at the same points, we conclude that, existing horizons, $F(z)$ necessarily vanishes at some point $z = z_c$ such that $0 < z_c \leq z_h$. However, as we pointed out before, for $k = 0$ or $k = -1$ there is only one positive root of $F(z)$. As $F(z) < 0$ for $z < z_c$, then $F(z) > 0$ for $z > z_c$. Thus, because $z_c \leq z_h$, $F(z) > 0$ for $z > z_h$ contrary to what was required in (175). This implies that there are no shortcuts with $k = 0$ or $k = -1$ when horizons exist.

In five dimensions the proof is very similar and we arrive to the same conclusion.

14.2 $k = 1$ Case

As we saw in the previous section, $F(z)$ has two real, positive and distinct roots for $k = 1$,

$$r_1^3 = \frac{5}{4}M - \frac{1}{4}\sqrt{25M^2 - 64Q^2}\,, \tag{194}$$

$$r_2^3 = \frac{5}{4}M + \frac{1}{4}\sqrt{25M^2 - 64Q^2}\,. \tag{195}$$

This is the only situation where the shortcuts can coexist with a shielded singularity. In fact, this situation necessarily requires the second root of $F(z)$ being at some point before the brane position z_0. This also implies $F(z_0) < 0$.

In addition, we must have both Q^2 and M positive.

Given the fact that we have horizons, if the brane is not between them or at a horizon position, then $h(z_0) > 0$. Furthermore, in order to guarantee that the brane is located after the event horizon, we also need $h'(z_0) > 0$.

From the discussion in the previous section we will have one or two horizons if and only if $h(r_1) \leq 0$.

In summary, shortcuts in bulks with shielded singularities can occur only if $k = 1$ and also if the following conditions are supplied,

1. $h(z_0) > 0$ and $h'(z_0) > 0$ to have both horizons before the brane.
2. $F(z_0) < 0$ and $r_2 < z_0$ to have shortcuts with shielded singularity.
3. $Q^2 > 0$ and $M > 0$, which assures the positivity of the black hole mass and charge.
4. $h(r_1) \leq 0$ in order to have horizons.

We will analyze each condition and impose certain restrictions on ω, ρ^2, and z_0.

14.2.1 Existence of Both Horizons Before the Brane

These conditions are the simplest to analyze since they restrict ω directly from the Darmois-Israel conditions (160) together with (161)

$$\begin{aligned} \frac{h(z_0)}{z_0^2} &= \varepsilon^2\,, & (196)\\ \frac{h'(z_0)}{2z_0} &= -(4\omega+3)\varepsilon^2\,. & (197) \end{aligned}$$

The condition (196) is automatically satisfied since $\varepsilon^2 > 0$.

From the condition (197)

$$-(4\omega+3)\varepsilon^2 > 0\,, \tag{198}$$

we have our first restriction

$$\omega < -3/4\,. \tag{199}$$

14.2.2 Existence of Shortcuts with Shielded Singularity

From the definition of $F(z)$, (175), and using (196) and (197) we see that

$$0 > F(z_0) = -4(\omega+1)\varepsilon^2 z_0 \,. \tag{200}$$

Thus we find another condition on ω

$$\omega + 1 > 0 \,. \tag{201}$$

Besides, from $r_2 < z_0$

$$\frac{5M}{4} - z_0^3 < -\frac{1}{4}\sqrt{25M^2 - 64Q^2} \,. \tag{202}$$

This equation will be satisfied if [4]

$$\frac{5M}{4} - z_0^3 < 0 \,, \tag{203}$$

or using (186)

$$\frac{3}{2}z_0^3 + \frac{10}{3}z_0^5 + \frac{10}{3}z_0^5\omega\varepsilon^2 < 0 \,, \tag{204}$$

and as $\omega < -3/4$

$$z_0^2\varepsilon^2 > \frac{1}{\omega}\left(-\frac{9}{20} - \frac{z_0^2}{l^2}\right) \,. \tag{205}$$

14.2.3 Positivity of the Black Hole Mass and Charge

Because we require the positivity of the black hole mass, from (186) we have

$$\frac{M}{z_0^3} > 0 \quad \Rightarrow \quad \frac{z_0^2}{l^2} + \omega\varepsilon^2 z_0^2 > -\frac{3}{4} \,, \tag{206}$$

thus,

$$z_0^2\varepsilon^2 < \frac{1}{\omega}\left(-\frac{3}{4} - \frac{z_0^2}{l^2}\right) \,. \tag{207}$$

[4] We assume that $25M^2 - 64Q^2 > 0$. We will return to this condition when we discuss the existence of horizons, where we will impose a stronger restriction, $M^2 - 4Q^2 > 0$.

Since $3/4 > 9/20$ this condition is certainly compatible with (205).

On the other hand, the positivity of the squared black hole charge requires

$$\frac{Q^2}{z_0^6} > 0 \quad \Rightarrow \quad 1 + \frac{5z_0^2}{3l^2} + \left(\frac{8}{3}\omega + 1\right) z_0^2 \varepsilon^2 > 0\,, \tag{208}$$

so that

$$z_0^2 \varepsilon^2 < \frac{1}{8\omega + 3}\left(-3 - \frac{5z_0^2}{l^2}\right)\,. \tag{209}$$

In spite of not being trivial, this equation is also compatible with (205). This requires

$$\frac{1}{\omega}\left(-\frac{9}{20} - \frac{z_0^2}{l^2}\right) < \frac{1}{8\omega + 3}\left(-3 - \frac{5z_0^2}{l^2}\right)\,, \tag{210}$$

or

$$-\frac{1}{5}\left(\omega + \frac{9}{4}\right) - \frac{z_0^2}{l^2}\left(\omega + 1\right) < 0\,, \tag{211}$$

what is always true for $-1 < \omega < -3/4$.

14.2.4 Existence of Horizons

This is the last and the more complicated of our conditions. We must have $h(r_1) \leq 0$. Let x be r_1^3,

$$\frac{x^{8/3}}{l^2} + x^2 - Mx + Q^2 \leq 0\,. \tag{212}$$

We do not need to do a complete study of this equation. For our purposes it will be enough to require

$$x^2 - Mx + Q^2 < 0\,. \tag{213}$$

Using (194) this implies

$$M^2 - 4Q^2 > 0\,. \tag{214}$$

This condition is necessary but not enough to have horizons. However, this restriction added to the others developed in this section will be enough to construct shortcuts with horizons as we will see. Notice that this condition is stronger than that one assumed before, $M > 8/5\,Q$.

Using (186) in (214),

$$(1-\varepsilon^2 l^2)+\frac{16}{9}\frac{z_0^2}{l^2}\left(1+\omega\varepsilon^2 l^2\right)^2>0\,. \qquad (215)$$

We know from (205) that $1-\varepsilon^2 l^2$ must be negative. Therefore, we must very carefully analyze (215). We can interpret (215) as a quadratic equation in the energy

$$\left(1+\frac{16}{9}\frac{z_0^2}{l^2}\right)+\left(\frac{32}{9}\omega z_0^2-l^2\right)\varepsilon^2+\left(\frac{16}{9}l^2 z_0^2\omega^2\right)\varepsilon^4>0\,, \qquad (216)$$

what implies

$$z_0^2\varepsilon^2>\frac{1}{32}\left(-32\omega z_0^2+9l^2+3\sqrt{-64\omega z_0^2 l^2+9l^4-64l^2 z_0^2\omega^2}\right)/(\omega^2 l^2)\,, \quad (217)$$

or

$$z_0^2\varepsilon^2<\frac{1}{32}\left(-32\omega z_0^2+9l^2-3\sqrt{-64\omega z_0^2 l^2+9l^4-64l^2 z_0^2\omega^2}\right)/(\omega^2 l^2)\,. \quad (218)$$

Notice that because $-1<\omega<-3/4$,

$$-64\omega z_0^2 l^2-64l^2 z_0^2\omega^2=-64\omega(\omega+1)z_0^2 l^2>0$$

and all the previous roots are real and positive.

Summarizing, from the considerations in the previous sections, we must have for ω

$$-1<\omega<-3/4\,. \qquad (219)$$

For the energy,

$$\tfrac{1}{\omega}\left(-\tfrac{9}{20}-\tfrac{z_0^2}{l^2}\right)<z_0^2\varepsilon^2<\tfrac{1}{\omega}\left(-\tfrac{3}{4}-\tfrac{z_0^2}{l^2}\right)\,, \qquad \text{or} \qquad (220)$$

$$\tfrac{1}{\omega}\left(-\tfrac{9}{20}-\tfrac{z_0^2}{l^2}\right)<z_0^2\varepsilon^2<\tfrac{1}{8\omega+3}\left(-3-\tfrac{5z_0^2}{l^2}\right)\,, \qquad (221)$$

depending on which condition is more restrictive.

In addition,

$$z_0^2\varepsilon^2>\tfrac{1}{32}\left(-32\omega z_0^2+9l^2+3\sqrt{-64\omega z_0^2 l^2+9l^4-64l^2 z_0^2\omega^2}\right)/(\omega^2 l^2), \quad (222)$$

or

$$z_0^2\varepsilon^2<\tfrac{1}{32}\left(-32\omega z_0^2+9l^2-3\sqrt{-64\omega z_0^2 l^2+9l^4-64l^2 z_0^2\omega^2}\right)/(\omega^2 l^2) \quad (223)$$

Now we are going to analyze the situations in which all these conditions are compatible.

Let us begin our analysis with equation (223). To be compatible with (220) and (221), we just need

$$\frac{1}{\omega}\left(-\frac{9}{20}-\frac{z_0^2}{l^2}\right) < \frac{1}{32}\left(-32\omega z_0^2+9l^2-3\sqrt{-64\omega z_0^2 l^2+9l^4-64l^2 z_0^2\omega^2}\right)/(\omega^2 l^2)\,, \tag{224}$$

that is,

$$-\frac{9}{20}\omega-\frac{9}{32}+\frac{3}{32}\sqrt{-64\omega\frac{z_0^2}{l^2}+9-64\frac{z_0^2}{l^2}\omega^2} < 0\,. \tag{225}$$

Since $3/4 <\mid \omega \mid< 1$,

$$-\frac{9}{20}\omega-\frac{9}{32}$$

will always be positive and thus, (225) will never be satisfied. Then, we conclude that (223) is not compatible either with (220) or (221). This implies that $z_0^2\varepsilon^2$ must satisfy (222) together with (220) or (221).

Let us initially compare (220) with (222). We must have

$$\frac{1}{\omega}\left(-\frac{3}{4}-\frac{z_0^2}{l^2}\right) > \frac{1}{32}\left(-32\omega z_0^2+9l^2+3\sqrt{-64\omega z_0^2 l^2+9l^4-64l^2 z_0^2\omega^2}\right)/(\omega^2 l^2)\,, \tag{226}$$

that is,

$$-\frac{3}{4}\omega-\frac{9}{32}-\frac{3}{32}\sqrt{-64\omega\frac{z_0^2}{l^2}+9-64\frac{z_0^2}{l^2}\omega^2} > 0\,. \tag{227}$$

In this case, since ω is negative and $3/4 <\mid \omega \mid< 1$,

$$-\frac{3}{4}\omega-\frac{9}{32} > 0$$

and (227) can be satisfied if

$$\left(-\frac{3}{4}\omega-\frac{9}{32}\right)^2 > \frac{9}{1024}\left(-64\omega\frac{z_0^2}{l^2}+9-64\frac{z_0^2}{l^2}\omega^2\right)\,, \tag{228}$$

or

$$\frac{9}{16}\omega(\omega+1)\frac{z_0^2}{l^2}+\frac{9}{64}(3+4\omega)\omega > 0\,. \tag{229}$$

Since $\omega + 1 > 0$ and $3 + 4\omega < 0$, for positive z_0 the inequality will be only fulfilled if

$$\frac{z_0}{l} < \frac{1}{2}\sqrt{-\frac{3+4\omega}{1+\omega}}\,. \tag{230}$$

So that (222) and (220) can be compatible.

Now we are going to analyze the compatibility between (222) and (221). We must have

$$\frac{1}{8\omega+3}\left(-3-\frac{5z_0^2}{l^2}\right)+\frac{z_0^2}{\omega l^2}-\frac{9}{32\omega^2} > \frac{3}{32\omega^2}\sqrt{-64\omega z_0^2 l^2 + 9l^4 - 64 l^2 z_0^2 \omega^2}\,. \tag{231}$$

or using that $8\omega + 3 < 0$, simplifying, and squaring both sides we can write (231) as

$$\frac{1}{16}\omega^2(3+4\omega)^2+\omega^2(\omega+1)^2\left(\frac{z_0^2}{l^2}\right)^2+\frac{\omega^2}{2}(3+4\omega)(\omega+1)\frac{z_0^2}{l^2} > 0\,. \tag{232}$$

This polynom has just one root for z_0^2/l^2

$$\frac{z_0^2}{l^2} = -\frac{1}{4}\left(\frac{3+4\omega}{1+\omega}\right)\,.$$

Since the coeficient of z_0^4/l^4 is positive, the inequality is satisfied with the same condition (230), so we verify that both (221) and (220) are compatible with (222) under the same restrictions.

Furthermore, let us compare the upper limits of (220) and (221). Suppose

$$\frac{1}{\omega}\left(-\frac{3}{4}-\frac{z_0^2}{l^2}\right) > \frac{1}{8\omega+3}\left(-3-\frac{5z_0^2}{l^2}\right)\,, \tag{233}$$

what can also be written as

$$-\frac{3}{4}(4\omega+3)-\frac{3z_0^2}{l^2}(\omega+1) > 0\,. \tag{234}$$

Thus, (233) is satisfied if and only if

$$\frac{z_0^2}{l^2} < -\frac{1}{4}\left(\frac{3+4\omega}{1+\omega}\right)\,, \tag{235}$$

which is just the same inequality (230), that z_0 must satisfy. Hence, between (220) and (221), it is enough to take into account the latter. Nevertheless, from (232) notice that (221) would be also compatible with (222) if

$$\frac{z_0^2}{l^2} > -\frac{1}{4}\left(\frac{3+4\omega}{1+\omega}\right) ,$$

and (233) would be satisfied with a change of sign implying that we should consider (220) instead of (221); however, as stated before, the compatibility of (220) and (222) requires

$$\frac{z_0^2}{l^2} < -\frac{1}{4}\left(\frac{3+4\omega}{1+\omega}\right) ,$$

which contradicts our hypothesis. Therefore, the only possible configuration is (235).

At last, we compare the lower limits of (221) and (222). Suppose

$$\frac{1}{\omega}\left(-\frac{9}{20}-\frac{z_0^2}{l^2}\right) < \frac{1}{32\omega^2 l^2}\left(-32\omega z_0^2 + 9l^2 + 3\sqrt{-64\omega z_0^2 l^2 + 9l^4 - 64l^2 z_0^2\omega^2}\right) , \tag{236}$$

or

$$-\frac{9}{20}\omega - \frac{9}{32} < \frac{3}{32}\sqrt{-64\omega\frac{z_0^2}{l^2} + 9 - 64\frac{z_0^2}{l^2}\omega^2} .$$

Squaring and simplifying we obtain

$$\frac{z_0^2}{l^2} > -\frac{9}{20(\omega+1)}\left(\frac{4}{5}\omega + 1\right) .$$

For $-1 < \omega < -3/4$ this inequality is always satisfied since the right hand side is negative. Hence, we conclude that (236) is valid and between the lower limits for the energy in (221) and (222), we just need to choose the latter.

In short, by purely analytic considerations we conclude that shortcuts in bulks having no naked singularities and a static brane embedded in can only appear if $k = 1$ and if the following conditions are satisfied,

1. We must choose ω such that $-1 < \omega < -3/4$;

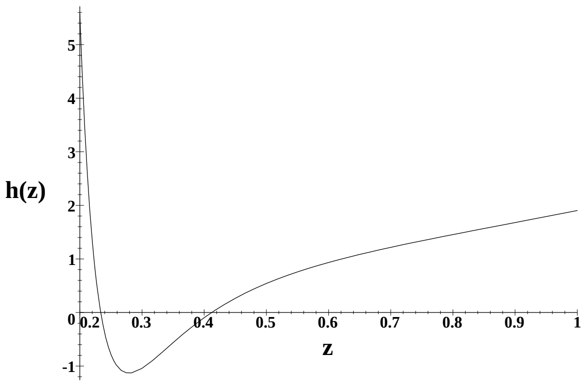

Figure 24: $h(z)$ in six-dimensional AdS-Reissner-Nordström bulk with the brane located at $z = 1$. Notice that the singularity is shielded by two horizons.

2. Given ω, the brane must be located at a position such that
$$\frac{z_0}{l} < \frac{1}{2}\sqrt{-\frac{3+4\omega}{1+\omega}}\,, \tag{237}$$
which is the same condition as AdS-Schwarzschild case (182);

3. Given (237), the energy ε must satisfy

$$\frac{1}{32\omega^2}\left(-\frac{32\omega z_0^2}{l^2}+9+3\sqrt{-64\omega\frac{z_0^2}{l^2}+9-64\frac{z_0^2}{l^2}\omega^2}\right) < z_0^2\varepsilon^2 < \frac{1}{8\omega+3}\left(-3-\frac{5z_0^2}{l^2}\right)\,. \tag{238}$$

In this way, it turns out to be simple to find shortcuts in bulks with shielded singularities.

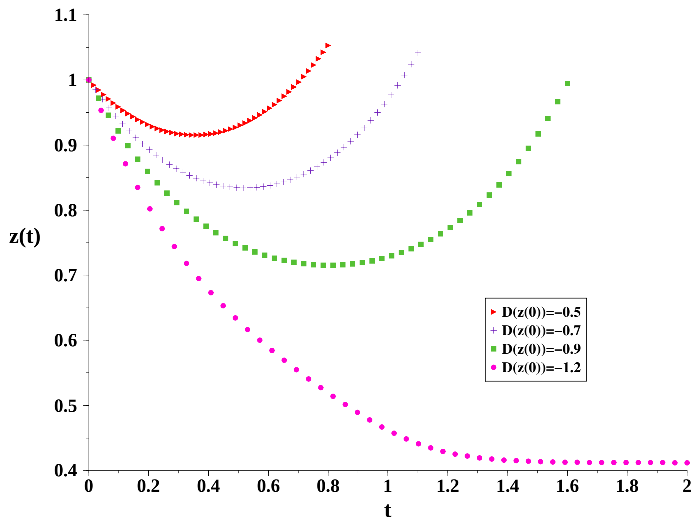

Figure 25: Shortcuts for several initial velocities in six-dimensional AdS-Reissner-Nordström bulk. Notice that there is threshold initial velocity for which the graviton can not return to the brane and falls into the event horizon.

As an example, let us choose $\omega = -9/10$. From (237) we must have

$$\frac{z_0}{l} < \frac{\sqrt{6}}{2},$$

then we choose $l = 1$ and $z_0 = 1$.

From (238) we have

$$\frac{35}{24} + \frac{5}{72}\sqrt{41} < \varepsilon^2 < \frac{40}{21},$$

so we choose $\varepsilon = \sqrt{238/125}$.

In figure (24) we plot $h(z)$ with these conditions. Notice that the singularity is protected by an event horizon and the brane is at $z = z_0 = 1$.

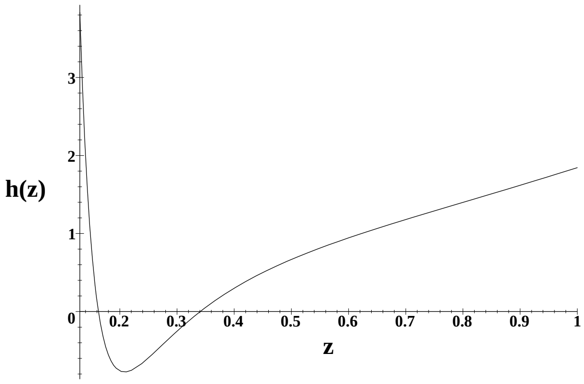

Figure 26: $h(z)$ in five-dimensional AdS-Reissner-Nordström bulk with the brane located at $z = 1$. We see that the singularity is protected by two horizons.

In figure (25) we plot the graviton paths obtained from (164) under the previous conditions for a variety of initial velocities showing that, in fact, shortcuts appear when we choose the parameters following the complete analysis shown in this section.

The analysis in five dimensions can be performed analogously to six-dimensional one with

$$h(z) = 1 + \frac{z^2}{l^2} - \frac{M}{z^2} + \frac{Q^2}{z^4}\,, \tag{239}$$

and

$$\frac{M}{z_0^4} = \frac{2}{z_0^2} + \frac{3}{l^2} + 3\omega\varepsilon_{(5)}^2\,, \tag{240}$$

$$\frac{Q^2}{z_0^6} = \frac{1}{z_0^2} + \frac{2}{l^2} + 3\omega\varepsilon_{(5)}^2 + \varepsilon_{(5)}^2\,, \tag{241}$$

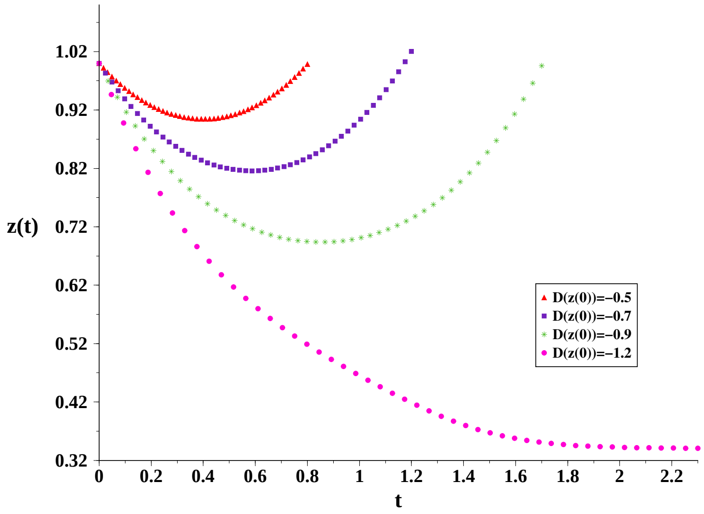

Figure 27: Shortcuts for several initial velocities in five-dimensional AdS-Reissner-Nordström bulk. We see that there is threshold initial velocity for which the graviton can not return to the brane and falls into the event horizon.

arriving to the following restrictions:

1. We must choose ω such that $-1 < \omega < -2/3$;
2. Given ω, the brane must be located at a position such that
$$\frac{z_0}{l} < \sqrt{-\frac{\omega + 2/3}{1+\omega}}\,; \tag{242}$$
3. Given (242), the energy $\varepsilon^2_{(5)} = \kappa^4_{(5)}\rho^2/36$ must satisfy
$$\frac{1}{9\omega^2}\left(2 - 9\frac{z_0^2}{l^2}\omega + 2\sqrt{1 - 9\frac{z_0^2}{l^2}\omega(\omega+1)}\right) < z_0^2\varepsilon^2_{(5)} < \frac{1}{3\omega+1}\left(-1 - \frac{2z_0^2}{l^2}\right). \tag{243}$$

As an example, we choose $\omega = -7/8$. From (242) we must have

$$\frac{z_0}{l} < \frac{\sqrt{15}}{3} \,,$$

so we choose $l = 1$ and $z_0 = 1$.

From (243) the energy must fulfill

$$\frac{632}{441} + \frac{16}{441}\sqrt{127} < \varepsilon_{(5)}^2 < \frac{24}{13} \,,$$

then we choose $\varepsilon_{(5)} = \sqrt{461/250}$.

In figure (26) we can see $h(z)$ according to the previous conditions. As in the six dimensional case, the singularity is protected by an event horizon, and the brane is at $z = z_0 = 1$.

In figure (27) we show several graviton paths obtained under the previous conditions for several initial velocities showing that shortcuts appear when we choose the parameters following the analysis shown in this section analogously to the six dimensional case.

15 The FRW-Brane evolving in the Bulk

The main reason to study the evolution of the brane from the point of view of the bulk is to simplify the analysis of gravitational signs leaving and subsequently returning to the brane. In fact in the static AdS backgound, the equation for a null geodesic in the bulk, $a = a(t)$, is particularly simplified [11],

$$\frac{\ddot{a}(t)}{a} + \frac{\dot{a}^2(t)}{a^2}\Big(1 - \frac{3h'(a)a}{2h(a)}\Big) + \frac{h(a)}{a}\Big(\frac{h'(a)}{2} - \frac{h}{a}\Big) = 0 \quad . \tag{244}$$

On the other hand, the evolution of the brane in the bulk, $a = a_b(t)$, at early times, $a_b << L_c$, is dictated by

$$\frac{da_b}{dt} = \frac{h(a_b)}{\sqrt{1 + \frac{h(a_b)}{\dot{a}_b(\tau)^2}}} = h(a_b)\Big(1 + \frac{k + \frac{a_b^2}{l^2}}{\frac{\Omega_0^2}{4(1+l^2\Lambda_4)}\frac{L_c^{2q}}{l^2 a_b^{2q-2}}}\Big)^{-1/2} \quad ,$$

where we used the fact that the quadratic term in the energy prevails. Thus,

$$\frac{da_b}{dt} = h(a_b)\Big(1 + \frac{4(1 + l^2\Lambda_4)}{\Omega_0^2}\frac{a_b^{2q}}{L_c^{2q}}(1 + kl^2/(a_b^2))\Big)^{-1/2} \quad ,$$

and, for $a_b << L_c$, since the observed cosmological constant is at most $\Lambda_4 \sim H_0^2$, $\Lambda_4 l^2 << 1$ we have

$$\frac{da_b}{dt} \approx h(a_b)\Big(1 - \frac{2(1+l^2\Lambda_4)}{\Omega_0^2}\frac{a_b^{2q}}{L_c^{2q}}(1+kl^2/(a_b^2))\Big) \quad . \tag{245}$$

Substituting the result for the evolution of the brane, $\dot{a}(t) = h(a)$, in the geodesic equation (244), we verify that it is satisfied. Therefore, the trajectory of the brane differs from the trajectory of the null geodesic by a term of the order $\left(\frac{a_b}{L_c}\right)^{2q}$.

This means that for $a_b << L_c$, the trajectory of the brane in the bulk is governed by

$$\frac{da_b(t)}{dt} = k + \frac{a_b^2}{l^2} \quad . \tag{246}$$

Thus, if $k = 0$,

$$a_b(t) = \frac{a_b(0)l^2}{l^2 - a_b(0)t} \tag{247}$$

and, if $k = -1$,

$$a_b(t) = \frac{2l(l + a_b(0))}{e^{2t/l}(l - a_b(0)) + l + a_b(0)} - l \quad . \tag{248}$$

In this last situation, if the Universe begins under the Randall-Sundrum scale, $a(0) < l$, it will recolapse to the singularity in a finite time,

$$t = \frac{l}{2}\ln\Big(\frac{l + a_b(0)}{l - a_b(0)}\Big) \quad .$$

Indeed, there is an event horizon when $a = l$ if $k = -1$.

In the case of an eliptic Universe,

$$a_b(t) = l\tan\Big(\frac{t}{l} + \tan^{-1}\Big(\frac{a_b(0)}{l}\Big)\Big) \quad . \tag{249}$$

Starting at the singularity $t_0 = \tau_0 = a_b(t_0) = 0$, we have

$$a_b(t) = l\tan\Big(\frac{t}{l}\Big) \quad . \tag{250}$$

Note that the evolution of the brane in the bulk is linear near the initial singularity ($a(t) \sim t$ for $t << l$), diverging at the critical time $t_c = \frac{\pi}{2}l$. In fact, the behaviour of all solutions is similar near the critical time

$$\begin{aligned} t_c &= \frac{l^2}{a_b(0)} \quad ; \\ t_c &= \frac{l}{2}\ln\Big(\frac{l+a_b(0)}{a_b(0)-l}\Big) \quad ; \\ t_c &= \frac{\pi}{2}l - l\tan^{-1}\Big(\frac{a_b(0)}{l}\Big) \end{aligned} \tag{251}$$

for $k = 0,\ -1,\ +1$ respectively.

As we approach the critical time $a_b(t)$ increases quickly. When $a_b(t) \sim L_c$ equation (246) is no longer valid, and the trajectory of the brane is no longer a geodesic. Thus, for a very short period, from the point of view of the bulk the brane undergoes a phase transition. In figure 28 this behaviour is shown in terms of the numerical solution of eq. (130) for a radiation dominated eliptic Universe.

Before the critical time, from the point of view of the bulk, there is no time left for the remaining graviton geodesics to reach the brane. This is in fact the kind of behaviour that we find in numerical studies of the complete equation for the evolution of the brane and null geodesics as in the example of figure 29.

On the other hand, for later times the evolution of the brane is softer, and shortcuts appear, as exhibited in fig. 30.

15.1 The Effect of Shortcuts in Late Times Universes

The shortcuts just found for late times Universes could be used to probe the extra-dimensionality by the aparent violation of causality in the brane. Thus, suppose that in $\tau = t = 0$ an object could emit eletromagnetic and gravitational waves and that we could be able to detect both signs in times τ'_γ and τ'_g. We compute now the order of magnitude of the advance in time of the graviton. Since the signals cover the same distance in the brane,

$$\int_0^{\tau'_\gamma} \frac{d\tau_\gamma}{a_b(\tau_\gamma)} = \int_0^{t'_g} \frac{dt_g}{a(t_g)}\sqrt{h(a) - \frac{\dot{a}(t_g)^2}{h(a)}} \quad . \tag{252}$$

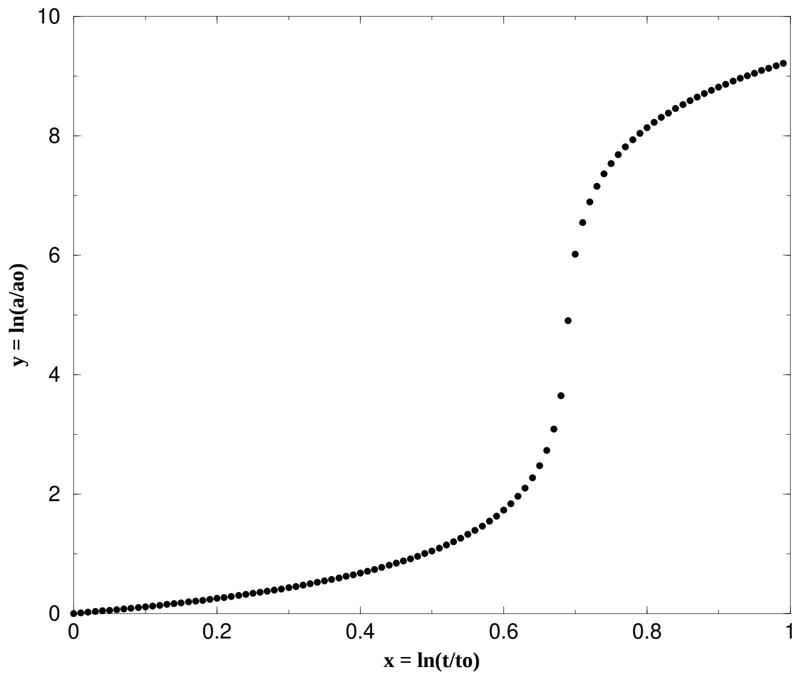

Figure 28: Evolution of the brane in the bulk at the intermediate epoch $a_b \sim 0.01 L_c$ until $a_b \sim 200 L_c$, radiation dominated era (RDE), $\Omega_0 = 2$.

Here, a denotes the coordinate defining the geodesic in the bulk, and differs from the coordinate of the brane a_b. In terms of the dimensionless parameters y and x, $a = Ly$ and $t = Tx$ the last integral reads

$$\int_0^{t'_g} \frac{dt_g}{a(t_g)} \sqrt{h(a) - \frac{\dot{a}(t)^2}{h(a)}} \quad = \quad \int_0^{t'_g} \frac{dt_g}{l} \sqrt{1 + \frac{l^2}{L^2 y^2} - \frac{l^2}{T^2} \frac{\dot{y}(x)^2}{y^2 + y^4 \frac{L^2}{l^2}}} \quad .(253)$$

Using the relation between the time in the brane and that of the bulk we convert the above expressions in terms of the interval of time of the observer in the brane,

$$\begin{aligned} \int_0^{\tau'_\gamma} \frac{d\tau_\gamma}{a_b(\tau_\gamma)} &= \int_0^{\tau'_g} \frac{d\tau_g}{l} \frac{dt_g}{d\tau_g} \sqrt{1 + \frac{l^2}{L^2 y^2} - \frac{l^2}{T^2} \frac{\dot{y}(x)^2}{y^2 + y^4 \frac{L^2}{l^2}}} \\ &= \int_0^{\tau'_g} \frac{d\tau_g}{l} \frac{1}{h(a_b)} \sqrt{h(a_b) + \dot{a}_b(\tau_g)^2} \sqrt{1 + \frac{l^2}{L^2 y^2} - \frac{l^2}{T^2} \frac{\dot{y}(x)^2}{y^2 + y^4 \frac{L^2}{l^2}}} \, . \end{aligned}$$

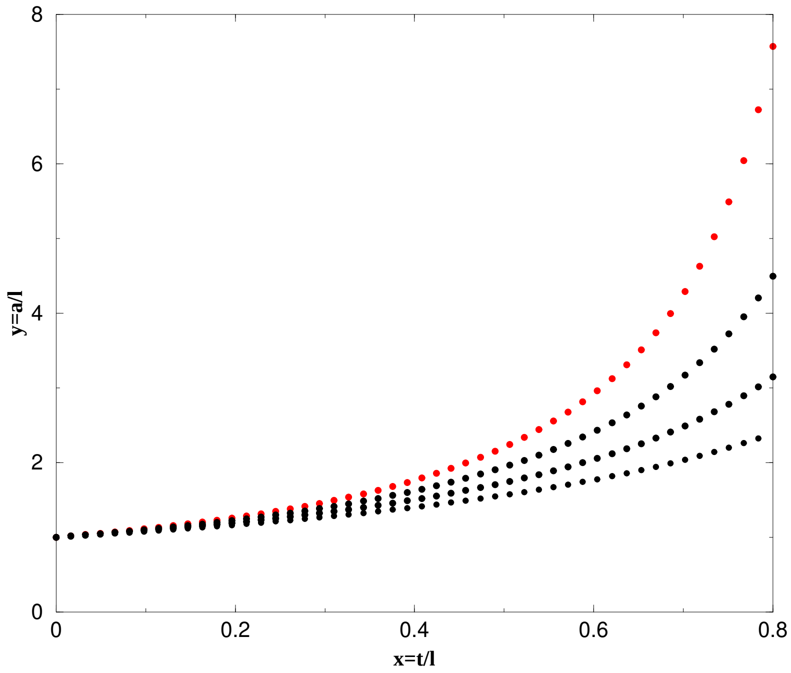

Figure 29: The trajectory of the brane in the bulk for $\Omega_0 = 2$. Other curves are geodesics that start in the brane with different initial velocities.

The Friedmann equation implies

$$\int_0^{\tau_g'} \frac{d\tau_g}{l}\frac{1}{h(a_b)}\sqrt{\frac{y_b^2L^2}{l^2}+\Lambda_4L^2y_b^2+\frac{\Omega_0}{y_b^{q-2}}\frac{L_c^q}{l^2L^{q-2}}}\sqrt{1+\frac{l^2}{L^2y^2}-\frac{l^2}{T^2}\frac{\dot{y}(x)^2}{y^2+y^4\frac{L^2}{l^2}}}$$

$$=\int_0^{\tau_g'} \frac{d\tau_g}{l}\frac{1}{h(a_b)}\frac{y_bL}{l}\sqrt{1+l^2\Lambda_4+\frac{\Omega_0}{y_b^q}\frac{L_c^q}{L^q}}\sqrt{1+\frac{l^2}{L^2y^2}-\frac{l^2}{T^2}\frac{\dot{y}(x)^2}{y^2+y^4\frac{L^2}{l^2}}}$$

$$=\int_0^{\tau_g'} \frac{d\tau_g}{a_b(\tau_g)}\frac{1}{1+\frac{l^2}{L^2y_b^2}}\sqrt{1+l^2\Lambda_4+\frac{\Omega_0}{y_b^q}\frac{L_c^q}{L^q}}\sqrt{1+\frac{l^2}{L^2y^2}-\frac{l^2}{T^2}\frac{\dot{y}(x)^2}{y^2+y^4\frac{L^2}{l^2}}} \quad .$$

Therefore, if $L >> L_c >> l$ we obtain, at second order in L_c/L and l/L,

$$\int_0^{\tau_g'} \frac{d\tau_g}{a_b(\tau_g)}\Big(1-\frac{l^2}{L^2}\frac{1}{y_b^2}\Big)\Big(1+\frac{1}{2}l^2\Lambda_4+\frac{1}{2}\frac{\Omega_0}{y_b^q}\frac{L_c^q}{L^q}\Big)\Big(1+\frac{1}{2}\frac{l^2}{L^2y^2}-\frac{1}{2}\frac{l^2}{T^2}\frac{\dot{y}(x)^2}{y^2+y^4\frac{L^2}{l^2}}\Big) \quad .$$

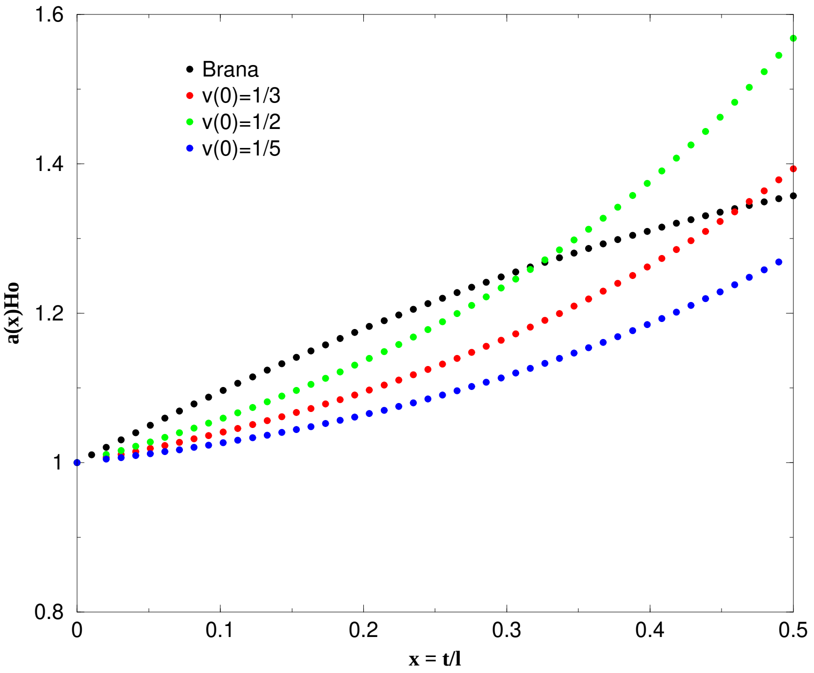

Figure 30: The trajectory of the brane in the bulk for $\Omega_0 = 2$, matter dominated era (MDE) with $k = 1$. Also null geodesics starting in the brane with various initial velocities.

Finally,

$$\int_0^{\tau'_\gamma} \frac{d\tau_\gamma}{a_b(\tau_\gamma)} = \int_0^{\tau'_g} \frac{d\tau_g}{a_b(\tau_g)} \Big[1 + \frac{1}{2}\frac{\Omega_0}{y_b^q}\frac{L_c^q}{L^q} + \frac{1}{2}l^2\Lambda_4 - \frac{l^2}{L^2}\frac{1}{y_b^2} + \frac{1}{2}\frac{l^2}{L^2 y^2} - \frac{1}{2}\frac{l^4}{T^2 L^2}\frac{\dot{y}(x)^2}{y^4}\Big] \quad .$$

Thus, at first order, the time difference between the photon and the graviton is corrected in the integrand by terms of the order $\frac{L_c^q}{a_b^q}$. Today this factor is at most 10^{-58} and in the time of decoupling 10^{-46}, showing that the time advance of the graviton can be safely neglected and is of no physical significance, in spite of the fact that the trajectory of the brane is distinctively different from the null geodesic.

15.2 The Effect of Shortcuts in Early Time Universe

From the analysis developed so far we learned that the periods of evolution of the Universe differ by the scale that defines the physical significance of the shortcuts. In an era where $a_b << L_c$, the trajectory of the brane in the bulk differs from the extreme geodesics by $(a_b/L_c)^{2q}$ and the shortcuts do not appear, since the brane itself provides the graviton geodesic.

In the period when $a_b >> L_c$, the trajectory of the brane is far from a null geodesic and shortcuts appear, but they are not significant, since the *skin depth* of the graviton in the bulk is defined by the parameter $l << L_c << a_b$. The difference between the time intervals of the photon and the graviton is of the order $(L_c/a_b)^q$.

However, from the continuity of the evolution of the brane in the bulk, we expect that there is also an intermediate situation $a_b \sim L_c$ when physically important shortcuts could appear, since the evolution of the brane is far enough from a geodesic. Indeed, in figure 31, rescaling the geodesics in the bulk we can observe the behaviour of the brane as compared to the geodesics that start in it at a later time. It is clear that these shortcuts are serious mediators of homogenization of the matter in the brane in the era before nucleosynthesis [13], [14].

From the evolution of the brane in the bulk in the intermediate epoch we thus conclude that there is a critical age t_c, after which the gravitational waves leaving the brane return before the arrival of the photons released at the same time as the gravitons. The behaviour of the geodesic in the bulk shows that any geodesic starting in the brane at a certain instant will be singular at a time later than the critical time, indicating that it will return to the brane. Thus, information leaks between regions which apparently are causally disconnected at times $t > t_c$.

In order to study the horizon problem, we now compare, at a certain time τ_n previous to nucleosynthesis, the graviton horizon R_g with the observable proper distance of the universe (from the radiation decoupling until today) [15]. Since the graviton evolves in a bulk geodesic,

$$R_g \equiv \int \frac{dr}{\sqrt{1-kr^2}} = \int \frac{dt}{a}\sqrt{h(a) - \frac{\dot{a}^2}{h(a)}} = \int \frac{d\tau}{a}\frac{\sqrt{h(a_b)+\dot{a}_b^2}}{h(a_b)}\sqrt{h(a) - \frac{\dot{a}^2}{h(a)}}$$

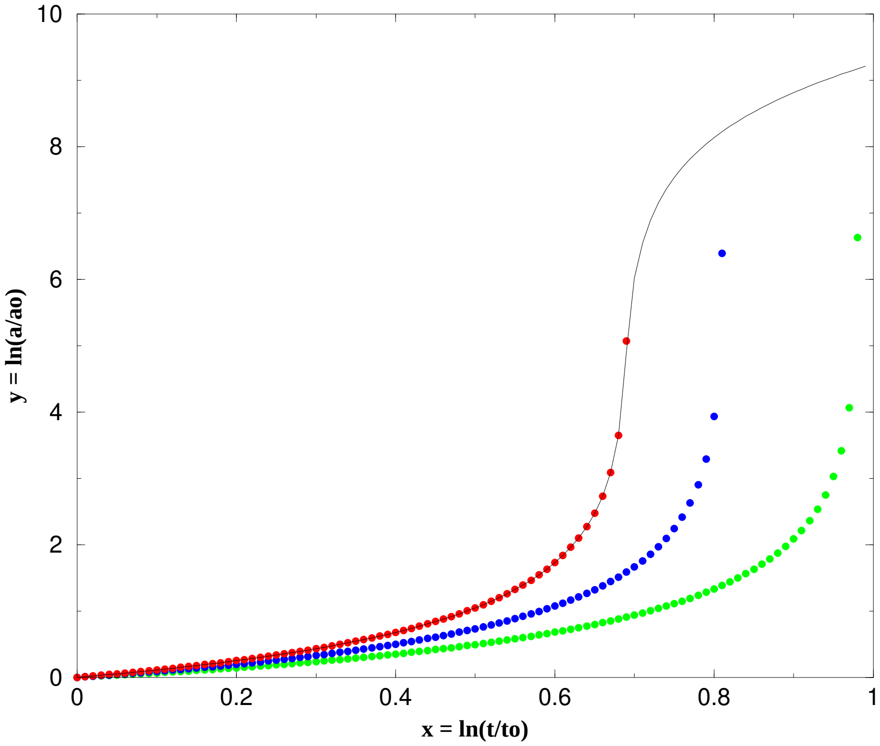

Figure 31: The trajectory of the brane in the bulk leaving $a = 0.01L_c$ in the RDE. Geodesics in the bulk with different initial velocities are exhibited intercepting the brane after the critical time t_c.

$$= \int_0^{\tau_n} \frac{d\tau}{a_b} \frac{1}{1 + l^2/a_b^2} \sqrt{1 + \Lambda_4 l^2 + \frac{\Omega_0 L_c^q}{a_b^q}\left(1 + \frac{\Omega_0 L_c^q}{4a_b^q(1+\Lambda_4 l^2)}\right)} \times$$

$$\times \sqrt{1 + \frac{l^2}{L^2 y^2} - \frac{l^2}{T^2} \frac{\dot{y}(x)^2}{y^2 + y^4 \frac{L^2}{l^2}}} \quad , \tag{254}$$

while in the brane, the size of the observable Universe is $R = \int \frac{d\tau}{a_b(\tau)}$.

We use the known results for the usual particle horizon

$$R = \frac{1}{\sqrt{\Omega_0} H_0 a_{b0}} \int_{z(\tau)}^{z(0)} z^{-q/2} dz = \frac{2}{(q-2)\sqrt{\Omega_0} H_0 a_{b0}} \left(z(\tau)^{1-q/2} - z(0)^{1-q/2}\right) \quad .$$

where $z(\tau) = a_{b0}/a_b(\tau)$. Today,

$$R \sim \frac{2}{\sqrt{\Omega_0} H_0 a_{b0}} \equiv R_0 \quad .$$

For the computation of the graviton horizon, we work in a primordial era before nucleosynthesis. Thus, in the Friedmann equation we can neglect the usual cosmological term as well as the curvature term. At an epoch between Planck era and nucleosynthesis, $l << a_b << H_0$, it is safe to neglect terms involving l^2/L^2 in (254), and we find

$$R_g \approx \int_0^{\tau_n} \frac{d\tau}{a_b} \sqrt{1 + \frac{\Omega_0 L_c^q}{a_b^q} + \frac{\Omega_0^2 L_c^{2q}}{4 a_b^{2q}}} \quad .$$

Using the Friedmann equation we get

$$R_g = \frac{1}{\Omega_0^{1/2} H_0 a_{b0}} \int_{z(\tau_n)}^{z(0)} \frac{dz}{z^2} \frac{\left(1 + \frac{\Omega_0 H_0^2 l^2}{2} z^4\right)}{\sqrt{1 + \frac{\Omega_0 H_0^2 l^2}{4} z^4}} \quad . \tag{255}$$

The integral diverges for arbitrarly high redshifts, proving that the horizon problem is potentially solvable. The behaviour of this integral can be determined. We have

$$R_g \approx \frac{l}{a_{b0}} z(0) \quad .$$

Comparing with the size of the Universe today,

$$\frac{R_g}{R_0} \sim \frac{\sqrt{\Omega_0}}{2} H_0 l z(0) \quad .$$

It looks like shortcuts are not enough to solve the horizon problem, since we would need to go back in time to $z(0) \sim (H_0 l)^{-1} \sim 10^{29}$, 10^{11} times higher than the redshift at the Planck time in the brane associated with the fundamental scale of gravity, κ_5.

For the time being, lets assume the validity of the theory in such high energies. In the next section we will argue that, in order to provide a solution to the usual cosmological problems, inflationary models must use of those high redshifts. We may note, however, that there are actually two related time scales. In the primordial Universe the brane is evolving as a part of the bulk, with velocities close to that of light, and time intervals in the brane correspond to much longer intervals in the bulk. In fact, the relation between these scales is obtained from $t_0 = \tau_0 = a_b(\tau_0) = 0$ and from

$$t = \int_0^\tau d\tau \frac{\sqrt{h(a_b) + \dot{a}_b^2(\tau)}}{h(a_b)} \quad .$$

For $a_b << L_c$ we have $\tau << l$, and one finds, as a consequence

$$t \approx \int_0^\tau d\tau \frac{\dot{a}_b(\tau)}{h(a_b)} = \int_0^{a_b(\tau)} \frac{da_b}{k + a_b^2/l^2} \quad .$$

This implies, for the example of a closed universe with $\Omega_0 = 2$,

$$t = l \arctan\Big(\frac{a_b(\tau)}{l}\Big) \quad .$$

Therefore, when $a_b(\tau) \sim l$, that is, when the brane time is $\tau \sim 10^{-67}s$, the corresponding bulk time $t \sim \frac{\pi}{4} l \sim 10^{-11}$s is much larger than the Planck scale, $t >> M_{(5)}^{-1}$.

If we assume that quantization is mandatory according to the bulk Planck energy scale, geodesics that start in the bulk with $z(0) \sim (H_0 l)^{-1}$ should be sufficient to homogenize the Universe before nucleosynthesis, reaching $R_g \sim 1$. In order to verify this, we have numerically integrated the expression for the distance reached by geodesics $a(t)$ starting in the brane at $a_b = l$, corresponding to a time $t = \pi/4l$, for $k = 1$ with $\Omega_0 \sim 2$ $(a_{b0} \sim H_0^{-1})$:

$$R_g = \int_{l\pi/4}^{t_f} \frac{dt}{a} \sqrt{h(a) - \frac{\dot{a}^2}{h(a)}} \quad . \tag{256}$$

The solution of the geodesic equation is given in figure 32. The brane evolves initially as a geodesic with speed $v_b \sim 2$ $(a_b \sim l)$ and we exhibit a geodesic with zero initial speed in the bulk. The point of inflexion in its trajectory is $t_f = 2.356 l > t_c = \frac{\pi}{2} l$. As we saw before, the brane evolves smoothly after the transition and the geodesics return to the brane if we wait until t_f, see (256). Although the trajectory diverges near this point, the integrand in (256) is finite and we can perform the integration, finding

$$R_g = 2.526 \quad .$$

Thus, the observable Universe is smaller than the reach of the relic gravitons that start in a previous era.

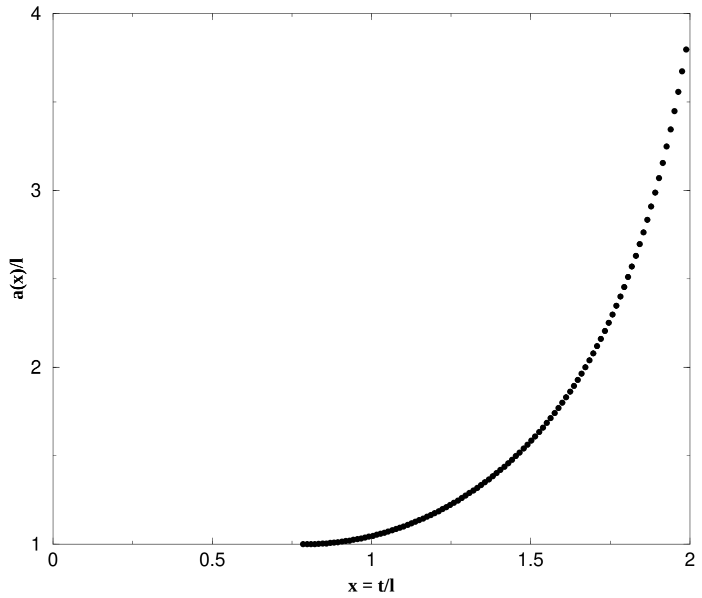

Figure 32: Null geodesic starting at $a = l$, $t = \pi/4l$ with initial velocity $v(\pi/4) = 0$.

16 Causal Gravitational Structure

In the last section we learned about the behaviour of null-geodesics for closed Universes. We can, however, study analytically the whole causal structure of the gravitational signs for a $k = 0$ Universe.

The geodesic equation, (244), is quite simple for purely AdS $k = 0$ space-times

$$\frac{1}{a^2}\frac{da}{dt} = \frac{v(0)}{a(0)^2} \quad . \tag{257}$$

Thus, a geodesic that starts in the brane at $a = a(0)$ ant $t = 0$, with initial veolcity $v(0)$, returns to it when

$$t_r \approx \frac{a(0)}{v(0)} \quad .$$

The expression for the gravitational horizon can also be integrated

$$\begin{aligned} R_g &= \int_0^{t_r} \frac{dt}{a}\sqrt{h(a)-\frac{\dot{a}^2}{h(a)}} = \int_0^{t_r} \frac{dt}{l}\sqrt{1-\frac{l^4\dot{a}^2}{a^4}} \\ &= \frac{t_r}{l}\sqrt{1-\frac{v(0)^2l^4}{a(0)^4}} \quad . \end{aligned} \tag{258}$$

Using the relation between the returning time and the initial velocity,

$$R_g = \frac{t_r}{l}\sqrt{1-\frac{l^4}{a(0)^2t_r^2}} \quad . \tag{259}$$

In order to relate the returning time to the redshift, we must integrate the relation between time of the bulk and time of the brane (130). We already know that from $a(0)$ to the critical period of transition a time of $t_c \sim \frac{l^2}{a(0)}$ has passed. After that, the evolution is dominated by the usual term in Friedmann equation and we can approximate

$$\begin{aligned} t_r &\approx \frac{l^2}{a(0)} + \int_{L_c}^{a_r} l\frac{da_b}{a_b^2 H} \approx \frac{l^2}{a(0)} + \int_{L_c}^{a_r} da_b \frac{l}{\sqrt{\Omega_0}H_0} a_b^{q/2-2} \\ &\approx \frac{l^2}{a(0)} + \frac{2l}{(q-2)\sqrt{\Omega_0}H_0 a_{b0}}\left(z_r^{-q/2+1} - 10^{-15}\right) \quad , \end{aligned} \tag{260}$$

where z_r must, of course, be greater than the redshift in the transition, $z_{Lc} \sim 10^{15}$.

Substituting back in the expression of the gravitational horizon,

$$\begin{aligned} R_g &= \Big[\frac{l}{a(0)} + \frac{2}{(q-2)\sqrt{\Omega_0}H_0 a_{b0}}\left(z_r^{-q/2+1} - 10^{-15}\right)\Big] \\ &\times \sqrt{1-\Big[1+\frac{2a(0)}{(q-2)\sqrt{\Omega_0}lH_0a_{b0}}\left(z_r^{-q/2+1} - 10^{-15}\right)\Big]^{-2}} \quad . \end{aligned} \tag{261}$$

When considering the interesting situation of a high initial redshift $z(0) = a_{b0}/a(0) > (H_0 l)^{-1}$, this expression can be approximated by

$$R_g \approx \frac{l}{a(0)}\sqrt{\frac{4a(0)}{(q-2)\sqrt{\Omega_0}lH_0a_{b0}}\left(z_r^{-q/2+1} - 10^{-15}\right)} \quad . \tag{262}$$

Comparing with the size of the horizon today, we find

$$\left(\frac{R_g}{R_0}\right)_{z_r} \approx \sqrt{\sqrt{\Omega_0}\frac{lH_0}{(q-2)}}\sqrt{z(0)\left(z_r^{-q/2+1} - 10^{-15}\right)} \quad . \tag{263}$$

We note, as we did in the last section, that if sufficiently large redshifts were available, the graviton horizon in a past epoch could be larger than the present size of the observable Universe.

We argue, however, that those high redshifts could be available even when the energy density in the brane is not quantized yet. Indeed, if inflation takes place in the brane high redshifts could be present in the beginning of the inflationary epoch.

Denoting the redshift when inflation ends by z_e, if the size of the present Universe, R_0, is expected to be in causal contact during inflation, we must reach at least a redshift in the beginning of inflation, $z(0)$, that solves

$$\frac{a_{b0}R_0}{z(0)} = H^{-1}(z_e) \quad .$$

The unusual results in brane-world cosmology are expected if inflation ends before the transition time, when the quadratic term in Friedmann equation dominates. In this case, we get

$$\frac{a_{b0}R_0}{z(0)} = \frac{1}{\Omega_0 H_0^2 l z_e^4}$$

and

$$z(0) = 2\sqrt{\Omega_0}H_0 l z_e^4 \quad . \tag{264}$$

If $H(z_e)l >> 1$, it is simple to note, from equation (130), that the evolution of the brane in the bulk is not altered during inflation. Thus, we can substitute the result(264) in the complete expression for the causal gravitational horizon (263),

$$\left(\frac{R_g}{R_0}\right)_{z_r} \approx \sqrt{\frac{2\Omega_0}{(q-2)}}H_0 l z_e^2\sqrt{\left(z_r^{-q/2+1} - 10^{-15}\right)} \quad . \tag{265}$$

This equation tells us that, in the time of nucleosyntesis, when $z_r \sim 10^{10}$, $R_g/R_0 \sim 1$ for a model with inflation ending just before what would be the Planck era, with $z_e \sim 10^{17}$ (where $z_{Pl} \sim 10^{18}$). This proves that successfully inflationary models ending before the transition time necessarily make relevant changes in the causal structure of the universe.

We are able to sketch the gravitational horizon for this kind of configuration. In figure 33 we show the behaviour of the Hubble horizon in comoving coordinates $H^{-1}a_b^{-1}/R_0$ and the graviton horizon R_g/R_0 for an inflationary model ending just before the Planck era, $z_e = 10^{17}$ and producing the necessary number of e-folds to solve the horizon problem. The fraction of the Universe in causal contact by gravitational signs in the nucleosynthesis epoch is just the present horizon R_0. Today, the gravitational horizon would be $10^5 R_0$.

17 Conclusions

Studying the shortcut problem in braneworld cosmology from the point of view of the bulk we have explicitly shown that shortcuts are indeed common in late time Universes, though they are extremelly small and the time advance of the graviton can be safely neglected. However, we have also learned that gravitational signs may leave and subsequently return to the brane even in early times Universes. We have showed that those shortcuts exist and that the new scale of the model, l, implies in a minimum time scale for the reception of those signs by an observer in the brane. Before that critical time, the brane itself evolves like a null-geodesic in the bulk.

If high initial redshits were available the shortcuts just found could solve the horizon problem without inflation. More important however, may be the effect of those shortcuts with an inflationary epoch in the brane.

Brane-world models incorporate two changes in the cosmology, namely, the modified Friedmann equation and the possibility of leaking of gravity in the extra dimension. Using the first of those modifications, it was shown that, remarkably, the consistency equation is mantained in the brane-world formalism when the inflation is guided by a scalar field minimally coupled in the brane [59]. This consists in bad news for those who expect that brane cosmological configurations could probe the extra dimensionality of our Universe.

However, we have showed that if there was an inflationary epoch in the brane evolution, the causal structure of the universe could be strongly modified. This could be a sign of an unusual evolution of the perturbations from

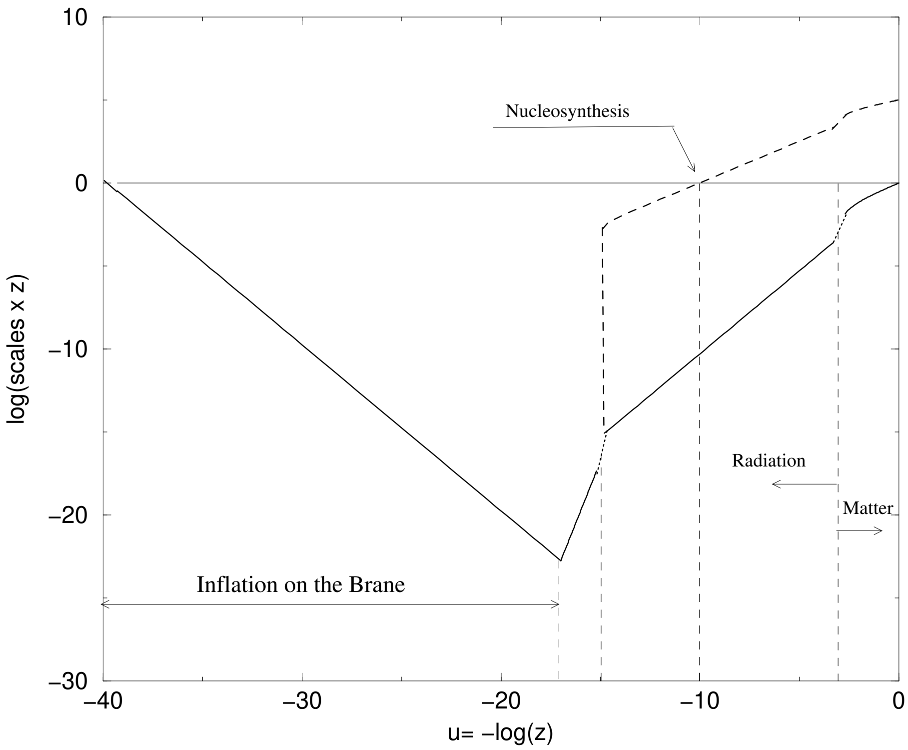

Figure 33: We plot in log-log scale the evolution of the fraction of graviton horizon and the present observable size, R_g/R_0 (dashed line) and the same for the Hubble horizon $a_b^{-1}H^{-1}/R_0$ (solid line), for an inflationary model in the brane that ends after Planck time ($u_{PL} = -\log(z_{PL}) = -18$), and before transition time ($u_{TR} = -15$), in $u_{end} = -\log(z_{end}) = -17$. The present scale would be under the de-Sitter horizon if redshifts like $u(0) = -39$ were available. This imply in strong modifications of the causal structure for gravitational signs after the transition time.

the time they cross the de Sitter horizon, H^{-1}, during inflation, through the time they became causally connected again. In this case, there could be distinct predictions for the microwave background radiation structure even with the same consistency equation during inflation. Thus, further investigation on the dynamics of perturbations in inflationary brane-world models may prove useful to probe the dimensionality of space-time.

Acknowledgements: This work has been supported by Fundação de Amparo à Pesquisa do Estado de São Paulo **(FAPESP)** and Conselho Nacional de Desenvolvimento Científico e Tecnológico **(CNPq)**, Brazil.

References

[1] M. Gasperini, G. Veneziano, The pre big-bang scenario in String Cosmology, **CERN-TH** (2002) 104; [hep-th/0207130].

[2] J. Polchinski, *Superstring Theory* vols. 1 and 2, Cambridge University Press 1998.

[3] G. t'Hooft

[4] Sugra

[5] Green Schwarz

[6] Duality

[7]

[8] kaluzaklein

[9] Arkani Hamed

[10] Horava and E. Witten

[11] E. Abdalla, A. Casali, B. Cuadros-Melgar, *Nucl. Phys.* **B644** (2002) 201; [hep-th/0205203].

[12] C. Csáki, J.Erlich, C. Grojean, *Nucl. Phys.* **B604** (2001) 312; [hep-th/0012143].

[13] H. Ishihara, *Phys. Rev. Lett.* **86** (2001) 381.

[14] R. Caldwell and D. Langlois, *Phys. Lett.* **B511** (2001) 129; [gr-qc/0103070].

[15] D. J. Chung and K. Freese, *Phys. Rev.* **D62** (2000) 063513; [hep-ph/9910235]. *Phys. Rev.* **D61** (2000) 023511; [hep-ph/9906542].

[16] C. Csáki, M.Graesser, L. Randall and J. Terning, *Phys. Rev.* **D62**, (2000) 045015, [hep-th/9911406]; P. Binetruy, C. Deffayet, D. Langlois *Nucl.Phys.* **B615**, (2001) 219, [hep-th/0101234].

[17] E. Abdalla, B. Cuadros-Melgar, S. Feng, B. Wang, *Phys. Rev.* **D65** (2002) 083512; [hep-th/0109024].

[18] G. Starkman, D. Stojkovic and M. Trodden, *Phys. Rev. Lett.* **87** (2001) 231303; *Phys. Rev.* **D63** (2001) 103511.

[19] D. J. Chung and K. Freese; [astro-ph/0202066].

[20] E. Abdalla and A. G. Casali; [hep-th/0208008].

[21] G. Dvali and S. H. Tye *Phys. Lett.* **B450** (1999) 72, hrp-th/9812483.

[22] F. Quevedo

[23] S. Kashru, R. Kallosh, A. Linde, J. Maldacena, L. McAllister and S. Trivedi, hep-th/0308055

[24] K. D. Kokkotas, B. G. Schmidt, gr-qc/9909058 and references therein.

[25] C. W. Misner, K. S. Thorne and J. A. Wheeler, Gravitation (Freeman, San Franciso, 1973).

[26] E. Poisson and W. Israel, Phys. Rev. D 41, 1796 (1990).

[27] R. H. Price, Phys. Rev. D 5, 2419 (1972); 5, 2439 (1972).

[28] C. Gundlach, R. H. Price and J. Pullin, Phys. Rev. D 49, 883 (1994).

[29] R. Gomez, J. Winicoar and B. G. Schmidt, Phys. Rev. D 49,2828 (1994).

[30] E. Leaver, J. Math. Phys. 27, 1238 (1986); Phys. Rev. D 34,384 (1986).

[31] N. Andersson, Phys. Rev. D 55, 468 (1997).

[32] J. Bicak, Gen. Relativ. Gravit. 3, 331 (1972).

[33] C. Gundlach, R. H. Price and J. Pullin, Phys. Rev. D 49, 890 (1994).

[34] L. M. Burko and A. Ori, Phys. Rev. D 56, 7820 (1997).

[35] S. Hod and T. Piran, Phys. Rev. D 58, 024017 (1998).

[36] S. Hod and T. Piran, Phys. Rev. D 58, 044018 (1998).

[37] P. R. Brady, C. M. Chambers, W. G. Laarakkers and E. Poisson, Phys. Rev. D 60, 064003 (1999).

[38] P. R. Brady, C. M. Chambers, W. Krivan and P. Laguna, Phys. Rev. D 55, 7538 (1997).

[39] E. S. C. Ching, P. T. Leung, W. M. Suen and K. Young, Phys. Rev. D 52, 2118 (1995); Phys. Rev. Lett. 74, 2414 (1995).

[40] J. M. Maldacena, Adv. Theor. Math. Phys. 2, 231 (1998).

[41] E. Witten, Adv. Theor. Math. Phys. 2, 253 (1998).

[42] S. S. Gubser, I. R. Klebanov and A. M. Polyakov, Phys. Lett. B428, 105 (1998).

[43] G. T. Horowitz and V. E. Hubeny, hep-th/9909056; G. T. Horowitz, Class. Quant. Grav. 17, 1107 (2000).

[44] Gravitational wave experiments.

[45] Accelerated Expansion.

[46] de Sitter

[47] B. Wang, C. Molina and E. Abdalla, *Phys. Rev.* **D63**, 084001 (2001), hep-th/0005143.

[48] B. Wang, C. Lin and E. Abdalla, *Phys. Lett.*

[49] Jiong-Ming Zhu, Bin Wang and Elcio Abdalla, *Phys. Rev.* **D63** (2001)124004 hep-th/0101133; Bin Wang, Elcio Abdalla and R.B. Mann, *Phys. Rev.* **D65** (2002) 084006 hep-th/0107243.

[50] Leaver

[51] Gamow

[52] Elcio Abdalla, Bin Wang, A. Lima-Santos and W.G. Qiu, *Phys. Lett.* **B538** (2002) 435-441 hep-th/0204030; E. Abdalla, K.H.C. Castello-Branco, A. Lima-Santos, *Mod. Phys. Lett.* **A** gr-qc/0301130.

[53] B. F. Schutz and C. M. Will, *Astrophys. J.* **291**, L33 (1985).

[54] S. Iyer and C. M. Will, *Phys. Rev.* **D35**, 3621 (1987).

[55] J. W. Moffat; [hep-th/0208122].

[56] E. W. Kolb and M. S. Turner, *The Early Universe*, Addinson-Wesley 1990.

[57] G. Giudice, E. Kolb, J. Lesgourgues and A. Riotto, **CERN-TH** (2002) 149; [hep-ph/0207145].

[58] Shin'ichi Nojiri, Sergei D. Odintsov, Akio Sugamoto, *Mod. Phys. Lett.* **A17** (2002) 1269; [hep-th/0204065]. Shin'ichi Nojiri, Sergei D. Odintsov, *JHEP* **0112** (2001) 033; [hep-th/0107134]. Bin Wang, Elcio Abdalla, Ru-Keng Su, *Mod. Phys. Lett.* **A17** (2002) 23; [hep-th/0106086].

[59] G. Huey and J. Lidsey, *Phys. Lett.* **B514**, 217 (2001), [astro-ph/0104006]; A. Liddle and A. Taylor, *Phys. Rev.* **D65**, 041301 (2002), [astro-ph/0109412].

[60] A. R. Liddle and D. H. Lyth *Phys. Rep.* V. F. Mukhanov, H. A. Feldman and R. H. Brandenberger *Phys. Rep.* **215** (1992) 203.

[61] A. H. Guth *Phys. Rev.* **23** (1981) 347; A. A. Starobinsky *Phys. Lett.* **B 91** (1980) 99.

[62] J. R. Oppenheimer and H. Snyder *Phys. Rev.* **56** (1939) 455; S. Weinberg *Gravitation and Cosmology.*

[63] Gibbons and S. Hawking, *Phys. Rev.* **D15** (1977) 2738.

[64] C. Lanczos, *Phys. Zeits.* **23** (1922) 539; *Ann. der Phys.* **74** (1924) 518.

[65] W. Israel, *Nuovo Cimento* **44B** (1966) 1. Erratum: **48B** (1967) 2.

[66] G. Darmois, *Mem. Sciences Math.* **XXV** (1927) ch. V.

[67] H.A. Chamblin and H.S. Reall, *Nucl. Phys.* **B562** (1999) 133.

[68] G. Gibbons and S. Hawking, *Phys. Rev.* **D15** (1977) 2752.

[69] P. Bintruy, C. Deffayet and D. Langlois, *Nucl. Phys.* **B565** (2000) 269.

[70] P. Bintruy, C. Deffayet, U. Ellwanger and D. Langlois, *Phys. Lett.* **B477** (2000) 285.

[71] H. A. Chamblin and H. S. Reall, *Nucl.Phys.* **B562** (1999) 133; [hep-th/9903225].

[72] P. Kanti, R. Madden and K. A. Olive, *Phys. Rev.* **D64** (2001) 044021; [hep-th/0104177].

[73] D. Ida, *JHEP* **0009** (2000) 014; [gr-qc/9912002].

[74] L. Randall and R. Sundrum, *Phys. Rev. Lett.* **83**, (1999) 3370, [hep-th/9905221]; *Phys. Rev. Lett.* **83**, (1999) 4690, [hep-th/9906064].

[75] P. Kraus, *JHEP* **9912** (1999) 011; [hep-th/9910149].

[76] P. Bowcock, C. Charmousis and R. Gregory, *Class. Quant. Grav.*, **17** (2000) 4745 ; [hep-th/0007177].

[77] P. Binétruy, C. Deffayet and D. Langlois, *Nucl. Phys.* **B565** (2000) 269; [hep-th/9905012].

[78] C. Csáki, M. Graesser, C. Kolda and J. Terning, *Phys. Lett.* **B462** (1999) 34; [hep-ph/9906513].

[79] J. Cline, C. Grosjean and G. Servant, *Phys. Rev. Lett.* **83** (1999) 4245; [hep-ph/9906523].

[80] P. Binétruy, C. Deffayet, U. Ellwanger and D. Langlois, *Phys. Lett.* **B477** (2000) 285; [hep-th/9910219].

[81] P. Binétruy, C. Deffayet and D. Langlois, *Nucl. Phys.* **B565** (2000) 269; [hep-th/9905012].

[82] P. de Bernardis *et al.*, *Nature* **404** (2000) 955; *Astrophys. J.* **536** (2000) L63; [astro-ph/9911445]. R. Stompor *et al.*, *Astrophys. J.* **561** (2001) L7; [astro-ph/0105062].

[83] T. Regge and J.A. Wheeler, Phys. Rev. **108**, 1063 (1957).

[84] S. Chandrasekhar, *The Mathematical Theory of Black Holes*, (Oxford University Press, Oxforf, 1983).

[85] K. D. Kokkotas and B. G. Schmidt, Living Rev. Relativity **2** (1999).

[86] A. Riess et al. Astrophy. J., **116**, 1009 (1998).

[87] V. Cardoso and J. P. S. Lemos, Phys. Rev. D **64**, 084017 (2001);

[88] B. Wang, C. Lin and E. Abdalla, Phys. Lett. B, **481**, 79 (2000); B. Wang, C. Molina and E. Abdalla, Phys. Rev. D **63**, 084001 (2001); V. Cardoso, R. Konoplya, J. P. S. Lemos, gr-qc/0305038.

[89] B. Wang, C. Molina and E. Abdalla, Phys. Rev. D **63**, 084001 (2001);

[90] V. Cardoso and J. P. S. Lemos, Class.Quant.Grav. **18**, 5257 (2001); V. Cardoso and J. P. S. Lemos, Phys. Rev. D **63**, 124015 (2001); J. Zhu, B. Wang and E. Abdalla, Phys. Rev. D **63**, 124004 (2001); B. Wang, E. Abdalla and R. B. Mann, Phys. Rev. D **65**, 084006. (2002).

[91] H. Nariai, Sci. Rep. Tohoku Univ. **34**, 160 (1950); H. Nariai, Sci. Rep. Tohoku Univ. **35**, 62 (1951).

[92] E. Leaver, Phys. Rev. D **34**, 384 (1986).

[93] E. S. C. Ching, P. T. Leung, W. M. Suen and K. Young, Phys. Rev. D **52**, 2118 (1995).

[94] G. Gamow, Zeits. F. Phys. **51** 204 (1928).

[95] Elcio Abdalla, Bin Wang, A. Lima-Santos and W.G. Qiu, Phys. Lett. B **538**, 435 (2002); E. Abdalla, K.H.C. Castello-Branco, A. Lima-Santos, Mod. Phys. Lett. A **18**, 1435 (2003).

[96] B. F. Schutz and C. M. Will, Astrophys. J. **291**, L33 (1985).

[97] S. Iyer and C. M. Will, Phys. Rev. D **35**, 3621 (1987).

[98] S. Iyer, Phys. Rev. D **35**, 3632 (1987); K. D. Kokkotas and B. F. Schutz, Phys. Rev. D **37**, 3378 (1988).

[99] R. Ruffini, J. Tiomno, C. Vishveshwara, Lettere al Nuovo Cimento **3**, 211 (1972).

[100] R. Price, Phys. Rev. D **5**, 2419 (1972).

[101] V. Cardoso and J. P. S. Lemos, Phys. Rev. D **67**, 084020 (2003).

[102] C. Molina, gr-qc/0304053, to be published on Phys. Rev. D.

[103] A. Zhidenko, gr-qc/0307012.

[104] R. A. Konoplya, gr-qc/0303052.

[105] P. Brady, C. Chambers, W. Krivan and P. Laguna, Phys. Rev. D **55**, 7538 (1997).

[106] P. Brady, C. Chambers, W. Laarakkers and E. Poisson, Phys. Rev. D **60**, 064003 (1999).

[107] E. Abdalla, B. Wang, A. Lima-Santos and W. G. Qiu, Phys. Lett. B **538**, 435 (2002).

[108] E. Abdalla, K. Castello Branco and A. Lima Santos, Mod. Phys. Lett. A, **18**, 1435, (2003).

[109] *Higher Transcedental Functions, V.* ***II*** *(Bateman Manuscript Project)*, ed. by A. Erdlyi (McGraw-Hill, New York, 1953); I. S. Gradshteyn and I. M. Ryzhik, *Tables of Integrals, Series and Products* (Academic Press, 2000).

[110] G. 't Hooft, gr-qc/9310026; L. Susskind, *J. Math. Phys.* **36** (1995) 6377.

[111] J. Maldacena, *Adv. Theor. Math. Phys.* **2** (1998) 231; S. Gubser, I. Klebanov and A. Polyakov, *Phys. Lett.* **B 428** (1998) 105; E. Witten, *Adv. Theor. Math. Phys.* **2** (1998) 253.

[112] E. Witten, *Adv. Theor. Math. Phys.* **2** (1998) 505.

[113] S. W. Hawking and D. Page, *Comm. Math. Phys.* **87** (1983) 577.

[114] W. Fischler and L. Susskind, hep-th/9806039; N. Kaloper and A. Linde, *Phys. Rev.* **D 60** (1999) 103509; R. Easther and D. A. Lowe, *Phys. Rev. Lett.* **82** (1999) 4967; G. Veneziano, *Phys. Lett.* **B454** (1999) 22; R. Brustein, *Phys. Rev. Lett.* **84** (2000) 2072; R. Brustein, G. Veneziano, *Phys. Rev. Lett.* **84** (2000) 5695; R. Bousso, *JHEP* **7** (1999) 4, ibid **6** (1999) 28, *Class. Quan. Grav.* **17** (2000) 997; B. Wang, E. Abdalla, *Phys. Lett.* **B 466** (1999) 122, **B 471** (2000) 346.

[115] R. Tavakol, G. Ellis, *Phys. Lett.* **B 469** (1999) 37; B. Wang, E. Abdalla and T. Osada, *Phys. Rev. Lett.* **85** (2000) 5507.

[116] E. Verlinde, hep-th/0008140

[117] B. Wang, E. Abdalla and R. K. Su, hep-th/0101073, Phys. Lett. B 503 (2001) 394.

[118] S. Nojiri and S. D. Odintsov, Int. J. Mod. Phys A16 (2001) 3237; D. Kutasov, F. Larsen, JHEP 0101 (2001) 001, hep-th/0009244; F. Lin, Phys. Lett. B 507 (2001) 270; R. Brustein, S. Foffa and G. Veneziano, Nucl. Phys. B 601 (2001) 380; D. Klemm, A. C. Petkou and G. Siopsis, hep-th/0101076; R. G. Cai, Phys. Rev. D 63 (2001) 124018 hep-th/0102113; D. Birmingham and S. Mokhtari, Phys. Lett. B 508 (2001) 365 hep-th/0103108.

[119] I. Savonije and E. Verlinde, Phys. Lett. B 507 (2001) 305.

[120] L. Randall and R. Sundrum, Phys. Rev. Lett. 83, 3370 (1999); ibid 83, 4690 (1999).

[121] A. K. Biswas and S. Mukherji, JHEP 0103 (2001) 046; S. Nojiri and S. D. Odintsov, hep-th/0103078; Y. S. Myung, hep-th/0102184

[122] D. Youm Phys. Lett. B 515 (2001) 170; S. Nojiri, O. Obregon, S. Odintsov, H. Quevedo and M. Ryan Mod. Phys. Lett. A16 (2001) 1181; D. Klemm, A. Petkou, G. Siopsis and D. Zanon hep-th/0104141.

[123] T. Banks and W. Fischler astro-ph/0307459.

[124] Bin Wang, Elcio Abdalla and Ru-Keng Su *Mod. Phys. Lett.* **A17** (2002) 23.

[125] S. Dodelson and L. Hui, astro-ph/0305113.

[126] A. R. Liddle and S. M. Leach astro-ph/0305263.

[127] W. Israel, *Nuovo Cim.* **44B** (1966) 1; erratum: **48B** (1967), 463.

[128] E. Abdalla and B. Cuadros-Melgar

[129] A. Chamblin, R. Emparan, C. V. Johnson and R. C. Myers, Phys. Rev. D 60, 064018 (1999)

[130] J. Garriga and M. Sasaki, Phys. Rev. D 62, 043523 (2000)

[131] P. Kraus, JHEP 12, 011 (1999)

[132] R. Maartens, D. Wands, B. A. Bassett and I. P. C. Heard, *Phys. Rev.* **D62** (2001) 041301.